UNIVERSITY OF GENOA

PhD Programme: HEMATO-ONCOLOGY AND CLINICAL-TRANSLATIONAL INTERNAL MEDICINE

Curriculum: CANCER GENETICS AND MOLECULAR PATHOLOGY

Cycle: XXXVIII

DOCTORAL THESIS

PATHOLOGY-LED DIGITAL COLLAGEN QUANTIFICATION FOR RISK PROFILING OF MESENTERIC DISEASE IN SMALL-INTESTINAL NEUROENDOCRINE TUMORS

PhD Candidate:	Murad Ali
Supervisor:	Prof Federica Grillo
Department:	Department of Internal Medicine and Medical Specialties (DIMI)
Position:	PhD student, XXXVIII cycle

Academic Year: 2022/2025

Abstract

Mesenteric disease is a major determinant of morbidity and operative complexity in small-intestinal neuroendocrine tumors (SI-NETs), yet routine pathology alone can be insufficient for risk profiling of mesenteric involvement and distinguishing mesenteric tumor deposits (MTDs) from nodal metastases. This study evaluated a pathology-led framework integrating standardized clinicopathologic reassessment with digital collagen quantification on picrosirius red (PSR) whole-slide images and an interface-based assessment of vessel-wall modification (VWM). This single-center retrospective cohort included 70 resected, well-differentiated SI-NET cases from 2010 to 2024. Mesenteric disease was present in 49 of 70 SI-NET cases (primary tumor with mesenteric metastasis, either nodal metastasis or mesenteric tumor deposit), whereas 21 of 70 were primary-only cases with no mesenteric metastasis. PSR collagen proportionate area (CPA) was quantified using region-of-interest annotation and color deconvolution for compartment-specific primary bowel-wall regions and for mesenteric lesions. Mesenteric lesions were typed on H&E using prespecified architecture-based criteria as MTDs versus nodal metastases. A binary patient-level analysis compared primary-only cases versus any mesenteric lesion, and a lesion-level analysis assessed discrimination of MTDs versus nodes using CPA and VWM. In the binary analysis, patients with mesenteric lesions had larger primary tumors (median 2.0 vs 1.5 cm; $p = 0.0378$; ROC AUC = 0.66) and markedly higher frequencies of primary vascular invasion (OR = 10.2; $p = 0.0014$) and perineural invasion (OR = 8.5; $p = 0.00042$). In contrast, primary-tumor CPA showed minimal discrimination for mesenteric involvement (ROC AUC 0.49 to 0.54). In the lesion-level analysis (19 mesenteric tumor deposits; 29 mesenteric nodal metastases), CPA was higher in MTDs than in nodes (median 21.1% vs 15.7%; $p = 0.00158$; ROC AUC = 0.709); a Youden-derived CPA threshold of at least 18% yielded sensitivity 0.77 and specificity 0.61. VWM was strongly enriched in MTDs (89.5% vs 41.4%; OR = 12.04; $p = 0.000828$), with sensitivity 0.895 and specificity 0.586, and concordant positivity for CPA ≥18% together with VWM most strongly supported an MTD diagnosis in this dataset. In this cohort, larger primary-tumor size and the presence of vascular and/or perineural invasion were associated with mesenteric involvement, whereas an interface-focused combination of VWM and higher lesion CPA supported distinction of MTDs from nodal metastases.

Keywords: SI-NET; mesenteric spread; mesenteric tumor deposits (MTDs); nodal metastasis; mesenteric fibrosis; digital pathology; picrosirius red (PSR); collagen proportionate area (CPA); vessel-wall remodeling

Table of Contents

List of Figures

List of Tables

List of Abbreviations

Abbreviation	Meaning
5-HIAA	5-hydroxyindoleacetic acid
68Ga	Gallium-68
177Lu	Lutetium-177
AJCC	American Joint Committee on Cancer
AUC	Area under the curve
CAF	Cancer-associated fibroblast(s)
CAP	College of American Pathologists
CgA	Chromogranin A
CHD	Carcinoid heart disease
CI	Confidence interval
CPA	Collagen proportionate area
CT	Computed tomography
CTA	Computed tomography angiography
CTGF	Connective tissue growth factor
DAE	Device-assisted enteroscopy
DPX	Resinous mounting medium (DPX)
ECM	Extracellular matrix
EMVI	Extramural venous invasion
ENETS	European Neuroendocrine Tumor Society
EOD	Extent of disease
FDG	Fluorodeoxyglucose
FFPE	Formalin-fixed paraffin-embedded
GI	Gastrointestinal
GEP-NEN	Gastroenteropancreatic neuroendocrine neoplasm
H&E	Haematoxylin and eosin
HRQoL	Health-related quality of life
IHC	Immunohistochemistry
IQR	Interquartile range
Ki-67	Ki-67 proliferation index
LC-MS	Liquid chromatography mass spectrometry
MRI	Magnetic resonance imaging
MTD	Mesenteric tumor deposit
NCDB	National Cancer Database
NEN	Neuroendocrine neoplasm
NEC	Neuroendocrine carcinoma
NET	Neuroendocrine tumor
NETest	Multigene blood transcript assay (NETest)
NT-proBNP	N-terminal pro-B-type natriuretic peptide
OR	Odds ratio
ORR	Objective response rate

OS	Overall survival
PET	Positron emission tomography
PFS	Progression-free survival
PRRT	Peptide receptor radionuclide therapy
PSR	Picrosirius red
QA	Quality assurance
ROC	Receiver operating characteristic
ROI	Region of interest
SBCE	Small-bowel capsule endoscopy
SD	Standard deviation
SEER	Surveillance, Epidemiology, and End Results
SI-NET	Small-intestinal neuroendocrine tumor
SMA	Superior mesenteric artery
SMV	Superior mesenteric vein
SSA	Somatostatin analogue
SSTR	Somatostatin receptor
SSTR2	Somatostatin receptor 2
TGF-β	Transforming growth factor beta
TPH1	Tryptophan hydroxylase 1
VWM	Vessel-wall modification
WHO	World Health Organization
WSI	Whole-slide image

Chapter 1: Introduction

1.1 Background and Significance of SI-NETs

1.1.1 Overview of SI-NETs: Classification and Clinical Context

Small-intestinal neuroendocrine tumors (SI-NETs) are well-differentiated gastroenteropancreatic neuroendocrine neoplasms (GEP-NENs) that arise most commonly from enterochromaffin cells of the ileum and are formally classified by morphology with grading based on mitotic count and Ki-67 proliferative index in the 2022 WHO framework, which also clarifies distinctions between NET and NEC across digestive sites [1]. Recent European guidelines treat well-differentiated small-intestinal neuroendocrine tumors as a distinct entity within GEP-NENs, and recommend that staging and treatment selection be driven by tumor grade (G1 to G3), functional status, overall disease extent, and somatostatin receptor expression [2,3]. Epidemiologically, large US registry analyses have shown that NEN incidence and prevalence have risen substantially over time, accompanied by improvements in survival that extend to patients with distant-stage gastrointestinal primaries, underscoring the growing clinical impact despite its relative rarity [4]. Population data from England similarly document steadily increasing NEN incidence and progressive survival gains, reflecting enhanced detection and evolving management within national health systems [5]. Clinically, SI-NETs often progress silently for years and are frequently discovered at advanced stages either following the identification of hepatic metastases or after nonspecific abdominal symptoms. A possible pattern of presentation is mesenteric involvement with mesenteric tumor deposits of variable, even considerable, size, often with a relatively small primary tumor [6]. From a biological perspective, midgut NENs typically exhibit a relatively low tumor mutational burden and substantial epigenetic and microenvironmental influences, producing heterogeneity in growth kinetics and therapeutic responsiveness across patients [7]. Consensus oncology guidelines, therefore, emphasize taxonomy (NET vs NEC), grade, and functional status as the backbone for staging, prognostication, and initial treatment selection across the GEP-NEN spectrum [3].

1.1.2 Mesenteric Fibrosis: Clinical Impact and Rationale

Mesenteric fibrosis, a stromal, desmoplastic reaction that develops around mesenteric metastases or involved lymph nodes, is a signature complication of SI-NETs and is strongly implicated in symptoms, operative feasibility, and downstream morbidity [8]. Recent prospective tissue studies and systematic reviews estimate that clinically relevant mesenteric fibrosis occurs in a substantial fraction of patients with SI-NETs and can precipitate intestinal obstruction, mesenteric ischemia, severe abdominal pain, and malabsorption [9]. In surgical planning, mesenteric extension is often the principal limiting factor because fibrotic retraction and vascular encasement constrain safe dissection planes and raise the risk of short-bowel syndrome after resection [10]. Emergency presentations with obstruction or ischemia remain common and are associated with worse perioperative and oncologic outcomes compared to elective surgery, highlighting the stakes of timely recognition and judicious intervention [11]. Expert surgical commentary further emphasizes that operative strategy should balance symptom relief and oncologic control with vascular safety and preservation of small-bowel length, alongside growing interest in carefully selected minimally invasive approaches in high-expertise centers [12]. While peptide-receptor radionuclide therapy has transformed systemic disease control for somatostatin-receptor–positive midgut NETs, dedicated imaging analyses indicate that mesenteric masses rarely undergo major morphologic regression after peptide receptor radionuclide therapy (PRRT), so desmoplastic risk may persist despite radiologic stability elsewhere [13]. Contemporary US database studies report improving survival in GEP-NENs, but also show substantial resource use and care complexity, particularly in patients with disease patterns that include mesenteric involvement [14]. Mechanistic profiling supports a biological basis for these clinical observations: proteomics of SI-NET primaries and paired mesenteric lesions demonstrates enrichment of profibrotic extracellular-matrix proteins and complement components in fibrotic mesenteric metastases [15]. Recent oncology reviews note that, despite expanding systemic options, mesenteric complications remain a major driver of symptoms and quality-of-life impairment, supporting multidisciplinary pathways that integrate surgery, nuclear medicine, radiology, pathology, and supportive care [16].

1.2 Epidemiology and Natural History of SI-NETs

1.2.1 Incidence, Prevalence, and Survival Trends

Age-adjusted incidence and prevalence of neuroendocrine neoplasms (NENs) have risen steadily in the 21st century, with small-bowel primaries among the most common gastroenteropancreatic (GEP) sites [4]. Globally, small-intestine cancers (including SI-NETs) showed an estimated 64,477 new cases in 2020 and a higher disease burden in older adults, underscoring rising detection and reporting [17]. Population-based analyses indicate that age-standardized small-intestine cancer incidence (including NETs) has more than doubled over recent decades, reflecting both true increases and improved case ascertainment [18]. Within the United States, recent registry work confirms rising small-intestine cancer incidence across histologic subgroups from 2000 to 2020, with attention to age, sex, and racial/ethnic differences [19]. Contemporary ENETS guidance specifically notes that the incidence and prevalence of well-differentiated SI-NETs are gradually increasing across health systems [2]. Across NENs, 1-, 5-, and 10-year relative survival have improved alongside incidence, contributing to accumulating prevalence as patients live longer with the disease [20]. From 2004 to 2016, annual GEP-NEN cases increased ($n = 4{,}010$ to $n = 9{,}379$), largely driven by low-stage, low-grade disease [14]. Regional series focusing on SI-NETs report contemporary incidence ranges around 0.8–2.7/100,000, consistent with the broader trend of gradual increases observed in clinical datasets [21]. Surgical-oncology perspectives emphasize that SI-NETs have become the most frequent entity among small-intestinal tumors, with increasing identification and prolonged survival, inflating point prevalence [22]. Basic and translational syntheses similarly highlight the disproportionate rise of midgut (small-intestinal) NENs compared with many other solid tumors, paralleling advances in imaging and classification [23]. Notably, some population-based European studies describe more stable SI-NET incidence over limited periods, suggesting that geographic heterogeneity and ascertainment differences can modulate observed trends [24].

1.2.2 Clinical Presentation

SI-NETs are most often diagnosed in older adults, with the highest proportion between ages 65–74 (29.8%) and a median age at diagnosis of 66 years [25]. SI-NETs may remain clinically silent for many years, often with non-specific symptoms; cross-sectional and functional

imaging are therefore central to case detection once symptoms prompt evaluation [26]. When symptomatic, SI-NETs often present with abdominal pain, as well as diarrhea, and carcinoid syndrome in <10-20% of patients who are generally metastatic to the liver. Symptoms may derive from complications, including intermittent or progressive obstruction, or ischemic features related to mesenteric desmoplasia, as well as metastatic disease at first diagnosis (often liver but may be seen in diverse and unexpected sites) [27]. Primary-care–to-specialist pathways can be protracted for SI-NETs; recent machine-learning work in an 11.7-million-person UK primary-care cohort documented low absolute incidence and diagnostic delay, motivating targeted case-finding approaches [28]. Carcinoid syndrome (CS) is a debilitating disease that affects approximately 10-20% of patients with NENs, most often with SI-NETs [29]. CS symptoms often involve flushing, diarrhea, tachycardia, and bronchospasm with wheezing/shortness of breath. Among those with CS, up to ~50% may develop carcinoid heart disease (CHD) over time, typically involving right-sided valvular dysfunction and progressive heart failure if unrecognized [30]. Hormone-mediated complications shape the disease course; in metastatic midgut NETs with carcinoid syndrome, CHD contributes to morbidity and mortality, warranting proactive screening and timely cardiology co-management [31]. Cardiac imaging is crucial for both diagnosis and management of CHD; in the past, imaging was accomplished largely by echocardiography, but more recently, imaging for CHD has increasingly become multimodal and warrants awareness of the particular diagnostic challenges of this disease [32,33]. Expert guidance from ENETS on CS recommends standardized diagnostic pathways and multidisciplinary management to mitigate hormone-mediated morbidity, including proactive screening for cardiac involvement [34]. Broader NET practice updates emphasize the heterogeneous symptom spectrum, from non-specific abdominal complaints to hormone-driven syndromes, necessitating high clinical suspicion and coordinated imaging/biochemical workups [35].

1.2.3 Anatomic Distribution and Multifocality

Most small-bowel NETs arise in the ileum (midgut), reflecting their origin from serotonin-producing enterochromaffin cells concentrated in the distal small intestine [36].

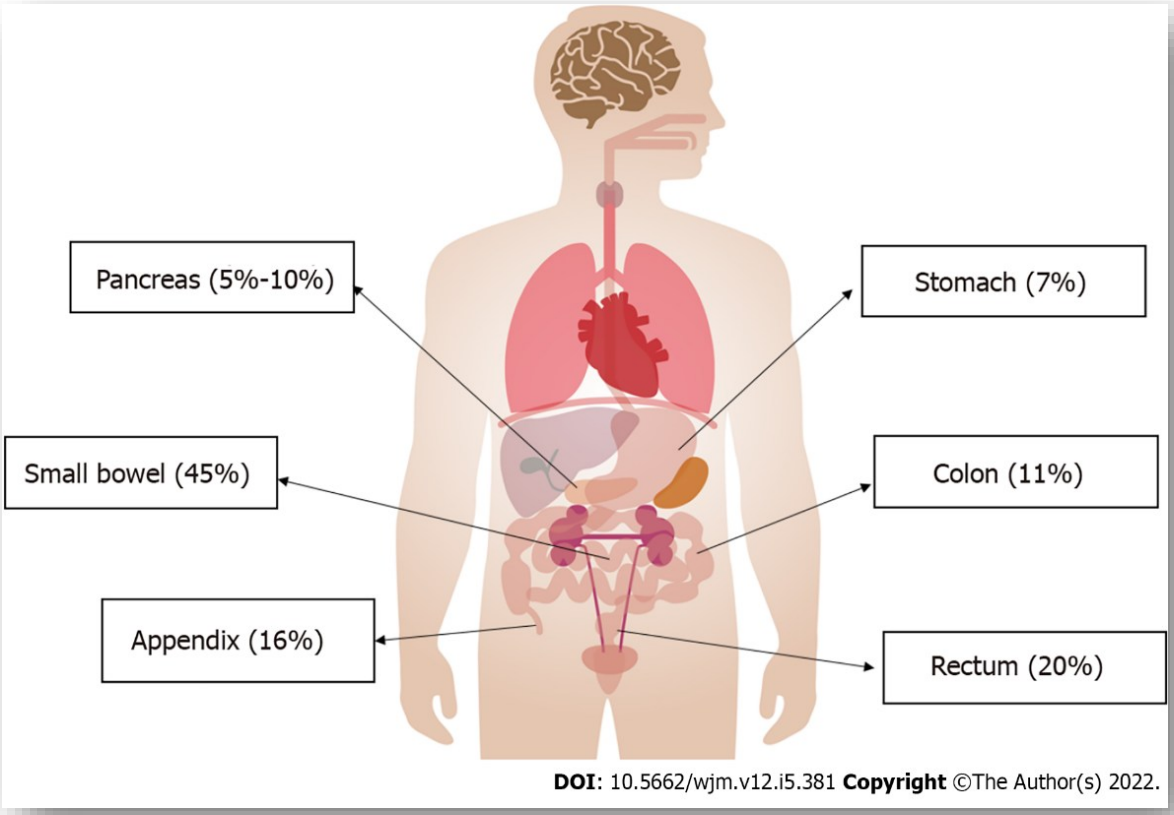

Figure 1. Anatomic distribution of primary sites in gastroenteropancreatic neuroendocrine tumors. Schematic overview of common primary locations with approximate relative frequencies: small bowel (45%), rectum (20%), appendix (16%), colon (11%), stomach (7%), and pancreas (5–10%). Percentages are illustrative and may vary across registries and case mix; values shown are adapted from published epidemiologic summaries and are broadly consistent with population-based analyses.

Radiologic and surgical reviews reiterate that SI-NETs are the most common malignant neoplasm of the small intestine and that recognition of their midgut biology guides imaging and surgery [37]. Multifocal primaries are a defining feature in a meaningful minority of patients; contemporary surgical series report multifocality rates that can approach 50% of cases, especially when the entire small bowel is meticulously palpated [38]. In jejunal and ileal NETs, endoscopy does not play a major role, while Ga-68 Dotatate PET/CT scan aids in identifying multifocal tumors before surgical resection, or localizing the primary lesion in metastatic NETs where the initial workup is unrevealing [39]. Modern CT planning tailored to SI-NETs assists in delineating mesenteric involvement and vascular encasement before surgery, complementing functional imaging to localize multifocal disease [10]. Single-cell and

genomic profiling underscore biological heterogeneity within SI-NETs, supporting observations that multifocal tumors can differ transcriptionally even within the same patient [40]. In multifocal SI-NETs, independent clonal and epigenetic evolution of synchronous primaries has been documented, supporting a 'field' effect in which shared local microenvironmental cues produce phenotypically similar yet clonally unrelated tumors [41,42].

1.2.4 Disease Course and Survival by Stage and Grade

Prognosis in SI-NETs is strongly stage- and grade-dependent, with Ki-67–based grading central to risk stratification in modern classifications and clinical decision-making. Ki-67 proliferation index was an independent predictor of recurrence, progression, and/or death in a large, multicenter cohort of patients with SI-NETs [43]. Meta-analytic data in metastatic SI-NETs show prolonged long-term survival for well-differentiated disease compared with many other metastatic solid tumors, yet outcomes remain heterogeneous across cohorts [44]. Longitudinal biomarker studies reveal that Ki-67 can increase over time with a change in grade, and such changes are associated with inferior survival, highlighting the value of dynamic re-assessment [45,46]. Across SI-NETs, population-level survival has improved in the last two decades: a contemporary US SEER analysis (2000–2021) shows lower mortality in later eras with gains extending to distant-stage gastrointestinal NETs, while regional and national European cohorts report clearer improvements for jejuno-ileal primaries [4]. Population-level survival for jejuno-ileal SI-NETs has improved over time; in a nationwide Swedish study, 5-year net survival rose from 0.69 in the 1960s to 0.81 in 2010–2015 [47]. After apparently curative surgery for SI-NETs, the risk of recurrence after intended radical surgery was high, with a recurrence-free survival rate of 40% after 10 years of follow-up in large, long-followed institutional cohorts, underscoring the need for extended surveillance [48]. Scandinavian cohorts indicate that although disease control after curative-intent resection of SI-NETs is generally durable, it remains imperfect, with ~30% of patients experiencing recurrence by about five years and a persistent risk extending into years five to ten postoperatively, thereby supporting standardized long-term follow-up protocols [49]. For high-grade digestive NENs (including NET G3), prospective population-based data confirm markedly worse outcomes than for G1-G2 well-differentiated SI-NETs, validating grade as a dominant prognostic determinant [50]. In a large single-center cohort of 615 patients with SI-NETs, intended radical surgery achieved durable, but imperfect, control with frequent late recurrences, disease-specific

survival in disseminated cases around seven years, and prognostication driven by Ki-67 as a continuous variable (while WHO G1 vs G2 did not discriminate outcomes), collectively justifying prolonged, standardized follow-up and supporting reconsideration of current grading [48].

1.3 Biology of SI-NETs

1.3.1 Enteroendocrine Lineage and Enterochromaffin (EC) Cell Origin

SI-NETs are serotonin-secreting well-differentiated NETs believed to originate from enterochromaffin (EC) cells [51]. SI-NETs most convincingly trace their lineage to intestinal enteroendocrine cells, with recent integrative whole-genome/transcriptome studies showing SI-NET transcriptomes that deconvolve to an enteroendocrine signature and, specifically, high expression of enterochromaffin (EC) markers such as TPH1, implicating EC cells as the likely cell of origin [52]. EC cells are the principal source of peripheral 5-hydroxytryptamine (5-HT) in the intestine, positioning this lineage as a likely cell of origin for serotonin-producing midgut NET biology [53]. Recent single-cell atlases show that enteroendocrine cells form discrete subtypes in the human gut and frequently co-express multiple peptide hormones, with the epithelium as a whole producing more than 20 gut hormones, features that underscore EEC lineage plasticity relevant to SI-NET hormone programs [54,55]. Developmental and lineage-mapping reviews detail how Notch, NEUROG3, and downstream bHLH factors drive EEC differentiation from intestinal stem cells, offering plausible routes for tumor initiation within the EC branch [56]. Chemosensory properties of L-type and other EECs, via G-protein–coupled receptor networks and RGS modulators, anchor the concept that transformed EECs can retain environmental responsiveness typical of their normal counterparts [57]. Spatially resolved SI-NET profiling at single-cell resolution demonstrates that tumor cells segregate into epithelial-like vs neuronal-like programs, implying that transformation and progression can capture distinct facets of EEC maturation [40]. Microenvironmental cues that shape EC biology (nutrients, bile acids, and the microbiota) also modulate epithelial serotonin availability, highlighting how niche inputs could influence both tumor initiation and symptom biology [58]. Beyond endocrine secretion, EECs exert local paracrine control of motility, barrier function, and immune tone, functions that may be co-opted or dysregulated in EC-lineage tumors [59]. Multifocal SI-NETs often originate independently from separate neoplastic clones within the same segment of small bowel, consistent with field effects acting on a susceptible EEC

compartment [41]. Across this lineage, robust somatostatin-receptor expression, especially SSTR2, serves as a hallmark of neuroendocrine differentiation and enables both high-affinity molecular imaging and targeted therapy in SI-NETs, with receptor density often aligning with hormone control, tumor growth suppression by SSAs, and prognosis [60].

1.3.2 Copy Number and Epigenetic Landscape of SI-NETs

Modern multi-omics converge on the view that SI-NETs have exceptionally low point-mutation burdens, with biology dominated by copy-number change and epigenetic reprogramming rather than canonical oncogenic mutational drivers [61,62]. While *CDKN1B* mutations occur in a minority of cases and implicate p27-mediated cell-cycle control, they do not account for the full disease spectrum or its heterogeneity [52]. Loss of chromosome 18 is the single most frequent genomic event in ileal SI-NETs, often hemizygous, and is detectable across multifocal primaries [63]. Longitudinal WGS and archival imaging indicate SI-NETs often originate in childhood and evolve over decades, with early truncal chromosome-18 loss (sometimes whole-genome doubling) and predominantly clock-like mutagenesis—consistent with their indolent clinical course [64]. In line with this view, expert overviews emphasize that broad chromosomal imbalances (especially 18q loss) drive downstream shifts in gene dosage and epigenetic state, supporting a copy-number–centric model of SI-NET that is distinct from classic mutation-driven oncogenesis [65]. Additional recurrent copy-number imbalances include gains on chromosomes 4, 5, 14, and 20, and evidence of acquired DNA-repair defects during progression, together suggesting a stepwise structural evolution [52]. Across advanced NENs, whole-genome analyses reveal site-specific molecular heterogeneity and highlight potentially actionable targets, underscoring that SI-NETs are a distinct genomic class within NENs [66]. DNA-methylation profiling identifies stable epigenetic subgroups that correlate with differentiation and clinical behavior, indicating that methylome states can function as molecular taxonomies in GI NETs [67]. A comprehensive multi-center portrait integrating copy-number, methylation, and expression delineates diverse SI-NET molecular groups, linking epigenetic states to tumor programs and clinical phenotypes [68]. In SI-NETs, lower DNA methylation at the SSTR2 promoter is associated with higher SSTR2 mRNA expression, supporting a role for promoter methylation in regulating SSTR2 expression [69]. In preclinical NET models, the hypomethylating agent guadecitabine increased SSTR2 expression and radiotracer uptake on PET, suggesting that epigenetic therapy might re-sensitize NETs to somatostatin-targeted diagnostics and peptide receptor radionuclide therapy [70]. In preclinical

NET models, histone deacetylase inhibition upregulates SSTR2, increases 177Lu-DOTATATE tumor uptake, and enhances antitumor efficacy, linking epigenetic chromatin modulation to somatostatin-targeted radionuclide delivery [71]. Cohort-level clinical genomics also documents grade-linked expression shifts and variable neuroendocrine marker intensity, reflecting how molecular heterogeneity maps onto diverse growth rates and therapeutic responsiveness [72]. Across cancers, accumulating evidence shows that ECM and stromal programs are not only shaped by oncogenic and therapeutic pressures but also feed back to drive progression and treatment resistance, underscoring the rationale for microenvironment-targeted strategies [73].

1.3.3 Serotonin Biology, Mesenteric Fibrosis, and Carcinoid Heart Disease

Intestinal epithelial serotonin signaling is increasingly recognized as a central regulator of gut physiology and brain–gut axes, aligning with the EC-cell specialization that typifies SI-NETs [74]. EECs, including EC cells, integrate microbial and dietary cues and can act as gatekeepers of microbiome–gut–endocrine communication, a property that may be co-opted in hormone-secreting tumors [75]. Clinically, systemic 5-HT excess underlies CS in many midgut NETs and sets the stage for serotonin-mediated fibrotic complications [2]. Mesenteric fibrosis (MF) is a hallmark of SI-NETs and contributes to bowel obstruction, ischemia, and cachexia, which makes fibro-inflammatory biology relevant alongside tumor control [9]. Proteomic analyses of SI-NET mesenteric metastases identify collagen-rich, proteoglycan-enriched ECM signatures and matrisome remodeling consistent with active desmoplasia [15]. At the tissue level, mesenteric fibrosis in SI-NETs is associated with dense αSMA-positive fibrotic stroma adjacent to mesenteric lymph node metastases and with stromal enrichment of COMP-expressing cells, alongside increased stromal COMP and COL11A1 expression in MF-positive vs MF-negative patients [8]. Mechanistically, 5-HT can promote fibroblast proliferation and matrix production via 5-HT_{2B} receptor signaling, offering a plausible link between hormonal excess and fibrotic remodeling in NETs [76]. Serotonin-mediated fibrosis also manifests in the heart as CHD, driven by endocardial plaque deposition in long-standing, serotonin-secreting disease [32]. Targeting peripheral serotonin synthesis with the tryptophan hydroxylase inhibitor telotristat ethyl yields sustained improvements in CS-associated diarrhea and durable reductions in urinary 5-HIAA, with a favorable long-term safety profile in extension follow-up [77]. Preclinical co-culture data indicate that telotristat ethyl downregulates

ECM/matrisome gene programs and disrupts tumor–fibroblast paracrine signaling, suggesting potential antifibrotic effects that warrant clinical evaluation [78].

1.3.4 Tumor Microenvironment: Angiogenesis, Extracellular Matrix, and Immunity

SI-NETs are highly vascular, stroma-rich neoplasms in which angiogenic signaling and fibroinflammatory remodeling are central to tumor ecology and progression [79]. Systematic profiling reveals scant intratumoral effector T cells with peri-tumoral accumulation in many midgut NETs, an immune-excluded ('cold') phenotype; prior studies also report low PD-L1 expression in this disease [80]. Consistent with this immune-excluded biology, pembrolizumab monotherapy achieved a low objective response rate (~3–4%) in previously treated well-differentiated NETs, reinforcing the need to combine PD-1 blockade with strategies that recruit T cells and reprogram the tumor microenvironment [81]. The ECM, through cross-linking, increased stiffness, and protease-driven remodeling, tunes mechanotransduction and drug distribution, thereby shaping invasion, intratumoral drug penetration, and therapeutic resistance [82]. Broad oncology frameworks indicate that ECM–stroma programs can govern immune-cell trafficking and response durability, making matrix-targeted or stroma-normalization strategies attractive partners for NET therapies [73]. Pan-tumor angiogenesis reviews emphasize VEGF/VEGFR as a central driver and discuss other growth-factor circuits (e.g., FGF, PDGF); NET-specific studies are needed to substantiate their activity in GEP-NET endothelium [83]. Clinically, the multikinase inhibitor cabozantinib significantly prolonged progression-free survival vs placebo in both previously treated, progressive extrapancreatic and pancreatic neuroendocrine tumors in the phase III CABINET trial, supporting anti-angiogenic targeting in NET microenvironments [84]. Additional randomized and phase-II data with anti-VEGF strategies, including pazopanib, support a class effect on disease control in extrapancreatic NETs [85]. Microenvironmental desmoplasia appears to blunt locoregional response: after PRRT, mesenteric masses typically show little morphologic regression and remain stable despite symptom improvement, consistent with stromal refractoriness [13]. Finally, cancer-wide perspectives argue that therapeutically reprogramming pathological ECM, via stromal normalization, integrin pathway modulation, or dampening TGF-β signaling, may enhance responses to other modalities, a rationale that warrants investigation in SI-NETs [86].

1.4 Mesenteric Disease in SI-NETs

1.4.1 Mesenteric Vascular, Lymphatic, and Neural Anatomy

The small-bowel mesentery is a broad, fan-shaped double fold of peritoneum that anchors the jejunum and ileum to the posterior abdominal wall and serves as a conduit for their arterial, venous, lymphatic, and autonomic nerve supplies; within its two leaves, the superior mesenteric artery gives rise to multiple jejunal and ileal branches that form arterial arcades and straight terminal vessels (vasa recta) [87]. Within the mesentery, jejunal and ileal branches of the superior mesenteric artery form arterial arcades that give rise to vasa recta; typically, the jejunum has 2–3 arcades with longer vasa recta, whereas the ileum has 4–5 arcades with shorter vasa recta [88]. During ileal tumor surgery, the paraintestinal marginal artery (ileal arcade) and the first arcade serve as key boundaries for lymphadenectomy and bowel-sparing ligation, underscoring the operative importance of mesenteric arcades [89]. The superior mesenteric artery (SMA) enters the small-bowel mesentery and terminates at the ileum, where it anastomoses with the ileal branch of the ileocolic artery; recognizing this junction is useful in preoperative planning when mesenteric disease abuts the ileocolic pedicle [90]. Lymphovascular bundles closely parallel the terminal and successive ileal arteries toward the SMA tripod, with sub-millimetric lymphatic–arterial separation in the proximal ileal mesentery, which explains how mesenteric tumor spread can endanger long small-bowel segments and informs bowel-sparing arterial ligation and lymphadenectomy [89]. Human anatomic studies describe dense periarterial neural cords and fine branches spiraling around the superior mesenteric artery as part of the superior mesenteric plexus, providing a structural basis for perineural involvement and helping explain how perivascular tumor extension can entrap nerves as well as vessels [91]. Autonomic neuroanatomy describes a contiguous prevertebral sympathetic network in the retroperitoneum with lumbar splanchnic inputs coursing through the aortic plexus and its prevertebral ganglia, including the prehypogastric and inferior mesenteric ganglia, to the superior hypogastric plexus, providing a framework to contextualize periarterial neural involvement around mesenteric vessels [92]. Clinically, knowledge of mesenteric perfusion and collateralization is essential because ischemic risk rises when encasement compromises multiple arcades, a scenario radiologists appraise by CT angiography in suspected mesenteric ischemia [93,94]. In practice, mesenteric vascular segmentation and lymphatic routing mean that even modest-appearing mesenteric lesions can

have outsized surgical and functional consequences when they track along mesenteric vessels and lymphatics [22].

1.4.2 Nodal Metastases vs Mesenteric Tumor Deposits (MTDs)

In most (approximately 80%) SI-NETs, mesenteric lymph-node metastases are present at the time of surgery and often extend to the mesenteric root, where desmoplastic fibrosis may encase the superior mesenteric artery (SMA) and superior mesenteric vein (SMV) [95]. Pathology literature defines mesenteric tumor deposits in SI-NETs as discrete, irregular mesenteric tumor nodules, discontinuous from the primary and lacking lymphoid tissue, thereby distinguishing them from conventional lymph-node metastases [96]. Importantly, MTDs are not simply enlarged lymph nodes; across pathology series, their presence independently predicts worse prognosis, challenging node-centric interpretations and prompting updates to staging schemas [97]. Across recent updates, mesenteric tumor deposits are explicitly recognized for their prognostic weight, and AJCC v9 incorporates mesenteric masses into nodal staging (pN2); several groups advocate careful documentation, though formal requirements to quantify them separately from nodal metastases are still evolving [98]. Dedicated surgical planning studies show that preoperative CT identifies a mesenteric mass with high sensitivity, reflecting current radiologic-pathologic understanding. This mass often corresponds to MTDs rather than enlarged nodes, especially when it encases branches of the SMA and appears retractile/spiculated; however, imaging criteria to reliably separate MTDs from nodes are not yet standardized [10]. MTDs are flagged as biologically adverse markers in midgut SI-NETs and appear at least as prognostically informative as, often stronger than, nodal burden, particularly for predicting liver metastasis, though formal staging still relies on existing N-category rules [96]. At the microanatomic level, SI-NET mesenteric disease can show extramural venous invasion (EMVI), which is strongly associated with hematogenous liver dissemination and adverse metastatic risk [99]. Proteomics of SI-NET mesenteric metastases with fibrosis show stromal enrichment of collagens (e.g., COL12A1) and proteoglycans, consistent with profibrotic ECM programs; these stromal changes may plausibly relate to the retractile mesenteric phenotype [15]. Mesenteric fibrosis commonly forms around NET-lymph node metastases, with stroma enriched for α-SMA–positive fibroblasts and COMP-expressing cells, consistent with a TGF-β–driven desmoplastic program that underlies obstruction and ischemia [8]. In daily practice, radiologists still stage mesenteric involvement along the SMA axis because the level of arterial contact or encasement predicts how much small bowel can be

preserved; however, this gradation does not, by itself, distinguish MTDs from nodal disease [100]. Surgical oncology viewpoints emphasize that mesenteric extension along the SMA/SMV pedicles is the principal constraint on resectability, with the risk of short-gut syndrome rising steeply once proximal branches are encased, hence the emphasis on mesenteric-sparing resections and accepting R1 margins when needed to preserve bowel length [22]. CT-based staging links the extent of mesenteric involvement to predicted residual small-bowel length and the likelihood of right colectomy, highlighting how the mesenteric mass can drive the operative plan [10]. Therapeutically, desmoplastic mesenteric masses often remain morphologically stable while extra-mesenteric disease is controlled, and peptide-receptor radionuclide therapy can improve symptoms despite little or no measurable reduction of the fibrotic mass [13]. Even when the mesenteric mass is unresectable, carefully selected patients can benefit from palliative debulking for obstructive or ischemic symptoms, with modern series from expert centers reporting high rates of symptom improvement and acceptable perioperative risk [101].

1.4.3 Clinical Consequences of Mesenteric Disease

Clinically, mesenteric involvement is a major driver of mechanical problems in SI-NETs: fibrotic retraction can kink or tether bowel loops and compromise mesenteric vessels, leading to intermittent subacute obstruction and ischemia that often require operative or endovascular intervention in selected patients [27]. When a desmoplastic mesenteric mass encases the SMA or its branches, patients are at risk of segmental mesenteric ischemia; although uncommon, it can present acutely and require prompt recognition and intervention because of its morbidity and mortality [94]. Guideline-level evidence identifies Computed Tomography Angiography (CTA) as the first-line test for suspected mesenteric ischemia; programs that standardize early CTA within ‘intestinal stroke’ pathways increase appropriate imaging, shorten time to intervention, and raise revascularization rates [102]. Even without an acute vascular event, mesenteric mass effect and fibrosis can drive abdominal pain and intermittent obstruction; in symptomatic, locally advanced cases, imaging–surgical correlation is used to select patients for vessel-sparing mesenteric debulking to decompress the root and improve bowel symptoms [101].

1.4.4 Distinguishing MTDs from Nodal Metastases on Imaging and Pathology

A central challenge is that CT/MRI often show a single mesenteric mass without reliably separating fibrotic tissue from active tumor/nodal metastases, a distinction with staging, prognostic, and surgical implications [101]. Even expert panel reviews acknowledge that while multimodality imaging accurately detects SI-NETs and their mesenteric masses, it is vulnerable to pitfalls and interpretive ambiguities in characterizing fibrotic deposits vs enlarged nodes [103]. To reduce variability, ENETS published standardized synoptic CT/MRI templates for GI-NETs, which require the structured reporting of mesenteric disease characteristics, SMA/SMV involvement, and suspected adjacent-organ invasion [104]. An interobserver study found substantial agreement among GI pathologists in separating SI-NET mesenteric tumor deposits from nodes, with irregular shape and nerve/vessel entrapment favoring MTDs, and peripheral lymphoid features and round shape favoring nodes [105]. In SI-NETs, outcome data show that the prognostic impact of MTDs tracks with their number rather than their size, supporting refinement of staging to emphasize deposit count and formal inclusion of deposits in nodal assessment [106]. Preoperative CT reliably identifies the mesenteric mass, yet has low sensitivity for retropancreatic lymph node involvement, and because validated imaging criteria to distinguish MTDs from nodal metastases are lacking, confidently "typing" mesenteric disease before surgery remains challenging [10]. Because MTDs, nodal disease, dense fibrosis, and entrapped neurovascular structures can coexist within a single mesenteric mass, radiology–pathology concordance is often limited, so multidisciplinary boards are used to reconcile findings and plan therapy [101].

1.4.5 Imaging-Guided Management of Mesenteric Masses

Mesenteric fibrosis appears to be an active stromal program with disease-specific proteomic signatures in mesenteric metastases, including increased collagens, proteoglycans, and complement components, suggesting therapeutic avenues beyond pure cytoreduction [15]. Although PRRT with 177Lu-DOTATATE often improves clinical symptoms and systemic disease control, mesenteric masses rarely regress radiographically (ORR ~4%), suggesting that the benefit reflects stabilization and relief of hormonal symptoms more than reversal of desmoplastic fibrosis [13]. When symptoms stem from vascular compromise or bowel obstruction, debulking of the mesenteric mass—after multidisciplinary review and in experienced centers—can decompress the mesenteric root and, in most carefully selected

patients, relieve pain and resolve obstructive symptoms [101]. Preoperative imaging classifications of mesenteric masses help anticipate vascular involvement and potential obstructive or ischemic complications, guiding timely, mesenteric-sparing surgery aimed at symptom control while avoiding short bowel syndrome [22]. Emerging preoperative vessel-based imaging classifications for SI-NET mesenteric masses stratify surgical risk and help plan bowel-preserving operations intended to mitigate future obstruction or ischemia [107,108].

1.5 Diagnostic Imaging and Endoscopy

1.5.1 Capsule Endoscopy and Device-Assisted Enteroscopy: Roles and Yields

Small-bowel capsule endoscopy (SBCE) and device-assisted enteroscopy (DAE), including double-balloon, single-balloon, and spiral systems, are established modalities that extend mucosal assessment beyond standard endoscopy and have defined roles in contemporary small-bowel diagnostic pathways, including the evaluation of small-bowel tumors such as SI-NETs. For small-bowel tumors, ESGE recommends SBCE for patients at increased risk, and when imaging already suggests a small-bowel tumor, DAE is preferred. Lesions identified at SBCE should be confirmed and, where appropriate, treated with DAE using biopsy and tattooing, and cross-sectional imaging is advised for staging when SBCE shows high diagnostic certainty [109]. When cross-sectional imaging raises high suspicion for a small-bowel tumor or when stenosis is likely, consider DAE to secure histology and to avoid capsule retention, particularly when SBCE may be contraindicated [110]. These principles are reinforced by practical clinical pathways that position SBCE upstream for occult bleeding and anemia but favor DAE when tissue acquisition or therapeutic intervention is immediately required [111]. Evidence in small-bowel NETs shows that double-balloon enteroscopy can identify additional lesions preoperatively and aid detection of multifocal disease [112]. A 2024 narrative review dedicated to endoscopic management of small-bowel NETs details how SBCE aids in initial detection, while DAE enables targeted biopsies, tattooing for surgical planning, and, in selected cases, endoscopic management of bleeding [113]. When suspicion for a mass is high, cross-sectional enterography is preferred first line because it depicts masses, wall thickening, and narrowing, while SBCE may miss submucosal lesions; imaging then guides both the route and urgency of device-assisted enteroscopy [114].

1.5.2 CT/MR Enterography, Liver MRI, and Radiomics

CT or MR enterography is central for detecting SI-NETs, delineating mesenteric disease, and contributing to staging, using neutral oral contrast for luminal distention and multiphasic IV enhancement to depict hypervascular tumors and associated desmoplastic change, typically alongside Somatostatin receptor PET and liver MRI for comprehensive staging [26]. A 2023 systematic review and meta-analysis reported high diagnostic accuracy for both MR enterography and CT enterography in small-intestinal tumors, supporting their use in clinical diagnosis and overall management, with modality choice tailored to context [115]. Pictorial and practical radiology reviews emphasize that CT/MR enterography, with neutral oral contrast, improves depiction of small-bowel tumors and their mesenteric manifestations compared with routine abdominopelvic CT, especially for mural and extramural features, though very small primaries can still be missed [116]. Comprehensive overviews of gastroenteropancreatic neuroendocrine neoplasms emphasize combining anatomic imaging with functional techniques to leverage complementary strengths for lesion detection, characterization, and staging [117]. Hepatobiliary contrast-enhanced MRI with gadoxetic acid is highly sensitive for detecting and volumetrically quantifying NET liver metastases, and hepatic tumor load measured on these scans informs response assessment and multidisciplinary treatment decisions [118]. Dedicated liver MRI reviews report that hepatocyte-specific contrast agents improve lesion-to-liver contrast on the hepatobiliary phase, enhancing baseline staging and follow-up response assessment of metastatic disease, while dynamic phases may still benefit from extracellular agents [119]. Radiology pictorial reviews detail classic direct and indirect CT signs of small-bowel tumors, such as enhancing mural nodules, kinking and tethering from mesenteric desmoplasia, and a mesenteric mass with radiating stranding [120]. Recent teaching cases reaffirm that CT enterography or enteroclysis enables thorough evaluation of small-bowel tumors and extra-enteric findings that inform surgical planning [121]. Cross-sectional reviews for GEP-NENs note that dedicated enterographic protocols are superior to routine CT for depicting subtle small-bowel parietal abnormalities and aiding detection of primary lesions [122]. Radiomics has emerged as a complementary layer, with CT-based models of mesenteric lesions in SI-NETs predicting the risk of mesenteric-fibrosis–related complications [123]. Broader imaging practice papers reiterate that no single modality suffices in NENs, and that combining contrast-enhanced CT/MRI for morphology, including liver MRI with hepatobiliary agents, with somatostatin-receptor PET (and FDG when indicated) yields the most complete picture for multidisciplinary decisions [124].

Contemporary reviews of small-bowel tumor imaging emphasize protocol-optimized CT/MR enterography for detecting primaries and multiphasic CT/MRI for staging and surgical planning, including evaluation of mesenteric and vascular involvement [125].

1.5.3 Somatostatin Receptor PET/CT: Indications and PRRT Selection

SSTR PET using 68Ga-DOTATATE/-DOTATOC or 64Cu-DOTATATE is a key part of NET workup, with high sensitivity for well-differentiated disease and whole-body mapping that directly informs management, while FDG or other tracers are preferred in selected low-SSTR or high-grade cases [126]. SSTR PET is preferred over ^{111}In-pentetreotide and conventional imaging for staging and restaging well-differentiated NETs [127]. Head-to-head comparative studies show higher patient-, lesion-, and region-level true-positive rates for SSTR PET than SPECT, including better detection in liver, bone, and nodal metastases, supporting PET as the preferred functional imaging modality for NETs where available [128]. ENETS 2024 recommends SSTR PET/CT or PET/MRI in the diagnostic and staging work-up of well-differentiated SI-NETs and uses SSTR uptake to guide therapy selection, including eligibility for SSA and PRRT [2]. For PRRT selection and triage, contemporary guidance requires adequate and preferably homogeneous SSTR uptake on PET across all lesions and recommends adding FDG PET in selected higher-grade or clinically heterogeneous cases to refine prognosis and guide treatment [129]. An institutional reassessment (n=124) found 68Ga-DOTATATE PET/CT most useful for initial staging and for surveillance or response monitoring in metastatic GEP-NETs, frequently revealing additional disease and changing management; its incremental value was limited for surveillance after curative-intent surgery, and in some cases, results prompted PRRT initiation [130]. A 2024 systematic review cataloged numerous false-positive patterns on 68Ga-DOTATOC PET/CT and emphasized that recognizing these pitfalls, often from non-NET conditions, is crucial to avoid misclassification [131]. Consensus statements on theranostic and molecular imaging emphasize multidisciplinary care pathways that connect SSTR PET staging, pathology-informed assessment, and systemic therapies, including PRRT, coordinated by experienced multidisciplinary teams [132].

1.6 Biomarkers and Grading in SI-NETs

1.6.1 Chromogranin A and 5-HIAA: Uses and Limitations

Chromogranin A (CgA) and 24-hour urinary 5-hydroxyindoleacetic acid (5-HIAA) remain the most widely used circulating biomarkers in gastroenteropancreatic neuroendocrine neoplasms; CgA can reflect overall tumor burden (with recognized confounders), and urinary 5-HIAA captures serotonin metabolism in functioning midgut disease [3]. Chromogranin A can aid baseline risk assessment and serial monitoring, but heterogeneous assays and common biologic confounders substantially limit diagnostic specificity and sensitivity, so results should be interpreted alongside imaging and histology rather than used in isolation [133]. Proton-pump inhibitors, chronic atrophic gastritis, renal impairment, systemic inflammatory conditions, and hepatic dysfunction can elevate CgA independently of tumor activity, so documenting and accounting for these factors and correlating results with clinical context and imaging are essential to mitigate false positives [134]. By contrast, 24-hour urinary 5-HIAA is a syndrome-specific biomarker recommended at presentation for advanced small-intestinal NETs, for lung or ovarian NETs of any stage, for unknown-primary NETs with liver metastases, and whenever carcinoid syndrome is suspected, with diet and medication counseling to reduce false results [135]. Higher 5-HIAA levels are linked to increased risk and progression of CHD; patients with 5-HIAA ≥300 μmol/24 h (or NT-proBNP >260 pg/mL) should undergo echocardiography and periodic cardiology follow-up [136]. Recent retrospective data show that serum 5-HIAA has diagnostic performance comparable to 24-hour urine 5-HIAA for carcinoid syndrome and offers a practical alternative that can simplify workflows while maintaining accuracy [137]. Recent reviews affirm 24-hour urinary 5-HIAA as the preferred biomarker for diagnosing and following NET-related CS and show that higher or rising levels and shorter doubling time correlate with progression, poorer outcomes, and increased risk of CHD [135].

1.6.2 Multigene Blood Biomarkers (NETest): Evidence and Current Role

Transcriptomic multi-analyte assays such as NETest measure blood mRNA signatures to reflect real-time tumor activity, offering superior performance for diagnosis, monitoring, and treatment response compared with single-analyte markers like CgA [138]. A 2020 Annals of Oncology meta-analysis found high diagnostic accuracy for the NETest and supported its clinical utility in distinguishing stable from progressive disease and in monitoring therapy

[139]. NETest scores were independently associated with progression-free survival (PFS) and overall survival (OS) in metastatic cohorts and showed promise for post-operative surveillance, complementing imaging and CgA, though the post-operative sample was small with limited follow-up [140]. ENETS guidance notes that multigene transcript assays, such as NETest, may help treatment monitoring, but their usefulness remains under evaluation; they are not widely available, and their real-world role in SI-NET management remains to be defined [2]. Proof-of-concept work on liquid-biopsy genome profiling in GEP-NENs likewise indicates that larger studies are needed to validate clinical impact [141]. Studies in high-grade GEP-NENs suggest that, while NETest is better established in G1 to G2 NETs, its role in high-grade disease is still being defined; available evidence appears mainly prognostic rather than treatment-predictive, supporting the need for further prospective validation before routine clinical use [142].

1.7 Pathology and Classification of SI-NETs

1.7.1 Primary Tumor Morphology and Immunohistochemistry

Small-intestinal neuroendocrine tumors are well-differentiated epithelial neuroendocrine neoplasms. In the 2022 WHO system, they are graded G1–G3 by mitotic count and Ki-67, and the framework distinguishes well-differentiated NETs from poorly differentiated NECs across all anatomic sites [143]. Primary SI-NETs typically display insular, trabecular, or nested growth of uniform cells with finely granular “salt-and-pepper” chromatin and often arise as multiple distal ileal EC-cell foci; correlation with site-specific markers supports ileal origin, and a conspicuous desmoplastic reaction around mesenteric nodal disease is characteristic, underpinning risks of bowel obstruction, ischemia, and mesenteric vascular compromise [22,144]. Core immunohistochemical markers remain the backbone of pathologic diagnosis in GEP tumors, with synaptophysin and chromogranin A routinely confirming neuroendocrine differentiation, often complemented by Insulinoma-associated protein 1 (INSM1) for added sensitivity [7]. The nuclear transcription factor INSM1 shows high, though slightly lower-than-synaptophysin, sensitivity with high specificity for neuroendocrine differentiation, and its combined use with synaptophysin and chromogranin A improves diagnostic accuracy [145]. CDX2 is a practical site marker that favors a midgut small-intestinal origin in metastatic NETs and, when interpreted with morphology and a panel including PAX8/PDX1 and TTF1, helps distinguish small-intestinal primaries from pancreatic and pulmonary sources [146]. Midgut neuroendocrine tumors commonly derive from enterochromaffin cells and produce serotonin,

which can be identified with immunohistochemistry [147]. Somatostatin receptor 2A immunohistochemistry often shows crisp membranous expression in well-differentiated NET and generally correlates with 68Ga-labeled somatostatin analog PET avidity, aiding integrated diagnostics [148,149].

1.7.2 WHO 2022 and ENETS Grading Criteria for SI-NETs

The 2022 WHO classification separates well-differentiated NETs from poorly differentiated NECs; NETs are graded primarily by proliferation using the Ki-67 index and mitotic count (G1–G3), whereas NECs are, by definition, high grade, reflecting distinct biology and clinical behavior [143]. ENETS 2024 notes that most SI-NETs present as G1 or G2, with NET G3 uncommon; management should integrate tumor grade with staging findings, functional status, and SSTR expression to guide therapy [2]. Guideline-based Ki-67 scoring uses hotspot selection with counting of at least 500 tumor cells to reduce variability; nonetheless, interobserver differences persist, supporting robust QA and the adoption of validated digital counting where available [150]. When Ki-67 and mitotic count are discordant, assign the higher grade; report both mitoses per 2 mm^2 and the Ki-67 index (counted on ~500–2000 tumor cells in hotspots) for prognostication and management [3]. Because Ki-67 shows marked spatial heterogeneity, small or non-hotspot biopsies can underestimate grade, contributing to biopsy–resection discordance; counting sufficient tumor cells in hotspots mitigates this bias [151,152]. Longitudinal SI-NET data show that Ki-67 can rise during follow-up and that increases or modified-grade progression (5% and 10% cut-offs) correlate with poorer survival, supporting re-biopsy and repeat grading when clinical, biochemical, or imaging findings suggest faster disease [45,46]. Baseline tumor growth rate predicts subsequent increases in Ki-67 and can refine risk stratification beyond static grade, helping identify patients at higher risk for grade progression [153]. Expert reviews note heterogeneous proliferation and recommend hotspot-based Ki-67 assessment; the 2022 WHO classification uses Ki-67 thresholds to grade digestive NENs, and close correlation with morphology is essential to prevent mislabeling high-grade NET as NEC or vice versa [154]. Digital pathology can improve objectivity and reproducibility in NET grading: automated or semi-automated Ki-67 assessment achieves agreement comparable to expert manual counting and helps avoid the variability of eyeball estimation, though it supplements rather than replaces the pathologist [155]. Emerging GEP-NEN data show that gradient-map-assisted hotspot selection can identify higher-grade hotspots, and that

digital image analysis reduces grading discordance vs eye estimation and aligns more closely with manual counting, improving the reliability of grade assignment [156].

1.7.3 Nodal Metastases and Mesenteric Tumor Deposits: Definitions and Criteria

In SI-NETs, MTDs are irregular nodules in the mesenteric fat that lack a lymphoid rim and often track along mesenteric neurovascular bundles. They correlate strongly with adverse dissemination, predicting liver metastasis more robustly than lymph node metastases and being associated with peritoneal carcinomatosis [96,157]. Version 9 of the AJCC acknowledges accumulating evidence on MTDs in jejunoileal NETs, cites data that MTDs may better predict adverse outcomes than nodal status, and underscores the need for improved data capture and staging refinements to better reflect prognosis [158]. Histologically, an MTD is a discrete mesenteric metastasis with no convincing residual nodal architecture and typically shows an irregular or angulated contour, entrapped nerves and/or thick-walled vessels, and prominent desmoplastic fibrosis [105]. By contrast, a positive lymph node generally preserves a rounded contour with at least a focal capsule, subcapsular sinuses, and a peripheral lymphoid rim or follicles when present [159]. Multicenter cohort data indicate that MTDs are common in resected SI-NETs and independently predict inferior relapse-free and overall survival [160]. In a single-center cohort of 615 patients with SI-NETs, stage, Ki-67 as a continuous variable, and plasma chromogranin A independently predicted recurrence after radical surgery, and Ki-67 independently predicted disease-specific survival in the total cohort; mesenteric nodal metastases were linked to higher recurrence risk [48]. Comprehensive management reviews report that mesenteric lymph-node metastases are present in most midgut NETs at diagnosis, and that desmoplastic mesenteric fibrosis and MTDs are common but often underestimated on staging imaging [161]. MTDs are associated with the presence of distant metastasis (pM) in SI-NETs, and this study supports their inclusion in staging; worse progression-free survival (PFS) was linked to higher modified nodal stage and to distant metastasis [162]. In SI-NETs, pathology frequently shows sclerosing fibrosis around mesenteric deposits that encompasses vessels and nerves; this pattern is associated with local complications such as bowel obstruction and ischemia [2]. Systematic reviews of nodal status indicate that nodal yield, lymph node ratio, and the adequacy of lymphadenectomy should be interpreted alongside MTDs, since these measures reflect different facets of regional spread and prognosis [163]. Interobserver studies show that experienced gastrointestinal pathologists can reach substantial agreement ($\kappa \approx 0.64$) in distinguishing MTDs from positive nodes when explicit architectural and stromal

criteria are applied [105]. In SI-NETs, SEER Inquiry 20230074 states that mesenteric soft-tissue deposits less than 2 cm should be documented but do not alter AJCC stage; for EOD staging, Regional Nodes is coded 000, only mesenteric masses greater than 2 cm receive a specific Regional Nodes code, and EOD primary tumor code 500 should not be used unless pathology explicitly states mesenteric invasion [164].

1.7.4 Staging and Reporting Standards (AJCC Version 9, CAP, ENETS)

AJCC Version 9 provides organ-specific staging protocols for jejunal and ileal NETs, outlines the T, N, and M categories with stage-specific survival from NCDB analyses, and notes areas needing refinement, such as lymph node assessment in the midgut, that will evolve as new evidence accumulates [158]. The College of American Pathologists requires synoptic reporting for jejunum and ileum NET resections using organ-specific checklists that capture core and conditional elements such as tumor site, multiplicity, grade, lymphatic and/or vascular invasion, and mesenteric involvement, with optional items including perineural invasion and mesenteric vascular elastosis [165]. ENETS has issued synoptic templates across pathology and companion documents for radiology and molecular imaging, promoting capture of standardized data elements and improving report completeness and cross-disciplinary comparability to support multidisciplinary care [166]. AJCC Version 9 delineates standardized, site-specific staging definitions for GEP-NETs, and as summarized in the Version 9 review, reports National Cancer Database–derived five-year survival stratified by site [158]. In preoperative planning, explicit classification of mesenteric nodal disease as distal vs proximal to the superior mesenteric vessels predicts the need for standard lymphadenectomy vs complex extended dissection, thereby informing whether a bowel-sparing segmental resection can be pursued or a more extensive approach is required, particularly when considering minimally invasive access [167]. Using CAP synoptic cancer protocols helps ensure complete capture of required data elements and standardized reporting that supports multidisciplinary care; specific distinctions like nodal metastasis vs mesenteric deposits should be recorded in appropriate fields [168]. Contemporary survival analyses in SI-NETs show that stratifying by lymphatic spread pattern and refining G2 subgrading improves prognostic grouping and can inform follow-up schedules and treatment planning [169].

1.8 Pathogenesis of Mesenteric Fibrosis and Vascular Remodeling

1.8.1 Cancer-Associated Fibroblasts and Extracellular Matrix Remodeling

Mesenteric fibrosis in SI-NETs, present in roughly half of patients, is commonly related to a desmoplastic reaction centered on mesenteric nodal metastases and manifests with abdominal pain from mesenteric angina, intermittent obstruction, ureteral obstruction, and ischemic symptoms, warranting targeted surgical assessment with mesenteric-sparing strategies [22]. Across solid tumors, cancer-associated fibroblasts arise from multiple lineages and encompass phenotypes that include myofibroblast-like states; they orchestrate extracellular-matrix deposition, contractility, and paracrine signaling that collectively sustain desmoplasia [170]. Mechanical features of the matrix are not passive because progressive collagen crosslinking and ECM stiffening amplify mechanotransduction, alter tumor cell transcriptional programs, and reinforce CAF activation in feed-forward loops [171]. Tumor microenvironments feature bidirectional signaling among epithelial, immune, endothelial, and stromal compartments that converges on matrix remodeling and fibrogenic cytokine networks [86]. In the stroma of mesenteric metastases, SI-NETs with mesenteric fibrosis show higher abundance of multiple collagens, proteoglycans, and complement proteins (for example, C9), with pathway enrichment consistent with profibrotic ECM dysregulation; no differential abundance was detected in tumor-cell compartments or primary-tumor stroma [15]. Histologic and transcriptomic analyses of mesenteric samples from patients with SI-NETs with mesenteric fibrosis show enrichment of α-smooth muscle actin-positive fibrotic stroma and a higher number of COMP-positive stromal cells compared with non-fibrotic cases [8]. At the metabolic level, CAFs upregulate de novo proline synthesis from glutamine via PYCR1 to sustain collagen production and deposition, linking stromal anabolic programs to the amount of collagen-rich extracellular matrix [172]. Matrix remodeling feeds back on therapy response, since dense ECM impedes drug penetration, alters interstitial fluid pressure and flow, and modulates receptor-mediated signaling relevant to targeted therapies [73]. Imaging correlates of this biology are well described in SI-NETs, where radiating sunburst strands, partially calcified mesenteric nodal masses, and encasement or occlusion of mesenteric vessels with engorged peripheral veins reflect the underlying desmoplastic architecture [26]. Taken together, mesenteric fibrosis in SI-NETs reflects cancer-associated fibroblast activity, extracellular matrix remodeling, and multicellular signaling that sustain a persistent, treatment-resistant desmoplastic stroma [9].

1.8.2 Serotonin-Driven Fibrogenesis and Tumor–Stroma Crosstalk

Serotonin is a central profibrotic signal in SI-NETs and, together with TGF-β and CTGF, promotes cancer-associated fibroblast activation and collagen deposition in the mesenteric stroma [173]. Proteomic and IHC data show downregulation of stromal tryptophan and serotonin-metabolizing enzymes in MF-positive SI-NETs, linking impaired local serotonin catabolism to profibrotic mesenteric remodeling [174]. Across cell, organoid, and in vivo models of SI-NETs, tumor-fibroblast paracrine crosstalk drives proliferation and desmoplasia, supporting strategies that therapeutically disrupt these signaling loops [175]. Serotonin 5-HT2B signaling in cardiac fibroblasts and myofibroblasts promotes proliferation, migration, and collagen remodeling; pharmacologic antagonism or cell-specific deletion reduces periostin-positive myofibroblasts, limits scar formation, and improves post-infarct remodeling [176]. The same receptor family has been implicated in lung fibroblast activation and matrix deposition; selective antagonism mitigates these effects, underscoring a broader role for serotonin GPCR pathways in tissue fibrosis beyond the gut [177]. Preclinical data show that peripheral 5-HT2A antagonism lowers hepatic fibrosis markers and collagen deposition in mouse MASH models, reinforcing that targeted serotonin-receptor modulation can alter fibrotic pathways [178]. Whether serotonin-targeted therapy mitigates carcinoid-related fibrosis remains uncertain; in a preclinical mouse model, telotristat with or without octreotide produced non-significant reductions in valve fibrosis and lowered NT-proBNP, underscoring the need for controlled studies to define any antifibrotic impact [179]. By contrast, PRRT can control systemic SI-NET disease, but mesenteric masses rarely shrink: in the MesenLuth study, the mesenteric-mass ORR was 4% and no metabolic responses were observed, with benefit mainly as mass stability and symptom improvement rather than radiographic regression [13]. Women, particularly those under 50 years, show a lower prevalence of mesenteric metastases and mesenteric fibrosis in SI-NETs; ERα is expressed in tumor cells and stroma, AR is confined to stroma, and ESR1 and AR mRNA are increased in tumors vs normal intestine, supporting a role for sex-steroid signaling in mesenteric disease [180]. Preclinical models show tumor-derived serotonin activates stromal cells through 5-HT2B signaling and profibrotic pathways like TGF-β and PDGF, sustaining mesenteric and other carcinoid-related fibrosis and revealing several therapeutic targets [181].

1.8.3 Mesenteric Vascular Involvement: Encasement, Ischemia Risk, and Operative Planning

The desmoplastic reaction around mesenteric metastases retracts the mesentery, can entrap bowel, and compromise mesenteric perfusion and venous drainage, creating a substrate for intermittent obstruction, ischemia, and pain [182]. On CT, mesenteric metastases from SI-NETs typically appear as a spiculated, sometimes calcified mass with radiating fibrotic strands ('spoke-wheel/sunburst'), accompanied by a desmoplastic reaction that retracts the mesentery and may encase mesenteric vessels [26,183]. There is a move toward standardized preoperative description of mesenteric extension, enabling anticipation of SMA/SMV involvement, likely resections, and the fraction of small bowel that can be preserved [10]. Reports describe acute mesenteric ischemia caused by encasement of the superior mesenteric artery and vein by mesenteric metastases in small-bowel NETs [94]. Systematic review evidence indicates that even with mesenteric root involvement or encasement, surgical exploration should not be considered an absolute contraindication, provided patients are carefully selected in multidisciplinary specialist centers, and appropriate hybrid or selective surgical strategies are available [100]. Emergency presentations are relatively common in SI-NETs, and emergency surgery is associated with worse oncologic outcomes, underscoring the need for early recognition of impending obstruction or ischemia and proactive elective management [11]. A standardized CT reading grid is under evaluation to improve the semiological description of mesenteric and lymph node extension on preoperative imaging, creating a shared language between radiology and surgery for operative planning [184]. ENETS 2024 advises that SI-NET care be coordinated in expert multidisciplinary teams; in patients with mesenteric involvement, decisions should consider the risk of short-bowel syndrome and the potential symptomatic benefit of intervention [2]. In practice, surgery aims to reduce tumor burden and hormone output and to prevent or treat locoregional complications from desmoplastic mesenteric fibrosis with vascular involvement [22]. Because mesenteric tumor deposits portend worse outcomes, systematic preoperative mapping and explicit reporting of mesenteric disease patterns provide prognostic insight and guide counseling and surgical planning [163].

1.8.4 Clinical Management of Mesenteric Fibrosis

First-line systemic therapy in well-differentiated SI-NETs typically uses somatostatin analogs for hormonal control and disease stabilization in SSTR-positive, slowly progressive disease, consistent with ESMO guidance [3]. For persistent carcinoid-syndrome diarrhea despite

optimized somatostatin analogs, telotristat ethyl reduces bowel-movement frequency and urinary 5-HIAA and is recommended as an adjunct for symptom control [185]. When disease progresses or symptom control is inadequate, peptide receptor radionuclide therapy is effective for tumor control, although objective shrinkage of the fibrotic mesenteric mass is uncommon, which limits stroma-directed benefit [13]. No medical therapy has convincingly reversed established mesenteric fibrosis in robust trials, so current pharmacologic strategies focus on hormonal control, tumor stabilization, and mitigation of downstream complications [182]. In carefully selected symptomatic patients with pain, obstructive episodes, or vascular compromise, debulking of the mesenteric mass in experienced centers can relieve symptoms with acceptable morbidity and sustained benefit for the majority [101]. Minimally invasive surgery is feasible in appropriately selected SI-NET cases, but selection should be cautious, and favor approaches that maintain safe mesenteric perfusion; bulky mesenteric root involvement or planned concurrent liver resection generally warrants open surgery [12]. Preoperative multiphasic contrast-enhanced CT, complemented by grade-appropriate SSTR or FDG PET/CT, is central to accurate staging and surgical planning in NENs [186]. Antifibrotic strategies targeting TGF-β signaling, fibroblast activation, and extracellular matrix turnover are under investigation in intestinal fibrosis [187]. Longitudinal care should also include surveillance for carcinoid heart disease, nutritional assessment, and symptom-directed supportive measures within multidisciplinary programs, consistent with expert guidelines [188].

1.9 Quantifying Fibrosis in SI-NETs

Digital pathology converts glass slides into whole-slide images that can be reviewed, shared, and analyzed, including with image analysis and machine-learning tools, and, when properly validated and integrated, can improve accuracy, efficiency, and the quality of patient care [189]. Quantification of mesenteric fibrosis in SI-NETs integrates Sirius Red histology with digital collagen proportionate area (CPA) and may be correlated with CT or MRI findings and intraoperative surgical evaluation [190].

1.9.1 Picrosirius Red and Color Deconvolution

On Picro-Sirius Red–stained sections, CPA quantifies the percentage of fibrosis and is the most validated morphometric approach for fibrosis assessment [191–194]. In automated pipelines,

picrosirius red–based whole-slide segmentation yields highly reproducible CPA suitable for translational preclinical fibrosis studies [195]. Algorithmic optimization of PSR detection increases specificity and sensitivity while minimizing operator input, yielding reproducible, multi-organ fibrosis quantification despite staining variation [196]. PSR-polarized-light analysis with CT-FIRE quantifies fiber length, straightness, alignment, and density to reveal microarchitectural remodeling beyond area-based metrics [197]. Biomedical studies continue to use PSR quantification as a primary readout of collagen deposition, embedding it within broader mechanistic experiments of fibrogenesis [198]. In hepatology models that inform pathology workflows, AI-assisted digital pathology with SHG/TPEF-based fibrosis quantitation and collagen morphometry is used to track treatment response and stromal dynamics [199]. Many pipelines apply stain normalization, including color-deconvolution–based methods, to mitigate between-site color variation, but their impact on model performance can be task-specific [200]. Contemporary reviews emphasize that normalization choices can materially alter downstream quantification, motivating explicit reporting and testing of multiple methods during pipeline development [201]. Virtual staining has shown high agreement with conventional stains in blinded pathology assessments, but broader multi-center clinical validation is still needed before routine clinical adoption [202]. Beyond simple area-based measures, semi-automatic, model-based analysis of polarized-light microscopy that combines bright-field and dark-field images can provide rapid, operator-light quantification of collagen fraction and spatial distribution, supporting batch analysis of large image datasets [203].

1.9.2 Whole-Slide Imaging and Compartmental Analysis

Guideline updates informed by multicenter concordance and noninferiority evidence indicate that whole-slide imaging can achieve diagnostic performance comparable to light microscopy for primary diagnosis, provided laboratories perform application-specific validation with high intraobserver concordance before clinical deployment [204]. Recent organ-focused reviews of label-free and rapidly stained virtual-H&E imaging summarize modality-specific strengths and limitations for generating H&E-like images on nonfixed tissue, underscoring that evaluation and interpretation should be tailored to the organ and tissue context [205]. Layer-specific quantification is appropriate in intestinal disease; in systemic sclerosis, collagen in the muscularis propria (circular vs longitudinal layers) has been measured on Sirius-Red sections using semi-automated image analysis [206]. Ex vivo human intestinal slice models demonstrate

distinct fibrogenic programs in mucosa vs muscularis, underscoring why compartment-specific readouts have mechanistic significance and translational relevance [207]. Human colon data show age-related, layer-specific shifts in total collagen, indicating that baseline differences by layer and age should be considered when interpreting fibrosis [208]. An international consensus defines stricture histology and sampling parameters to standardize assessments, enabling harmonized scoring frameworks and laying the groundwork for future quantitative, layer-specific metrics [209]. Analogous to fibrostenosing small-bowel Crohn's disease, consensus statements emphasize standardized definitions and multimodal assessment with cross-sectional imaging to guide endoscopic and surgical planning, highlighting how structured phenotyping can improve translational alignment between tissue pathology and imaging-based decision-making [210].

1.10 Study Aims

The overarching aim of this thesis was to develop a pathology-led and digitally reproducible approach to risk profiling of mesenteric disease in well-differentiated small-intestinal neuroendocrine tumors (SI-NETs) by integrating standardized clinicopathologic abstraction with whole-slide, picrosirius red (PSR) based collagen quantification and clearly defined histologic criteria for mesenteric lesion typing. Specifically, this work aimed to implement a robust digital pathology workflow that quantifies collagen as collagen proportionate area (CPA), defined as the percentage of analyzed tissue area occupied by PSR-positive collagen, and to apply this metric consistently across prespecified regions of interest in both the primary tumor and mesenteric lesions. A first, prespecified objective was to evaluate patient-level predictors of mesenteric involvement using a binary framework in which each case is treated as an observation and the endpoint is "any mesenteric lesion" (yes or no), irrespective of whether the mesenteric lesion is ultimately classified as a nodal metastasis, a mesenteric tumor deposit (MTD), or a mixed pattern; within this framework, the thesis aimed to test whether routinely reportable primary-tumor features, including maximum diameter, multiplicity, grade, mitotic count, Ki-67 index, vascular invasion, perineural invasion, and compartment-specific primary bowel-wall CPA (mucosa/submucosa and serosa/subserosa), can identify patients more likely to harbor a mesenteric mass. A second objective was to contextualize stromal patterns using a three-phenotype descriptive stratification (primary-only, primary with MTDs, primary with nodal metastasis), intended for exploratory, hypothesis-generating comparisons of collagen distributions and not as a separate inferential endpoint. A third, lesion-level

objective was to determine whether quantitative and semiquantitative pathology markers can discriminate MTDs from nodal metastases when each evaluable mesenteric lesion is treated as an observation, using H&E-based lesion typing as the morphologic reference standard; in this analysis, the aims were to evaluate discrimination based on lesion-level CPA and the presence of vessel-wall modification adjacent to the lesion interface, and to summarize diagnostic performance using receiver operating characteristic methods and operating characteristics derived from an exploratory Youden-optimal CPA threshold. Finally, we assessed whether, within individual patients, primary-tumor collagen burden correlates with mesenteric-lesion collagen burden, to evaluate whether stromal remodeling in the bowel wall and mesentery behaves as a coupled or partly independent process, thereby providing a quantitative pathology foundation that can be compared with, and ultimately integrated into, multidisciplinary imaging and clinical decision pathways for mesenteric disease assessment.

Chapter 2: Materials and Methods

2.1 Study Design

This single-center, retrospective observational study evaluated well-differentiated small-intestinal neuroendocrine tumors (SI-NETs) and associated mesenteric fibrosis at the Anatomic Pathology units of the University of Genoa/IRCCS Ospedale Policlinico San Martino. The study period encompassed small-bowel resections performed from 2010 to 2024 (inclusive). Analytic endpoints were derived from standardized clinicopathologic abstraction and whole-slide imaging; detailed histology, immunohistochemistry, and Sirius Red quantification protocols are reported in the dedicated Methods subsections. This Methods chapter integrates the prespecified analytic framework used in the Results: (i) a patient-level binary comparison (primary-only, with no mesenteric lesion vs with any mesenteric lesion), (ii) a three-phenotype stratification (primary-only, primary with mesenteric tumor deposits (MTDs), and primary with mesenteric nodal metastasis), and (iii) lesion-level analyses distinguishing MTDs from nodal metastases. Collagen was quantified as collagen proportionate area (CPA), defined as the percentage of analyzed tissue area occupied by picrosirius red-positive collagen. The analytic framework is detailed in Section 2.6, and collagen quantification (CPA) is detailed in Sections 2.4 and 2.5.

2.2 Case Accrual and Data Sources

With Institutional Review Board approval, consecutive jejuno-ileal neuroendocrine tumor resections performed from 2010 to 2024 were identified from pathology archives at the IRCCS Ospedale Policlinico San Martino/University of Genoa (Italy). Inclusion required (i) resection with at least one primary small-intestinal well-differentiated neuroendocrine tumor (SI-NET), (ii) confirmation of a well-differentiated neoplasm (G1 or G2) according to the 2022 WHO framework, and (iii) availability of formalin-fixed paraffin-embedded (FFPE) tissue suitable for picrosirius red staining of the primary tumor, with or without associated mesenteric lesions. Exclusions comprised poorly differentiated neuroendocrine carcinoma, non-neuroendocrine small-bowel primaries, small-bowel involvement by non-jejuno-ileal primaries, insufficient tissue for digital collagen quantification, missing essential variables, or indeterminate mesenteric lesion status after review. Cohort accrual, specimen availability, and mesenteric-lesion categories are reported in Results (Section 3.1 and Figure 2). Baseline clinicopathologic

variables were extracted from pathology reports, intraoperative notes, and clinical records into a structured dataset aligned with proposed minimum reporting elements for digestive-system neuroendocrine neoplasms [211]. Recorded variables included age at surgery, sex, primary-tumor site and multiplicity, maximum primary-tumor diameter, AJCC stage at presentation, presence and pattern of nodal involvement and distant metastases, mitotic count per 2 mm², Ki-67 labelling index, vascular and perineural invasion, mesenteric-lesion status and type, lymph-node yield and number positive, and neuroendocrine immunophenotype (synaptophysin and chromogranin A, with CDX2 and serotonin in selected patients).

2.3 Histopathologic Reassessment

All available hematoxylin and eosin (H&E) and picrosirius red (PSR) slides were re-reviewed by a dedicated gastrointestinal pathologist (F.G.) with real-time observation by a trained researcher (M.A.), blinded to clinical outcomes and downstream statistical analyses, to confirm key diagnostic features and prespecified variables. Primary-tumor features recorded included maximum diameter, multiplicity, deepest invasion, necrosis, vascular invasion, perineural invasion, mitotic activity, Ki-67 index, and pathologic TNM stage. Histologic grade was assigned according to the 2022 WHO framework, using mitotic count (mitoses per 2 mm²) and Ki-67 labelling index. When the two parameters disagreed, the higher grade was recorded. Mitotic activity was assessed on H&E sections in hotspots totalling 2 mm², and Ki-67 was scored in immunohistochemical hotspots by manual counting on a printed microphotograph, in line with local practice. Ki-67 immunohistochemistry was performed on freshly cut FFPE sections using standardized heat-induced antigen retrieval, recognising that nuclear antigens can show storage-associated immunoreactivity loss in archived precut sections and older blocks, which can be partly mitigated by deeper sectioning and/or prolonged or optimized heat-based retrieval conditions [151,212,213]. Vascular invasion was recorded when tumor cells were present within an endothelium-lined vascular space, with elastin stain confirmation used in equivocal cases where available; associated intraluminal thrombus or fibrin was noted as supportive evidence [214]. Perineural invasion was recorded when tumor cells tracked along or encased a nerve fascicle (involving the perineural sheath or space) [215]. When the requisite anatomic structures were not represented in the available material, invasion status was recorded as not assessable rather than assumed absent.

2.3.1 Lesion Typing Rules: Mesenteric Tumor Deposits Versus Nodal Metastases

On H&E, mesenteric lesions were classified as nodal metastases when a rounded metastatic focus showed residual lymphoid tissue (for example, a peripheral rim of lymphocytes), consistent with retained or partial nodal architecture. Mesenteric tumor deposits (MTDs) were defined as discrete, irregular mesenteric tumor nodules that were discontinuous from the primary tumor, lacked associated lymphoid (nodal) tissue, and were typically situated adjacent to mesenteric neurovascular bundles within a fibrotic (desmoplastic) stromal reaction [96]. For the patient-level analyses, each mesenteric lesion was first typed on H&E at the individual-lesion level, and these lesion-level calls were then aggregated to assign the binary endpoint (primary-only vs any mesenteric lesion) and the three-phenotype categories (primary-only, primary with MTDs, primary with nodes); the same lesion-level typing underpinned the direct lesion-level comparisons of MTDs vs nodal metastases.

2.4 Picrosirius Red Staining of FFPE Sections for Collagen Quantification

FFPE sections from primary SI-NETs and related mesenteric lesions were cut at 3-µm and dried at 60 °C for ≥30 min. Sections were deparaffinized in Histo-Clear/xylene (2×, ~5 min each) and rehydrated through graded ethanol to distilled water (100% ethanol 2×, 3–5 min each; 95% ethanol 3 min; 70% ethanol 3 min), then rinsed 2–5 min in distilled water. Without allowing sections to dry, slides were stained with 0.1% picrosirius red for 60 min at room temperature (Sirius Red for Collagen kit, code 010254), rinsed in distilled water, and differentiated with the kit Alcoholic Buffer for 10s (Diapath, Italy). Slides were then dehydrated rapidly to minimize dye leaching (70% → 95% ethanol, each ≤30s; 100% ethanol 2×, ~1 min each), cleared in Histo-Clear/xylene (2×, 3–5 min each), and coverslipped with a resinous medium (e.g., DPX/balsam). All reagents were handled in a certified chemical fume hood while wearing appropriate personal protective equipment (lab coat, nitrile gloves, and safety glasses) and were stored according to the manufacturer's instructions (photosensitive; +15 °C to +30 °C) (Diapath, Italy).

2.5 Digital Collagen Quantitation Workflow

Picrosirius red staining was performed on 3 µm FFPE sections from the primary tumor and, when present, from a representative mesenteric lesion. Sections were stained using a

standardized PSR protocol and digitized at 20× magnification on a Leica Aperio AT2 whole-slide scanner using bright-field illumination. Digital analysis focused on compartment-specific collagen proportionate area (CPA) in the primary bowel wall and in mesenteric lesions (MTDs/nodes). For each primary tumor, regions of interest (ROIs) representing mucosa/submucosa and serosa/subserosa were manually annotated on the PSR whole-slide image. For primary-tumor serosal/subserosal CPA, the ROI was confined to the bowel-wall serosa and immediate subserosa at the primary-tumor invasive front, and deliberately excluded mesenteric soft tissue, mesenteric tumor deposits, nodal tissue, and the desmoplastic stroma of any mesenteric mass; mesenteric-lesion CPA was quantified separately when available. ROIs explicitly excluded artefacts, necrosis, large vessels, smooth muscle, and non-neoplastic tissue. Within these ROIs, color deconvolution in Aperio ImageScope (v12.4.6) was applied to isolate the picrosirius red collagen signal from background staining, and collagen proportionate area (CPA) was computed as the percentage of PSR-positive pixels within the annotated ROI. Within each ROI, collagen was automatically quantified by the ImageScope algorithm, and compartment-specific mucosal/submucosal and serosal/subserosal CPA for each patient was expressed as the percentage of the analyzed area. Mesenteric-lesion collagen was quantified using the same pipeline. In mesenteric ROIs, the tumor–stroma interface was outlined, and collagen CPA was calculated for the perilesional fibrotic stroma. For the binary endpoint, primary-tumor CPA metrics (mucosa/submucosa and serosa/subserosa) were compared between primary-only cohort vs mesenteric disease cohort, and within-patient correlations paired primary serosal/subserosal CPA with a representative mesenteric-lesion CPA per case, after which analyses were extended to a three-group stratification (primary-only, primary with MTDs, primary with nodal metastasis) and to lesion-level comparisons directly contrasting MTDs vs nodal metastases using mesenteric-lesion CPA.

2.5.1 Mesenteric Lesion Vessel-Wall Modification Scoring

Vessel-wall modification (VWM) at the mesenteric-lesion interface was defined as fibrointimal hyperplasia with accompanying adventitial or perivascular fibrosis and recorded qualitatively on routine stains [216]. Perilesional vessels were defined operationally as arteries or veins whose outer wall lay within one low-power field of the lesion edge; more distant background vessels were not evaluated for VWM. Lesion typing and perilesional VWM were scored by a dedicated gastrointestinal pathologist (F.G.), with real-time observation by a trained researcher (M.A.). Equivocal cases were reviewed jointly and resolved by consensus. CPA outputs were

generated only after histologic scoring and were not available to raters; formal inter-rater reliability statistics were not calculated.

2.6 Variables, Endpoints, and Statistical Analysis

2.6.1 Analytic Overview And Units Of Analysis

This Methods chapter integrates three complementary analyses applied to the same curated resection cohort. First, a patient-level binary analysis treats each case as an observation and uses the endpoint “any mesenteric lesion” (yes or no). Second, a patient-level three-phenotype summary (primary-only, primary with MTDs, primary with nodal metastasis) is used to summarise and explore collagen patterns across phenotypes; any across-group statistical tests are exploratory and do not replace the prespecified binary endpoint. Third, lesion-level analyses treated each evaluable mesenteric lesion as an observation and evaluated discrimination of mesenteric tumor deposits vs nodal metastases.

2.6.2 Patient-Level Binary Analysis: Predictors of Any Mesenteric Lesion

For the patient-level binary framework, cases were dichotomized into a primary-only cohort with no mesenteric lesion and a mesenteric-lesion cohort with at least one mesenteric lesion, using the endpoint “any mesenteric lesion” irrespective of whether the mesenteric lesion was classified as nodal metastasis, tumor deposit, or a mixed pattern. Primary-tumor predictors included maximum diameter, multiplicity, grade, mitotic count, Ki-67 index, vascular invasion, perineural invasion, and compartment-specific primary bowel-wall CPA (mucosa/submucosa, and serosa/subserosa). When mesenteric CPA was required for within-case collagen correlations, one representative mesenteric lesion per patient was selected using prespecified criteria (largest, well-fixed lesion with an intact tumor–stroma interface), and these correlations were treated as exploratory.

2.6.3 Case-Level Descriptive Phenotype Comparisons

To contextualize stromal patterns, cases were additionally summarized into three mutually exclusive descriptive phenotypes: primary-only, primary with MTDs, and primary with nodal metastases. This three-phenotype structure was used for descriptive and exploratory

comparisons of collagen distributions; any across-group statistical tests are hypothesis-generating and do not represent a separate prespecified inferential endpoint. Where a mixed mesenteric pattern was present, it was described separately and not used to define the three-phenotype groups.

2.6.4 Lesion-Level Analysis: Mesenteric Tumor Deposits Versus Nodal Metastases

The primary lesion-level endpoint was discrimination of mesenteric tumor deposits vs nodal metastases using lesion-level PSR-derived collagen proportionate area (CPA) and the presence of vessel-wall modification (VWM) adjacent to the lesion. Lesion typing on H&E (Section 2.3.1) served as the morphologic reference standard. Lesion-level analyses were performed on all evaluable mesenteric lesions (48 lesions: 19 MTDs and 29 nodal metastases). CPA was quantified within prespecified regions of interest, and VWM was recorded qualitatively at the lesion interface.

2.6.5 Statistical Analysis

Continuous variables were summarized as median and interquartile range (with mean and range where useful), and categorical variables as counts and percentages; normality was assessed with the Shapiro–Wilk test. Case-level binary comparisons (primary-only vs any mesenteric lesion) used Mann–Whitney U tests for continuous predictors and Fisher's exact tests for categorical predictors; effect sizes were reported as Cliff's delta and Hodges–Lehmann median differences for continuous variables where applicable. The diagnostic performance for binary endpoints was evaluated using receiver operating characteristic (ROC) curves and the area under the curve (AUC), with exploratory Youden-optimal thresholds reported alongside sensitivity and specificity. Correlations between collagen metrics were estimated using both Pearson and Spearman coefficients. Lesion-level contrasts (tumor deposits vs nodes) used the Mann–Whitney U test for continuous measures and Fisher's exact test for categorical enrichments, reporting odds ratios and exact 95% confidence intervals. Analyses were conducted in Python 3 (NumPy, SciPy, statsmodels, scikit-learn, and Matplotlib). All statistical tests were two-sided; $p < 0.05$ was considered statistically significant.

2.6.6 Diagnostic Accuracy Sub-Study

A prespecified diagnostic-accuracy analysis evaluated the ability of lesion-level pathology markers to distinguish mesenteric tumor deposits from nodal metastases using H&E-based lesion typing as the reference standard. The index tests were PSR-CPA (analysed as a continuous marker using ROC analysis) and the presence of VWM at the lesion interface. An exploratory CPA threshold was derived using the Youden index, and operating characteristics were calculated at that threshold with exact confidence intervals.

2.6.7 Missing Data and Sensitivity Analyses

Analyses were restricted to evaluable material and are reported with explicit denominators; no imputation was performed. Variables were recorded as not assessable when the relevant anatomic structure was not represented in the reviewed material or when a stain was unavailable or non-informative (for example, due to tissue exhaustion or poor preservation). Archival Ki-67 values reported as ‘<x%’ were treated as upper bounds for descriptive summaries and evaluated in sensitivity analyses using alternative plausible codings. Where applicable, key findings were rechecked within the paired primary-tumor and mesenteric-lesion subset to confirm that conclusions were not driven by unpaired observations.

Chapter 3: Results

This chapter reports the patient-level and lesion-level analyses of mesenteric involvement.

3.1 Cohort and Specimen Overview

Of 117 records screened, 70 cases met eligibility criteria and formed a single-center cohort of resected well-differentiated SI-NETs treated from 2010 to 2024. The remaining 47 records were excluded for prespecified reasons (Methods, Section 2.2). Among the 70 cases, 49 showed mesenteric disease and contributed both primary and mesenteric tissue, while 21 had primary-tumor tissue only with no mesenteric involvement. Case accrual and mesenteric-lesion categories are summarized in Figure 2.

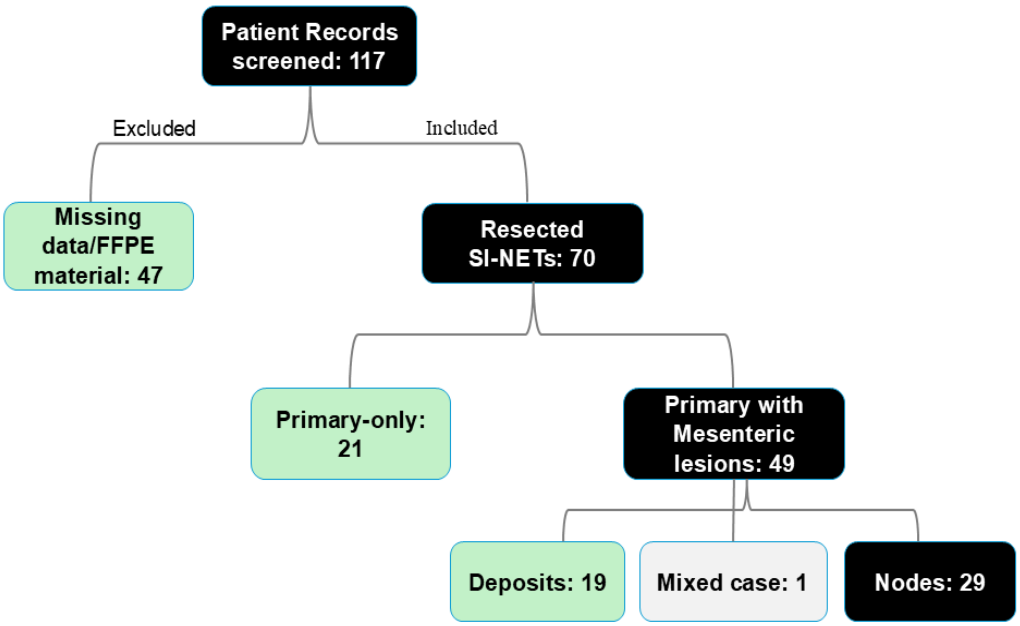

Figure 2. Lesion-inclusion flow diagram showing records screened (n = 117), included patients (n = 70), primary-only cases (n = 21), and cases with mesenteric lesions (n = 49), including mesenteric tumor deposits (n = 19), nodal metastases (n = 29), and one mixed case.

3.2 Clinicopathologic Characteristics of the Cohort

The cohort was predominantly male (48/70; 68.6%) with a median age of 70.5 years (IQR 61.75–77), a mean age of 68.9 years (SD 10.8), and an age range of 44–86 years. Discrete mesenteric lesions (MTDs and/or nodes) were present in 49/70 cases (70%) and absent in 21/70

(30%). At the case level within the mesenteric-lesion cohort (n = 49), lesion typing was: nodal metastasis only in 29/49 (59.18%), MTDs only in 19/49 (38.78%), and a mixed pattern in 1/49 (2.04%) characterized by two discrete mesenteric lesions (a node and an MTD). Expressed across the full cohort (n = 70), this corresponds to nodes 29/70 (41.4%), deposits 19/70 (27.1%), mixed 1/70 (1.4%), and no mesenteric lesions 21/70 (30%). Baseline clinicopathologic characteristics, including lymphadenectomy metrics (not restricted to mesenteric nodal disease), are summarized in Table 1. Pathological TNM staging showed a wide spectrum, ranging from early localized tumors (Stage I, 1/70 (1.4%); Stage II, 10/70 (14.3%)) to regionally advanced disease with lymph node involvement (Stage III, 41/70 (58.6%)), and to metastatic disease at presentation (Stage IV, 18/70 (25.7%)).

Table 1. Baseline characteristics

Characteristic	Evaluable n	Result
Male sex	70	48 (68.6%)
Chromogranin A positive	68	68/68 (100%)
Synaptophysin positive	66	66/66 (100%)
CDX2 positive	12	12/12 (100%)
Serotonin positive	38	38/38 (100%)
Ki-67, %	70	Median 1 (IQR 1–2.925)
Primary tumor size, cm	70	Median 1.8 (range 0.3–6.3)
Vascular invasion present	69	58/69 (84.1%)
Perineural invasion present	67	36/67 (53.7%)
Lymph nodes retrieved	65	Median 15 (IQR 8–22; range 0–68)
Metastatic nodes, count	65	Median 3 (IQR 1–6; range 0-15)
Mesenteric lesions available	70	49/70 (70%)
No mesenteric lesions	70	21/70 (30%)
AJCC stage at presentation	70	IV 25.7%; III 58.6%; II 14.3%; I 1.4%
Mesenteric lesion phenotype	70	Nodes 29 (41.4%); Deposits 19 (27.1%); Mixed 1 (1.4%); None 21 (30.0%)

Notes: Results are shown as n/N (%) for categorical variables and median (IQR) or range for continuous variables. Denominators vary for markers and variables not available in all cases. For immunohistochemistry, denominators reflect evaluable stains per marker; when a stain was unavailable or non-informative (for example, due to necrotic or ischemic material or tissue exhaustion), the marker was recorded as not assessable for that case.

3.3 Binary Analysis: Predictors of any Mesenteric Lesion (MTDs and Nodal Metastases)

The two-group analysis contrasted patients without any mesenteric lesion (primary-only, n = 21) against patients with at least one mesenteric lesion (n = 49), irrespective of whether the mesenteric lesion represented a nodal metastasis, an MTD, or a mixed pattern.

3.3.1 Baseline Clinicopathologic Comparability

Age and sex distributions were similar between groups. Primary-only patients had a median age of 73 years (IQR 65–78; mean 71.1; range 44–85), while patients with mesenteric lesions had a median age of 70 years (IQR 59–75; mean 67.9; range 47–86); Mann–Whitney U = 612.5, p = 0.21. Men accounted for 13/21 (61.9%) in the primary-only group and 35/49 (71.4%) in the mesenteric-lesion group. Grade distributions were balanced (G1/G2: 17/4 (81%/19%) in primary-only vs 35/14 (71.4%/28.6%) in the mesenteric-lesion cohort). As expected by design, AJCC stage differed between groups: in primary-only cases, 1/21 (4.8%) were Stage I, 10/21 (47.6%) Stage II, 6/21 (28.6%) Stage III, and 4/21 (19%) Stage IV, whereas all patients with mesenteric lesions were Stage III–IV (Stage III 35/49 (71.4%); Stage IV 14/49 (28.6%)).

3.3.2 Tumor Multiplicity, Necrosis, and Proliferative Indices

Tumor multiplicity distributions were comparable. In the primary-only group, 12/21 (57.1%) were unifocal, 5/21 (23.8%) had 2-4 lesions, and 4/21 (19%) were multifocal (5 or more lesions). In the mesenteric-disease cohort, 23/49 (46.9%) were unifocal, 17/49 (34.7%) had 2-4 lesions, and 9/49 (18.4%) were multifocal. Necrosis remained rare across both cohorts (1/21 (4.8%) vs 2/49 (4.1%)). Mitotic activity and Ki-67 index were low across both cohorts and did not differ meaningfully between groups. Overall, mitotic activity in the full cohort had a median of 1 per 2 mm² (IQR 0.5–1.0; range 0–12), with 98.5% of tumors showing ≤2 mitoses, and Ki-67 had a median of 1% (IQR 1–2.93; mean 2.25%; range 0.5–10). Ki-67 indices did not differ significantly between primary-only and mesenteric-lesion cohorts (Mann-Whitney U = 600, two-sided p = 0.27). In this cohort, proliferative indices were low in both groups and did not differ significantly.

3.3.3 Primary-Tumor Size as a Predictor of Mesenteric Involvement

In the two-group comparison, the primary tumor diameter was smaller in the primary-only cohort (median 1.5 cm; IQR 1.1–2.0; mean 1.66 (SD 1.01); range 0.3–5 cm) than in patients with mesenteric disease (median 2 cm; IQR 1.5–2.5; mean 2.09 ± 1.04; range 1–6.3). This difference was significant (Mann-Whitney U = 676, two-sided p = 0.0378) with a small to moderate effect size (Cliff's delta = 0.31). The Hodges–Lehmann estimator indicated a typical shift of approximately +0.4 cm in favour of the mesenteric-lesion group, suggesting that a "typical" mesenteric-cohort primary tumor is about 4 mm larger than a primary-only tumor, consistent with the idea that larger tumors are more likely to be associated with mesenteric disease. Still, the absolute size difference is moderate rather than dramatic. As a continuous classifier for the endpoint 'any mesenteric lesion', primary-tumor size showed modest discriminative performance (ROC AUC = 0.66), with operating thresholds around 1.7-2.0 cm offering a reasonable balance between sensitivity and specificity.

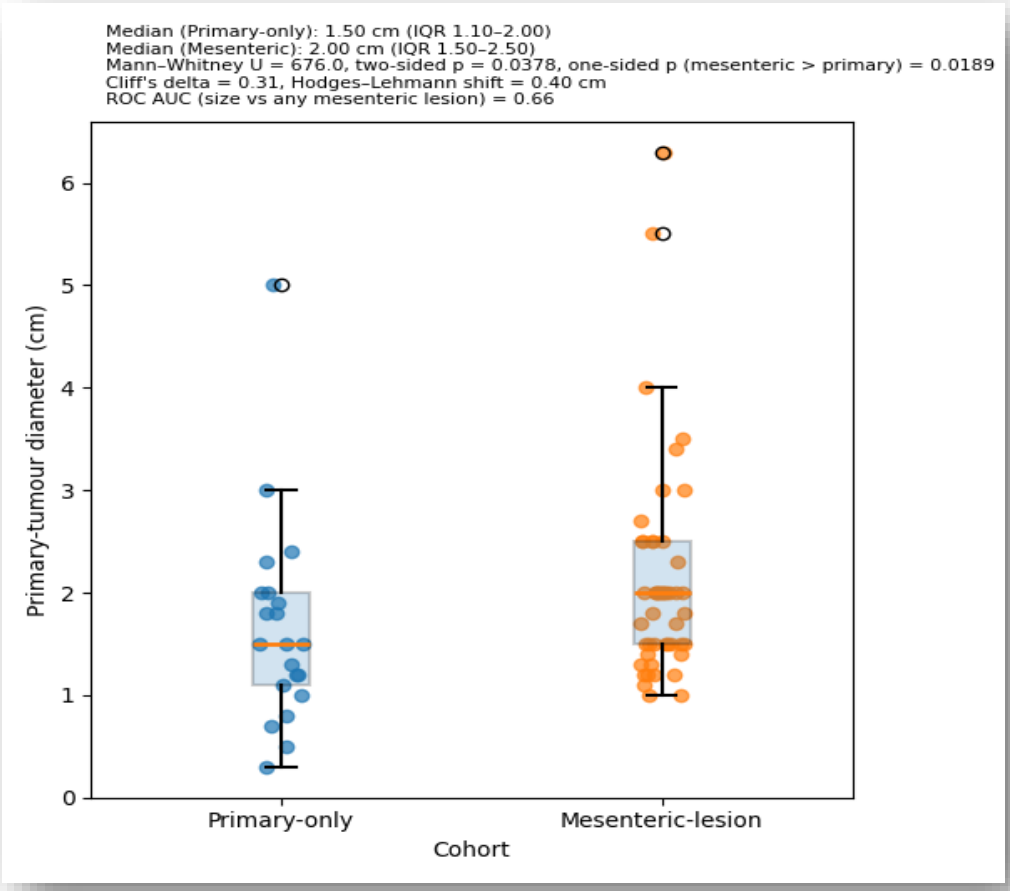

Figure 3. Primary-tumor size in the primary-only vs mesenteric-lesion cohorts.

3.3.4 Vascular and Perineural Invasion in the Primary Tumor

Primary-tumor vascular and perineural invasion were strongly enriched in patients with mesenteric disease. Vascular invasion was present in 12/20 evaluable primary-only cases (60%) vs 46/49 (93.9%) in the mesenteric-lesion group (Fisher's exact OR = 10.22; two-sided p = 0.0014), indicating roughly tenfold higher odds of vascular invasion in patients with mesenteric lesions compared with primary-only cases. Perineural invasion showed a similar pattern. In the primary-only group, perineural invasion was recorded in 4 of 20 evaluable cases (20%; 1 not assessable). In contrast, among patients with mesenteric disease, perineural invasion was present in 32 of 47 evaluable cases (68.1%; 2 not assessable). Fisher's exact test demonstrated a significant enrichment of perineural invasion in the mesenteric-lesion cohort (OR = 8.53; p = 0.00042). Taken together, these findings indicate that both lymphovascular and perineural permeation in the primary bowel wall function as proximate histologic correlates of mesenteric spread.

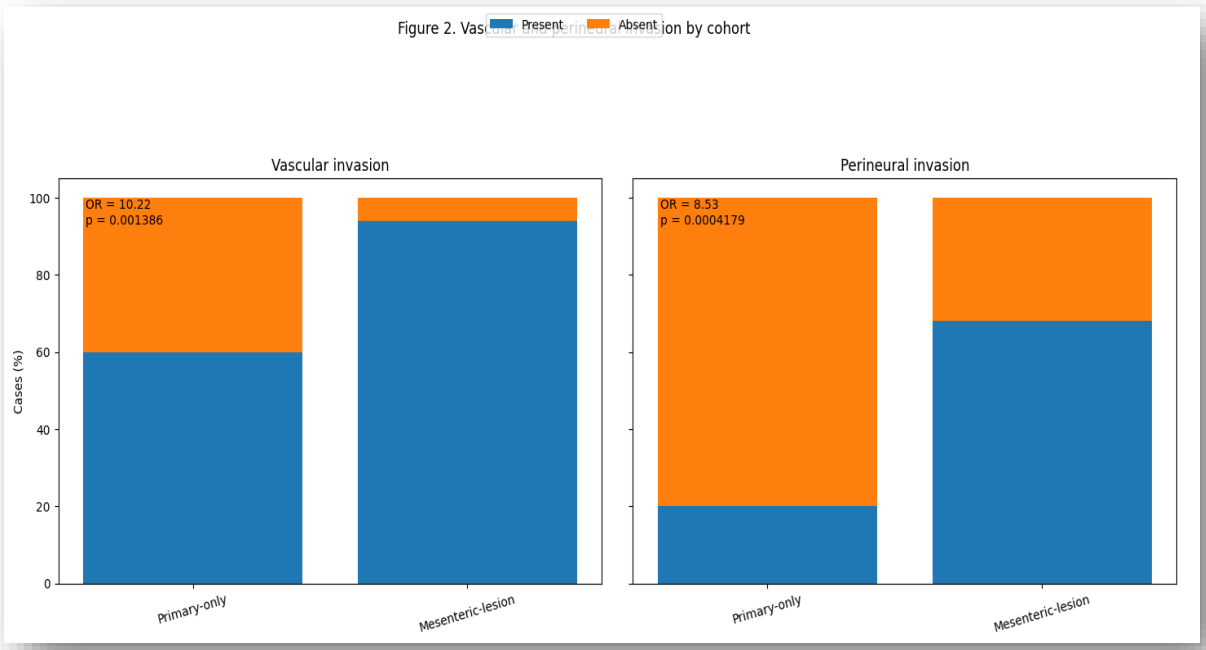

Figure 4. Vascular and perineural invasion in primary-only cases compared with cases with mesenteric disease

3.3.5 Primary-Tumor Collagen as a Predictor of Mesenteric Involvement

Primary-tumor collagen was quantified by picrosirius red color deconvolution and expressed as collagen proportionate area (CPA), defined as the percentage of the analyzed mucosal/submucosal and serosal/subserosal regions occupied by collagen. In the patient-level binary comparison (primary-only vs mesenteric lesion cohort), mucosal/submucosal collagen quantification showed near-complete overlap between the two groups. Among primary-only patients (n = 21), the median primary mucosal CPA was 15.8% (IQR 12.7–18.8%, mean 15.8%, range 9.3–25.9%). In patients with mesenteric lesions (n = 49), the median mucosal CPA was 15.4% (IQR, 11.7–19.2%; mean, 15.6%; range, 5.6–32.6%). A two-sided Mann–Whitney U test did not support any difference in patient-level mucosal/submucosal CPA between the two groups (U = 475, p = 0.95), with a negligible effect size (Cliff's delta = − 0.01) and a Hodges–Lehmann shift of only about − 0.038 percentage points. When patient-level mucosal/submucosal CPA was evaluated as a continuous classifier for any mesenteric lesion, performance was at chance level (ROC AUC = 0.49). The Youden-optimal threshold was approximately 20.7% CPA, but this cut-point provided high specificity (0.95) with very low sensitivity (0.17), limiting its practical usefulness as a stand-alone discriminator. Primary serosal/subserosal CPA showed only modest differences between cohorts. In the primary-only cohort (n = 21), the median serosal CPA was 21% (IQR, 19.1–26.3; mean, 22%; range, 13.3–30.4). In the mesenteric-lesion cohort (n = 49), median serosal CPA was slightly higher at 23.5% (IQR 18.9–27, mean 22.7%, range 10.5–31.5). The Mann–Whitney U test again showed no statistically significant difference between the cohorts (U = 303, p = 0.66), with a negligible effect size (Cliff's delta = 0.08) and a minimal median shift of less than 1 percentage point (Hodges-Lehmann = +0.94), indicating that the distributions were highly overlapping and clinically similar. As a binary classifier for the presence of any mesenteric lesion, serosal CPA showed poor performance (ROC AUC = 0.54), reflecting discrimination that is only slightly better than chance. Although the Youden index identified 20.4% as an operating cut-off, with sensitivity = 0.7 and specificity = 0.5, indicating that primary serosal/subserosal CPA has only weak discriminative value for predicting mesenteric involvement. Within the mesenteric-lesion cohort, primary serosal/subserosal collagen showed a modest, non-significant positive trend with mesenteric-mass collagen (Pearson r = 0.24, p = 0.14; Spearman ρ = 0.29, p = 0.074).

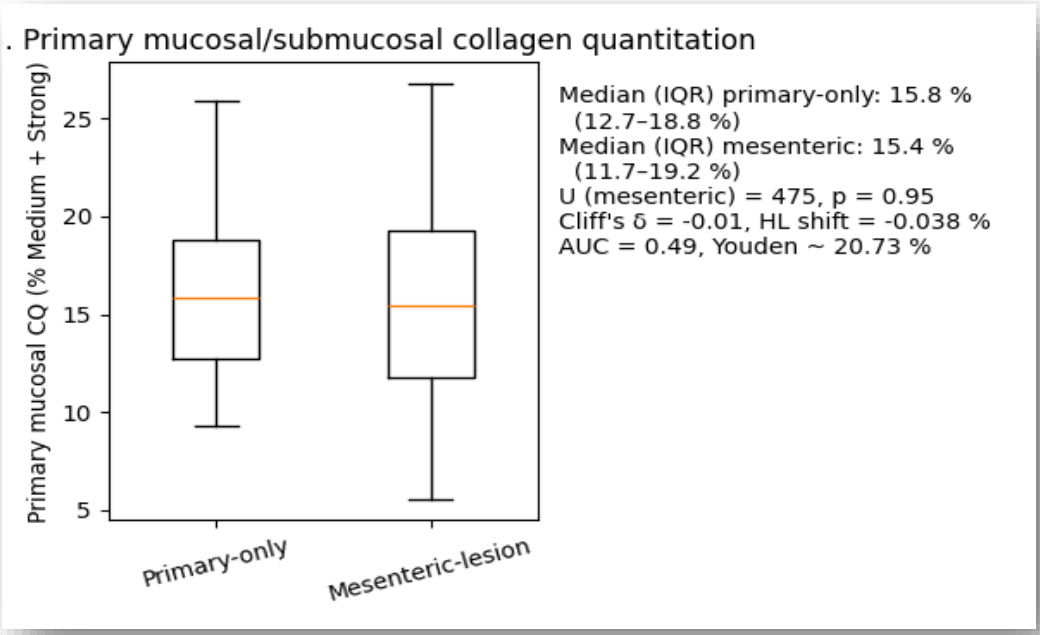

Figure 5. Primary-tumor PSR collagen proportionate area (CPA) by compartment (mucosal/submucosal and serosal/subserosal) in the primary-only vs mesenteric-lesion cohorts.

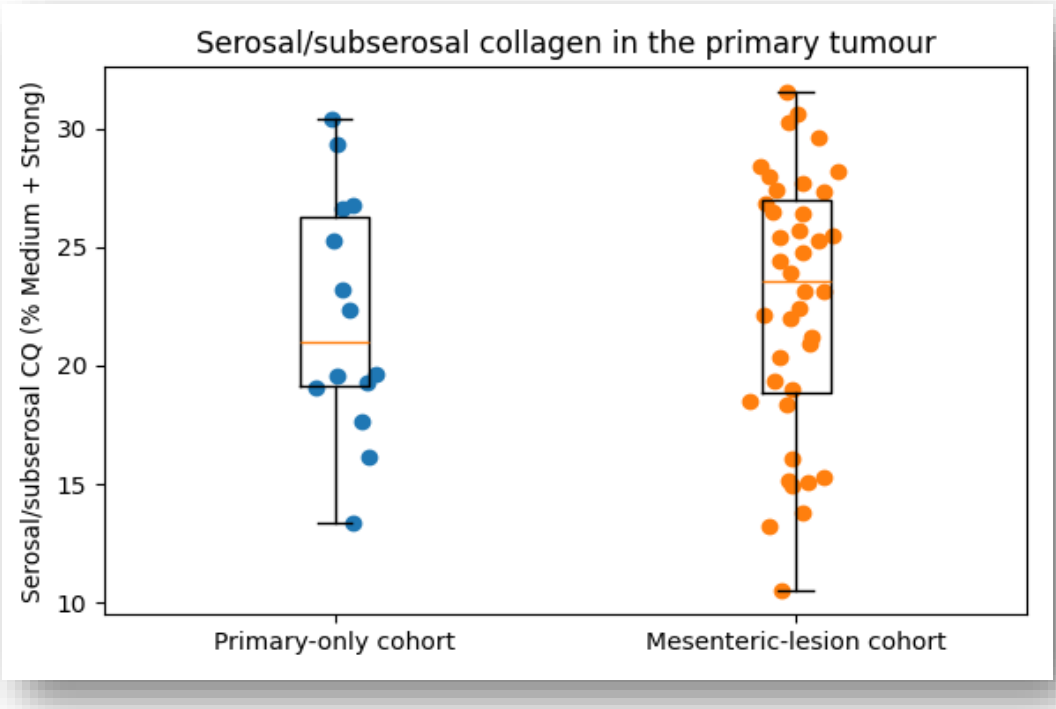

Figure 6. Primary-tumor serosal/subserosal collagen proportionate area (PSR-CPA) in the primary-only vs mesenteric-lesion cohorts.

3.3.6 Comparative ROC Performance of Primary-Tumor Predictors

When all primary-tumor features were compared as predictors of “any mesenteric lesion”, primary-tumor diameter clearly outperformed collagen metrics. Primary-tumor size yielded an ROC AUC of 0.66, whereas mucosa/submucosa CPA yielded an AUC of 0.49 and serosa/subserosa CPA yielded an AUC of 0.54.

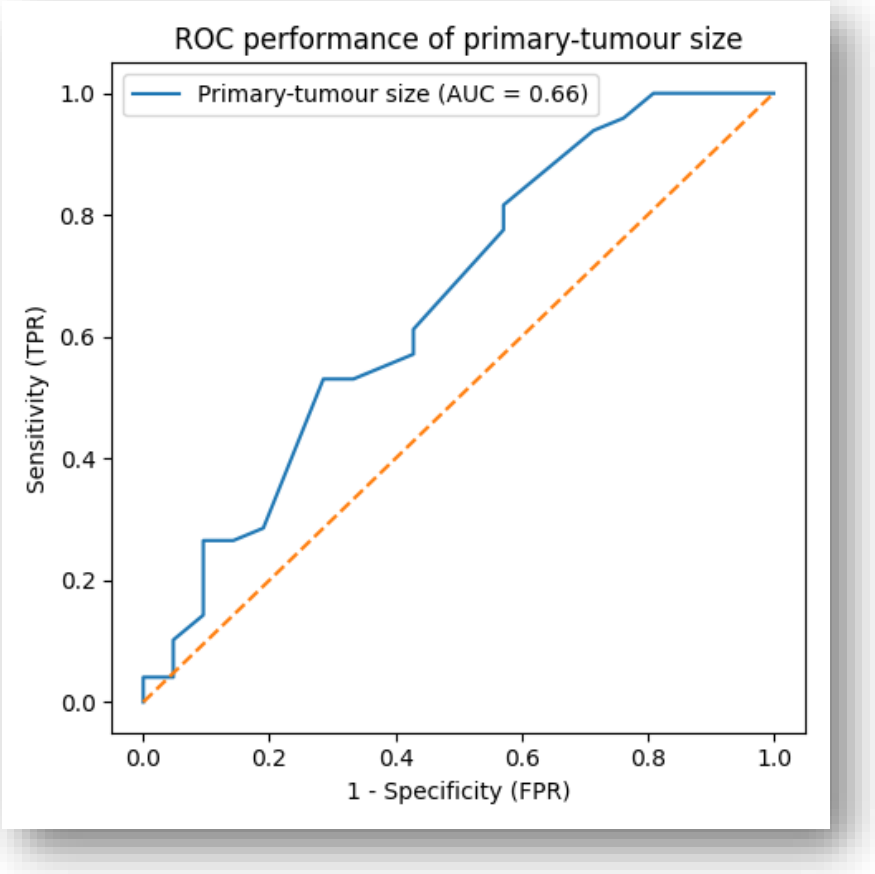

Figure 7. ROC performance of primary-tumor size and primary PSR-CPA (mucosal/submucosal and serosal/subserosal) for predicting any mesenteric lesion.

3.3.7 Summary of Binary Predictors of Mesenteric Involvement

In this binary analysis, patients with and without mesenteric lesions were similar in age, sex, and proliferative indices, but patients with mesenteric lesions had larger primary tumors (median 2 vs 1.5 cm; Mann-Whitney U = 676, p = 0.0378; Cliff's delta = 0.31; Hodges-Lehmann shift = +0.4 cm; ROC AUC = 0.66) and markedly higher frequencies of primary-

tumor vascular invasion (OR = 10.2; p = 0.0014) and perineural invasion (OR 8.5; p = 0.00042). By contrast, patient-level primary CPA metrics showed minimal or no discrimination for the presence of any mesenteric lesion. Taken together, these results indicate that primary-tumor size and the presence of vascular and perineural invasion are the most informative primary-tumor features for identifying patients with a mesenteric mass, whereas primary-tumor CPA is best interpreted as a descriptive stromal characteristic rather than a stand-alone classifier for mesenteric involvement.

Table 2. Binary analysis: primary-only versus any mesenteric lesion

Variable	Primary-only (n=21)	Mesenteric lesions (n=49)	Effect/ discrimination	p-value
Age, years	Median 73 (IQR 65-78)	Median 70 (IQR 59-75)	Mann-Whitney U=612.5	0.21
Male sex	13/21 (61.9%)	35/49 (71.4%)	-	-
Grade (G1/G2)	17/4 (81%/19%)	35/14 (71.4%/28.6%)	-	-
Multiplicity: unifocal	12/21 (57.1%)	23/49 (46.9%)	-	-
Multiplicity: 2-4 lesions	5/21 (23.8%)	17/49 (34.7%)	-	-
Multiplicity: ≥5 lesions	4/21 (19%)	9/49 (18.4%)	-	-
Necrosis present	1/21 (4.8%)	2/49 (4.1%)	-	-
Primary tumor size, cm	Median 1.5 (IQR 1.1-2)	Median 2 (IQR 1.5-2.5)	Cliff's delta=0.31; HL shift=+0.4 cm; ROC AUC=0.66	0.0378
Primary vascular invasion	12/20 (60%)	46/49 (93.9%)	OR=10.2	0.0014
Primary perineural invasion	4/20 (20%)	32/47 (68.1%)	OR=8.5	0.00042
Primary mucosa/submucosa CPA, %	Median 15.8 (IQR 12.7-18.8)	Median 15.4 (IQR 11.7-19.2)	U=475; ROC AUC=0.49; Youden ~20.7% (sens 0.17, spec 0.95)	0.95
Primary serosa/subserosa CPA, %	Median 21 (IQR 19.1-26.3)	Median 23.5 (IQR 18.9-27)	U=303; ROC AUC=0.54; Youden 20.4% (sens 0.70, spec 0.50)	0.66

Notes: Effect estimates and operating characteristics are reported where available. CPA refers to picrosirius-red collagen proportionate area.

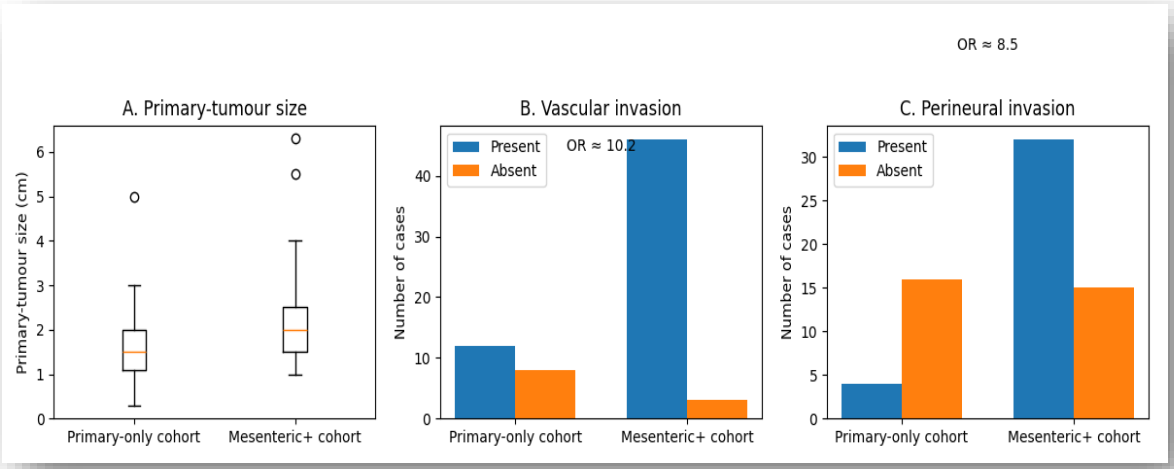

Figure 8. Summary of primary-tumor predictors of mesenteric involvement. (A) Primary-tumor size differs between the primary-only and mesenteric-lesion cohorts, with discrimination summarized by ROC AUC. (B) Vascular invasion is enriched among patients with mesenteric lesions. (C) Perineural invasion is similarly enriched, supporting primary size and vascular or perineural invasion as practical histologic risk markers for mesenteric disease.

3.4 Three-Phenotype and Lesion-Level Analyses: Distinguishing MTDs from Nodal Metastases

To extend the binary framework, three-way comparisons separated the mesenteric-lesion cohort into patients with MTDs and patients with nodal metastases only. Three mutually exclusive phenotypes were evaluated: (i) primary-only tumors without a mesenteric lesion, (ii) primary with MTDs, and (iii) primary with mesenteric nodal metastasis. The single case with both a mesenteric tumor deposit and a mesenteric nodal metastasis was included in descriptive summaries (Table 1) but excluded from three-group comparisons to preserve mutual exclusivity. Across-group p-values in this three-phenotype section are reported as exploratory. Mesenteric lesions were typed as MTDs vs nodal metastases on H&E using prespecified architecture-based criteria (Section 2.3.1).

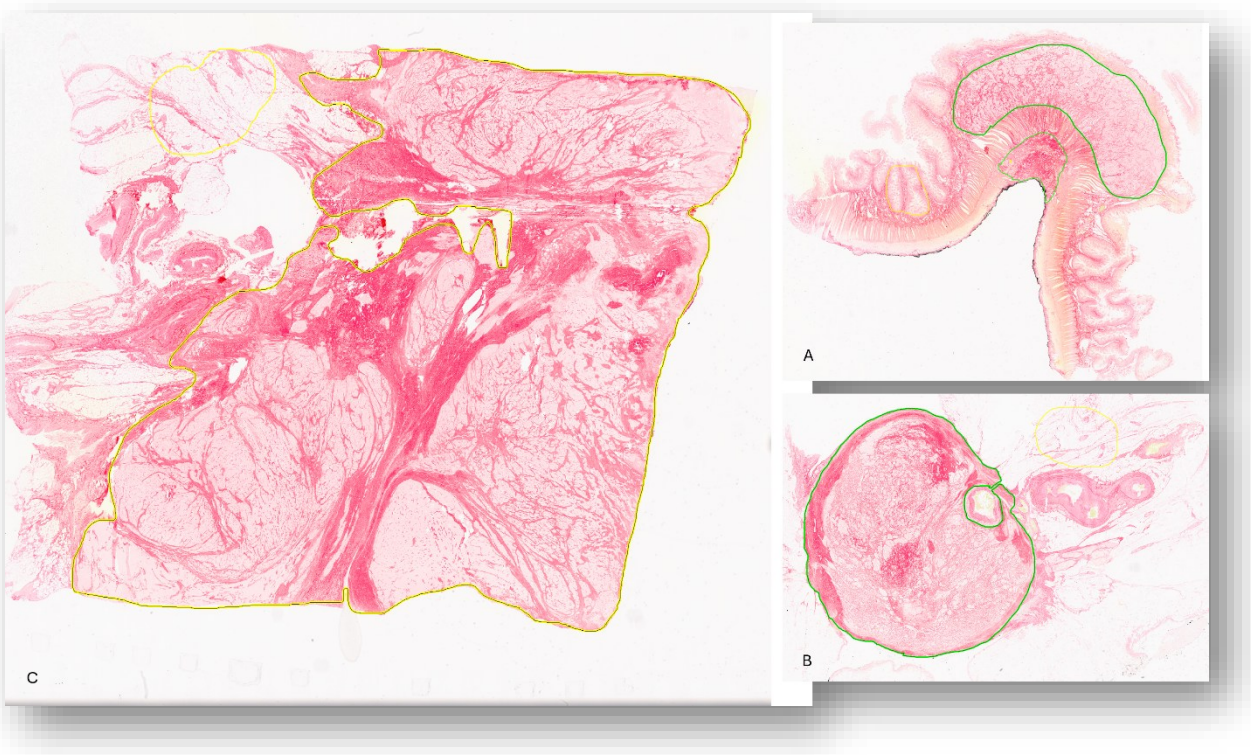

Figure 9. PSR-stained whole-slide images of a primary small-intestinal neuroendocrine tumor (SI-NET), a metastatic mesenteric lymph node, and a mesenteric tumor deposit (MTD). (A) Primary ileal SI-NET centered in the mucosa/submucosa with fibrotic stromal collagen along the mesenteric attachment. (B) Metastatic mesenteric lymph node with a rounded nodal mass and PSR-positive collagen. (C) Mesenteric tumor deposit with extensive fibrotic stroma forming a confluent collagenous plaque.

3.4.1 Baseline Clinicopathologic Profile Across Three Phenotypes

Age and primary-tumor Ki-67 were similar across groups (Kruskal-Wallis $p = 0.33$ and $p = 0.51$, respectively). In contrast, primary tumor size differed significantly across groups (Kruskal–Wallis $p = 0.018$), with the largest primaries observed in patients with mesenteric tumor deposits (median 2.0 cm, IQR 1.75–2.75), compared with the primary-only cohort (median 1.5 cm, IQR 1.08–2.0) and cases with mesenteric nodal metastases (median 1.7 cm, IQR 1.5–2.0).

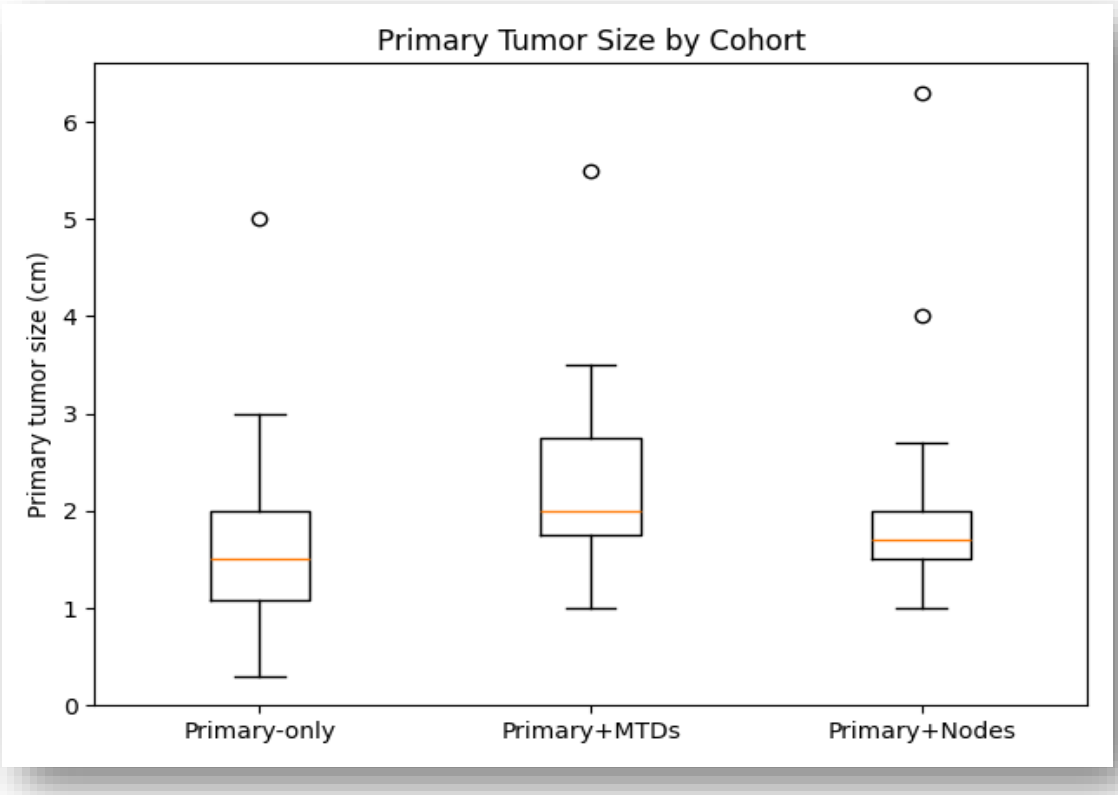

Figure 10. Primary tumor size (cm) across the three phenotypes (primary-only, primary with mesenteric tumor deposits, and primary with nodal metastases).

Multifocality did not differ significantly among cohorts (Kruskal-Wallis H = 0.765, p = 0.68); medians (IQR) were primary-only 1.0 (1.0–2.25), primary with MTDs 1.0 (1.0–3.0), and primary with nodes 2.0 (1.0–4.0). Metastatic lymph-node counts differed significantly across cohorts (Kruskal-Wallis H = 7.61, p = 0.022), highest in primary with nodes (median 4, IQR 2–6), intermediate in primary with MTDs (median 2, IQR 1–6), and lowest in primary-only (median 1, IQR 0–4.5).

3.4.2 Mesenteric Lesion Histology: Vascular and Perineural Invasion, and Vascular Remodeling

Vascular invasion was highly prevalent in both mesenteric phenotypes (primary with MTDs 17/19, 89.5% vs primary with nodes 28/29, 96.6%) with no statistically significant difference (Fisher's exact OR = 0.304, p = 0.554), indicating that transendothelial invasion is a shared, frequent feature rather than a discriminator between deposits and nodal disease. Perineural invasion within mesenteric lesions occurred frequently (primary with MTDs 15/19, 78.9% vs

primary with nodes 17/27, 63%) but did not reach statistical significance (OR 2.21, 95% CI 0.57–8.52; Fisher's p = 0.203), implying that PNI should be interpreted as a common mesenteric hallmark rather than a reliable differentiator of nodes vs MTDs. Mesenteric vessel-wall modification was more frequent in deposits than in nodal metastases (17/19, 89.5% vs 12/29, 41.4%), corresponding to an odds ratio of 12.04 (95% CI 2.33–62.14; Fisher's exact p = 0.000828). In the scored subset, vessel-wall modification showed a sensitivity of 0.895 and specificity of 0.586 for identifying an MTD; performance improved when combined with the CPA threshold derived from ROC analysis.

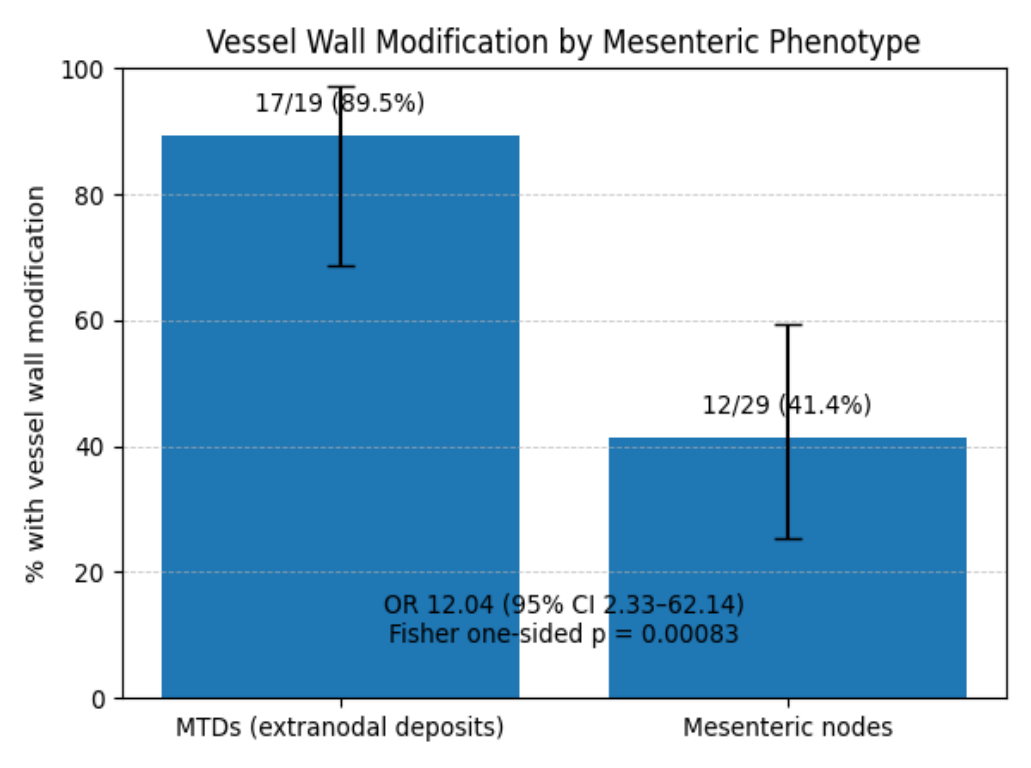

Figure 11. Vessel-wall modification at the mesenteric lesion interface in mesenteric tumor deposits vs nodal metastases.

Lesion size itself was not discriminative between deposits and nodes (both medians 3 cm; Mann–Whitney p = 0.374). Ki-67 within the mesenteric lesion trended higher for deposits (median 3%, IQR 0.75–4.30) than nodes (1%, 0.73–2.25), but this was not statistically significant (Mann–Whitney p = 0.213).

3.4.3 Primary-Tumor Collagen Burden Across Three Groups

Mucosal/submucosal CPA differed across the three phenotypes (Kruskal-Wallis H = 8.121, p = 0.017). Mucosal/submucosal collagen was highest in the primary with MTDs (median 18.4%, IQR 15.22–21.13) compared with primary-only (median 14.6%, IQR 11.06–19.14) and primary with nodal metastasis cohorts (median 15.8%, IQR 11.61–17.98).

Table 3. Primary-tumor collagen burden across three phenotypes

Metric	Primary-only (n=21)	Primary with MTDs (n=19)	Primary with nodes (n=29)	Across-group p-value
Mucosa/submucosa CPA, % (median, IQR)	14.6 (11.06-19.14)	18.4 (15.22-21.13)	15.8 (11.61-17.98)	0.017 (Kruskal-Wallis H=8.121)
Serosa/subserosa CPA, % (median, IQR)	22.4 (17.93-27.05)	25.4 (20.93-26.85)	22.5 (18.33-26.49)	0.666 (Kruskal-Wallis H=0.812)

Notes: Phenotypes are mutually exclusive; the single mixed-pattern case was excluded from the three-group comparisons. CPA (collagen proportionate area).

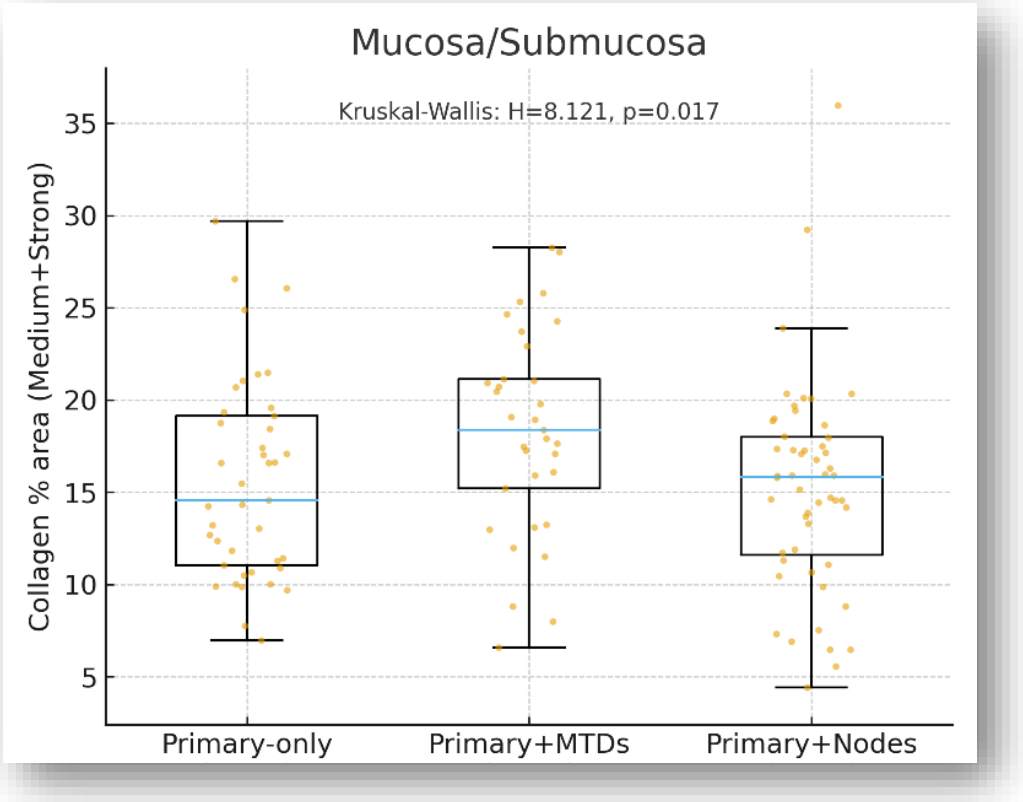

Figure 12. Primary-tumor mucosal/submucosal collagen burden (PSR-CPA) across the three phenotypes (primary-only, primary with mesenteric tumor deposits, and primary with nodal metastases).

By contrast, serosal/subserosal CPA showed similar distributions across phenotypes (Kruskal-Wallis H = 0.812, p = 0.666): primary-only, median 22.4% (IQR 17.93–27.05), primary with MTDs, median 25.4% (IQR 20.93–26.85), and primary with nodal metastasis, median 22.5% (IQR 18.33–26.49). Taken together, the non-significant Kruskal-Wallis result and the overlapping medians/IQRs indicate that serosal/subserosal collagen burden is broadly similar across the three cohorts.

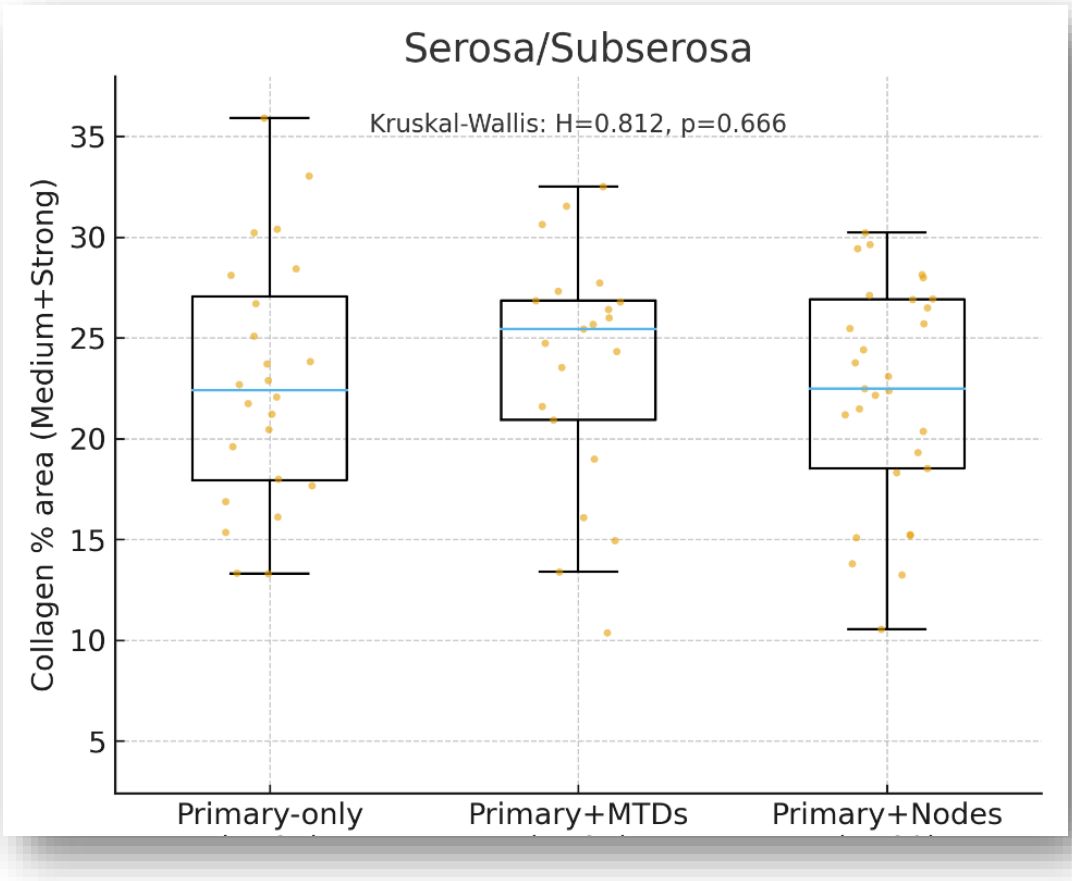

Figure 13. Primary-tumor serosal/subserosal collagen burden (PSR-CPA) across the three phenotypes (primary-only, primary with mesenteric tumor deposits, and primary with nodal metastases).

3.4.4 Lesion-Level Collagen and Diagnostic Performance for Deposit vs Node Typing

At the mesenteric-lesion level (deposits vs nodes), MTDs were more collagen-dense than nodal metastasis: median 21.1% (IQR 18.31–25.21) vs 15.7% (IQR 9.29–21.09), Mann-Whitney p = 0.00158.

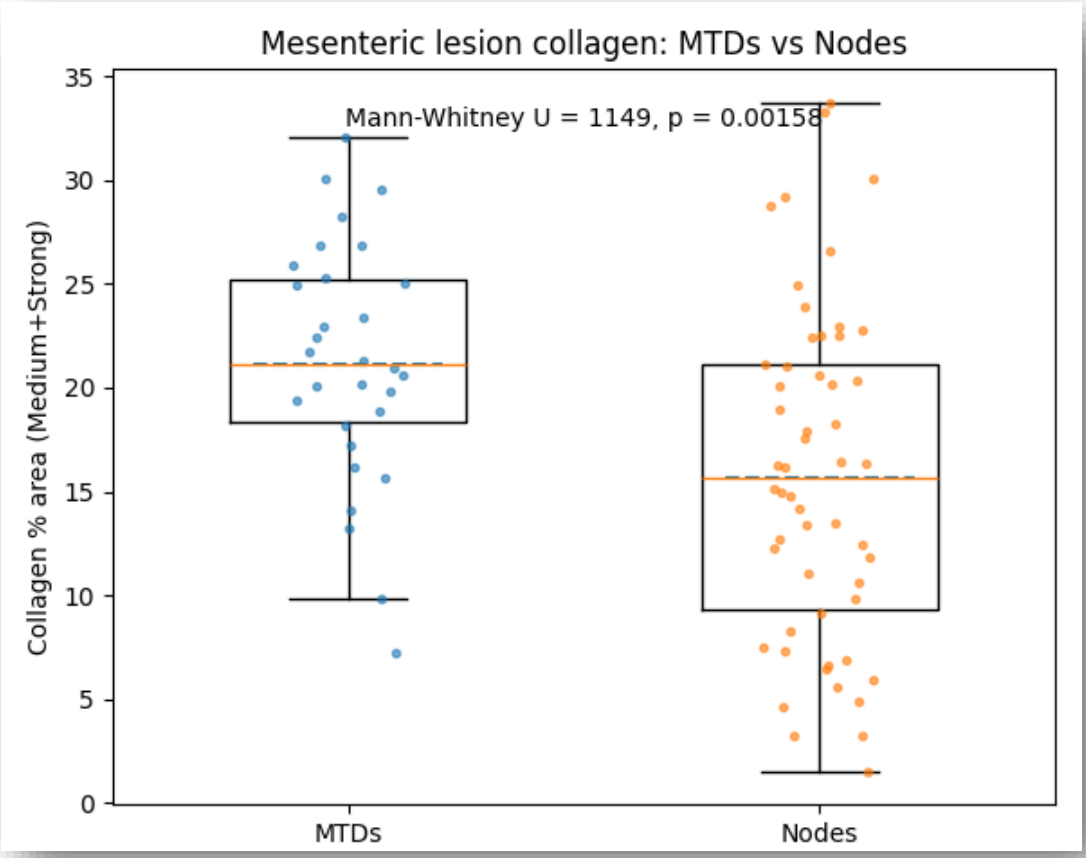

Figure 14. Lesion-level mesenteric collagen burden (PSR collagen proportionate area, CPA) in mesenteric tumor deposits vs nodal metastases.

Using PSR-CPA as a single predictor for deposit vs node typing, the ROC AUC was 0.709, indicating moderate discrimination, i.e., in ~71% of random deposit–node pairs, the deposit shows a higher collagen%, while operating sensitivity/specificity remains threshold-dependent. At the Youden-optimal 18% threshold, sensitivity was 0.77 and specificity 0.61, with PPV 0.52 and NPV 0.83.

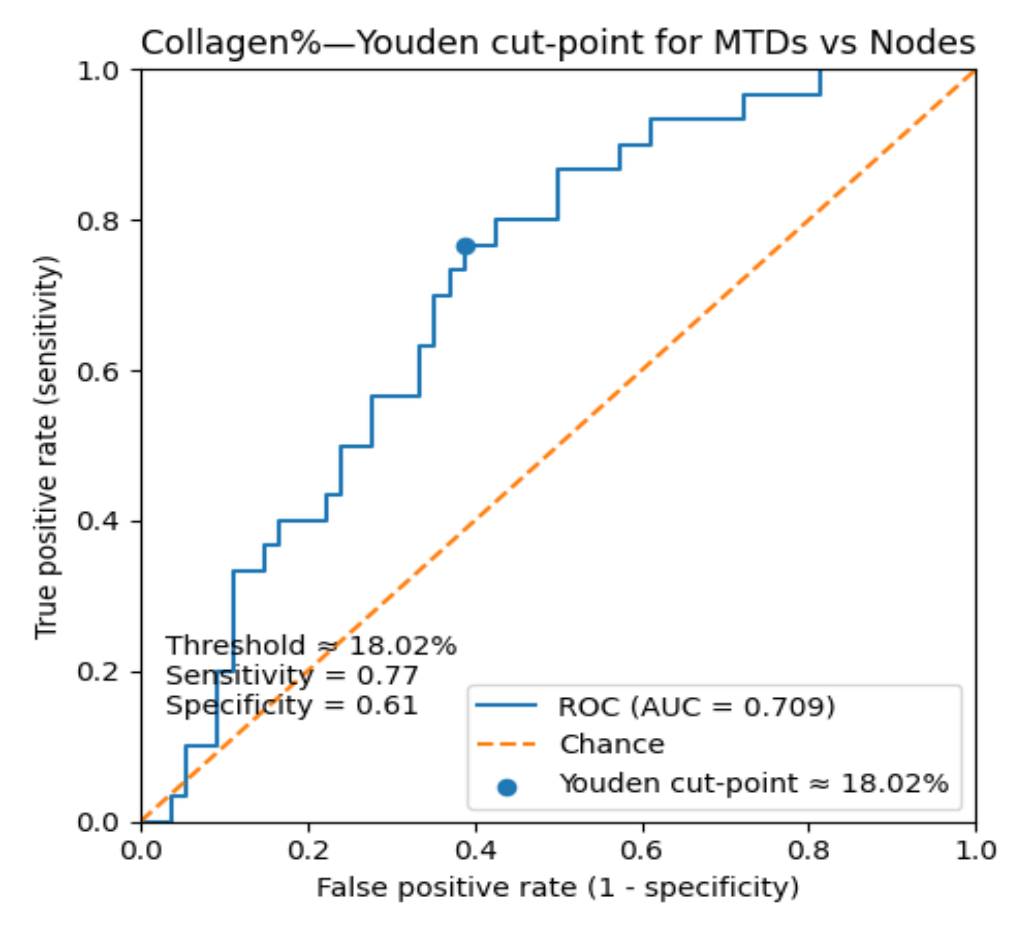

Figure 15. Receiver-operating-characteristic (ROC) curve for lesion-level PSR collagen proportionate area (CPA) in distinguishing mesenteric tumor deposits from nodal metastases.

3.4.5 Comparison of Collagen Thresholding and Vessel-Wall Modification as Practical Classifiers

Considered independently, both pathology-based indicators favoured a diagnosis of mesenteric tumor deposit (MTD) over nodal metastasis. Vessel-wall modification was markedly enriched around MTDs compared with nodes (17/19 (89.5%) vs 12/29 (41.4%)), yielding OR 12.04 (95% CI 2.33–62.14) with two-sided Fisher's p = 0.000828; operating characteristics were sensitivity 0.89, specificity 0.59, PPV 0.59, NPV 0.90, and Youden's J = 0.48. Across the mesenteric lesions (MTDs and nodes), a dichotomous collagen threshold of CPA ≥18% also discriminated MTDs from nodes, with OR 5.16 (95% CI 1.89–14.14) and two-sided Fisher's p = 0.000837; operating characteristics were sensitivity 0.77, specificity 0.61, PPV 0.52, NPV 0.83, and Youden's J = 0.378, consistent with moderate discrimination of CPA as a continuous measure (ROC AUC = 0.709). Overall, vessel wall modification was the stronger single

discriminator by Youden's J, and concordant positivity for CPA ≥18% plus vessel wall modification most strongly supports an MTD diagnosis over a nodal metastasis in this dataset.

Table 4. Lesion-level discrimination of mesenteric tumor deposits versus nodal metastases.

Marker	Effect/discrimination	Diagnostic performance
Lesion size	Not discriminatory (median 3 cm in both groups)	p = 0.374 (Mann–Whitney)
Lesion Ki-67, %	Trend higher in MTDs	p = 0.213 (Mann–Whitney)
Vascular invasion	OR = 0.304	p = 0.554 (Fisher's exact)
Perineural invasion	OR = 2.21 (95% CI 0.57–8.52)	p = 0.203 (Fisher's exact)
Lesion-level PSR-CPA, %	Higher in MTDs; ROC AUC = 0.709	p = 0.00158 (Mann–Whitney)
CPA ≥18% (exploratory cut-point)	OR = 5.16 (95% CI 1.89–14.14)	sens 0.77; spec 0.61; PPV 0.52; NPV 0.83; Fisher p = 0.000837
Vessel wall modification	OR = 12.04 (95% CI 2.33–62.14)	sens 0.895; spec 0.586; PPV 0.59; NPV 0.90; Fisher p = 0.000828

Abbreviations: MTD, mesenteric tumor deposit; PSR-CPA, picrosirius red collagen proportionate area; ROC AUC, receiver operating characteristic area under the curve; OR, odds ratio; PPV, positive predictive value; NPV, negative predictive value.

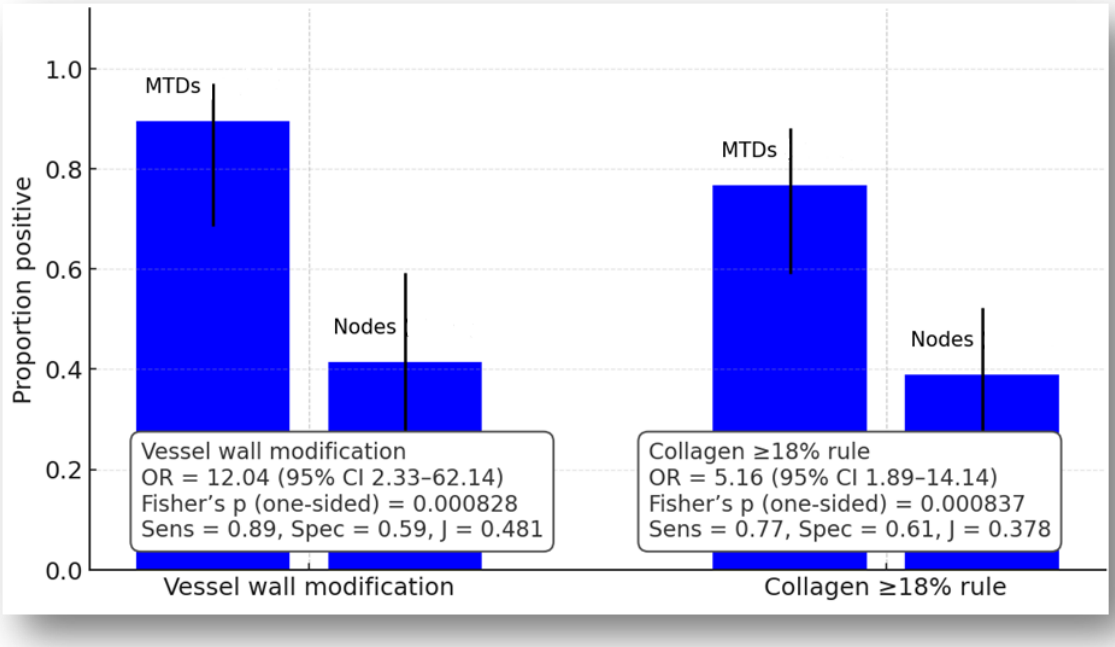

Figure 16. Comparison of vessel-wall modification and PSR-CPA thresholding (≥18%) for classifying mesenteric tumor deposits vs nodal metastases.

3.5 Summary of Key Pathology-Based Markers

In the binary comparison (primary-only vs any mesenteric lesion), primary-tumor size and the presence of vascular and/or perineural invasion were the main pathology-based markers associated with mesenteric involvement, whereas primary-tumor PSR-CPA showed minimal discrimination. In the exploratory three-phenotype summaries (primary-only vs MTD vs nodal metastasis), the MTD phenotype was characterized by larger primary-tumor size and higher primary mucosa/submucosa PSR-CPA relative to the other phenotypes. At the lesion level, two interface-focused features most consistently supported classification as MTD rather than nodal metastasis: vessel-wall modification adjacent to the lesion and higher lesion-level collagen burden, with an exploratory PSR-CPA threshold of at least 18 percent; concordant positivity for both features provided the strongest support for MTD classification in this dataset.

Chapter 4: Discussion

Mesenteric fibrosis is a desmoplastic stromal reaction around mesenteric metastases, including tumor deposits and/or involved lymph nodes, and is among the most clinically consequential complications of SI-NETs, contributing to symptoms, operative complexity, and long-term morbidity [8]. In large cohorts, extensive abdominal fibrosis has been associated with advanced metastatic patterns and has required palliative interventions such as superior mesenteric vein stenting, resection of mesenteric root metastases, nephrostomy or ureteric stents for obstructive uropathy, and repeated abdominal operations [217]. These complications contribute to emergency presentations and poorer outcomes compared with elective surgery, highlighting the stakes of timely recognition and risk stratification. Reported prevalence varies by definition and cohort, but clinically relevant mesenteric fibrosis occurs in a substantial fraction of patients with mesenteric disease and is strongly associated with hormonally functional tumors and elevated serotonin output [182,218]. Because SI-NETs are often indolent yet widely metastatic at diagnosis, MF can progress over years, driving morbidity and repeated hospitalizations even when tumor burden is stable. In most (approximately 80%) SI-NETs, mesenteric lymph-node metastases are present at diagnosis, and up to half show a prominent desmoplastic stromal response. In the mesentery, these tumors give rise to both nodal metastases and separate irregular mesenteric tumor deposits tracking along branches of the superior mesenteric vessels, and it is this mesenteric disease, rather than the usually small primary, that often drives symptoms, operative complexity, and long-term morbidity [2,3]. MTDs are increasingly recognized as a distinct pathologic entity and may carry prognostic information beyond traditional nodal staging, yet they remain variably reported and inconsistently incorporated into staging systems. Contemporary pathology studies suggest that the number of mesenteric tumor deposits, rather than their maximum size alone, may better stratify outcome in small-intestinal well-differentiated NETs [106]. Radiologic staging still commonly categorizes these lesions collectively as “mesenteric lymph nodes,” but this simplification can obscure differences in morphology, stromal composition, and vessel involvement that may matter for surgical planning and prognostication [98]. Pathology literature defines nodal metastases by the presence of residual nodal architecture, such as a capsule, subcapsular sinus, and peripheral lymphoid tissue, thereby distinguishing them from conventional lymph-node metastases [96]. By contrast, MTDs are discrete mesenteric soft-tissue nodules lacking convincing nodal architecture, often with irregular or angulated contours, prominent desmoplastic fibrosis, thick-walled vessels, and entrapped nerves, consistent with contemporary descriptions in SI-NETs

[8,10,15,99]. Clinically, mesenteric involvement is a major driver of mechanical complications in SI-NETs. Central mesenteric fibrosis may encase the superior mesenteric vessels and their branches, compromising perfusion and predisposing to ischemic strictures, chronic abdominal pain, and catastrophic bowel necrosis in severe cases [219]. Retroperitoneal extension can cause ureteric obstruction and hydronephrosis, sometimes requiring nephrostomy or ureteric stents [217]. Beyond obstruction and vascular events, mesenteric mass effect and fibrosis can drive abdominal desmoplastic tethering, kinking, and adhesions that complicate resection and increase the risk of short-bowel syndrome when extensive bowel sacrifice is necessary. These complications may persist or progress even when systemic therapy achieves tumor stabilization, underscoring the importance of identifying patients at risk for aggressive mesenteric disease and fibrosis. A central challenge is that CT/MRI often show a single mesenteric mass with radiating strands, calcification, or spiculated margins, but may not reliably distinguish MTDs from nodal metastases or quantify stromal fibrosis, and histologic fibrosis can be present even when CT appears negative [220]. Cross-sectional imaging can demonstrate mesenteric disease but may not reliably distinguish mesenteric tumor deposits from nodal metastases; definitive classification remains histologic, where nodal metastases retain residual nodal architecture, whereas tumor deposits lack nodal architecture [26,96,106]. CT tends to underestimate microscopic fibrosis and may misclassify lesions, contributing to under-recognition of clinically significant MF. This diagnostic gap motivates pathology-led approaches that directly quantify collagen burden and capture vessel-related changes at the lesion interface, providing a more granular stromal phenotype to link with imaging and clinical outcomes. In this single-center, pathology-led study of 70 resected small-intestinal neuroendocrine tumors (SI-NETs), we assessed primary-tumor predictors of any mesenteric involvement, grouping nodal metastases and mesenteric tumor deposits (MTDs) together as “any mesenteric lesion” to reflect the clinical reality that either pattern signals a more advanced disease phenotype. The key findings were that primary tumor size and the presence of vascular and perineural invasion were strongly associated with mesenteric involvement, whereas digitally quantified primary-tumor collagen burden showed more nuanced associations that did not translate into strong predictive performance. Specifically, mucosal/submucosal collagen proportionate area (CPA) was higher in the mesenteric-lesion cohort, but serosal/subserosal CPA was not meaningfully different between groups, and collagen metrics overall showed modest discrimination compared with tumor size and neurovascular invasion. These data align with the broader SI-NET literature, suggesting that mesenteric disease is driven by patterns of spread along lymphovascular and neurovascular routes, and that stromal reactions, although

biologically central to mesenteric fibrosis, do not necessarily manifest as simple, linearly predictive collagen burden within the primary bowel wall [218,221,222]. In addition, the findings are compatible with contemporary pathology frameworks that increasingly distinguish deposits from nodes and emphasize that deposit number rather than size may carry prognostic information [105,106,223,224]. Our binary endpoint was intentionally pragmatic, but the observed associations with vascular and perineural invasion provide a biologically coherent substrate for future models that stratify mesenteric disease more finely and integrate imaging and biomarker correlates [11,99,163,225]. The clinical stakes remain high because mesenteric fibrosis contributes to obstruction, ischemia, emergency surgery, and poorer outcomes, and these complications can occur even in indolent tumors with stable systemic disease [182,219,226–228]. In this context, a pathology-led focus on readily reportable primary-tumor predictors, combined with objective stromal quantification when feasible, may help identify patients at higher risk of mesenteric involvement and guide more deliberate surveillance and multidisciplinary planning [8,15]. Biologically, the strong association between mesenteric involvement and vascular and perineural invasion supports a model in which early extramural invasion along vessels and nerves facilitates dissemination to the mesenteric root and perivascular soft tissue. In SI-NETs, tumor cells infiltrate the submucosa and muscularis propria, where they interface with a dense neurovascular plexus, and invasion into these compartments may serve as a proximate histologic correlate of mesenteric spread. The findings also align with descriptions of MTDs as vessel-adjacent, nerve-entrapping lesions with prominent desmoplastic stroma, suggesting that neurovascular invasion in the primary bowel wall may relate mechanistically to deposit formation and subsequent stromal activation. While collagen burden is central to mesenteric fibrosis, our results indicate that collagen quantification within the primary tumor alone is not sufficient to predict mesenteric involvement with high accuracy, and that stromal metrics likely need to be interpreted within a broader biological and clinical context. These observations support integrated risk frameworks that incorporate tumor size, invasion patterns, and stromal features together with imaging and biomarker variables to improve stratification and clinical translation. Strengths of this work include standardized pathology re-review, integration of conventional predictors with digitally quantified collagen, and reporting of effect sizes and ROC analyses to contextualize associations. Limitations include the single-centre retrospective design and the absence of time-to-event outcomes such as progression-free survival or MF-related complications. These limitations highlight the need for larger, multicenter cohorts and prospective datasets that can link pathology-derived risk features to clinically meaningful endpoints and complications.

From a practical pathology perspective, our findings support careful and consistent reporting of primary tumor size and active assessment of vascular and perineural invasion in SI-NETs, given their strong association with mesenteric involvement. Maximum tumor diameter should be measured carefully and documented consistently, and the presence of vascular and perineural invasion should be actively sought and reported as readily interpretable histologic variables. While primary collagen quantification may add biologic nuance, our data suggest that collagen burden alone is not a dominant predictor of mesenteric spread and should be interpreted in the context of other variables. Future pathology-led risk stratification models could incorporate tumor size, invasion patterns, and stromal features together with radiologic correlates to identify patients at risk for clinically significant mesenteric disease and fibrosis. Future studies should validate the association of tumor size and vascular/perineural invasion across institutions and assess whether these features predict MF-related outcomes such as obstruction, ischemia, re-intervention, or bowel length preserved. Combining pathology ground truth with radiologic variables, including mesenteric mass morphology and radiomics-derived stromal signatures, may improve prediction and help connect invasion patterns with imaging phenotypes. Beyond collagen burden, expanded stromal profiling using proteomic or transcriptomic readouts could better capture fibrotic biology, and mechanistic models of the mesenteric niche may clarify how neurovascular invasion relates to deposit formation and stromal activation, including the potential influence of serotonin-targeted or antifibrotic approaches. In this study, we also analyzed lesion-level discrimination between mesenteric tumor deposits (MTDs) and nodal metastases using digitally quantified collagen burden and a qualitative assessment of vessel-wall modification (VWM) at the lesion interface. Across the mesenteric lesions, deposits showed higher picrosirius red collagen proportionate area (CPA) and were strongly enriched for VWM compared with nodal metastases, whereas lesion size alone did not reliably separate these entities. These findings support the concept that MTDs represent a stromally active, vessel-adjacent metastatic phenotype that is distinct from nodal metastasis and that pathology-led stromal quantification can add objective information beyond morphology alone [10,15,96,98,229]. In challenging cases, combining collagen quantitation with VWM may provide practical support for classification, aligning with contemporary descriptions of deposits as irregular, desmoplastic, neurovascular bundle-associated lesions that lack convincing nodal architecture and frequently entrap thick-walled vessels and nerves [99,106]. From a clinical standpoint, the improved distinction between deposits and nodes is important because deposits may carry prognostic information not captured by traditional nodal staging and may reflect patterns of spread and stromal interaction that are relevant to surgical

planning and the risk of mesenteric complications. The results also align with the broader SI-NET literature, indicating that mesenteric fibrosis and vessel encasement are significant drivers of obstruction, ischemia, operative complexity, and the need for re-intervention, even in tumors with indolent systemic trajectories [182,217,219]. At the same time, the data emphasize that routine cross-sectional imaging can underestimate microscopic fibrosis and may not reliably distinguish between deposits and nodal histology, which strengthens the case for pathology-led ground truth and for integrated imaging-pathology efforts, including radiomics approaches that attempt to capture stromal phenotypes non-invasively [123,220]. Future work should test reproducibility across observers and platforms, define robust operational criteria for VWM and perilesional vessel selection, and evaluate whether stromal and vascular signatures in deposits predict clinically meaningful outcomes such as obstruction-free survival, ischemia events, need for vascular intervention, preserved bowel length, and overall survival. Mesenteric fibrosis in small-intestinal neuroendocrine tumors has evolved from a poorly defined “desmoplastic reaction” to a recognisable stromal disease process with its own biology, imaging phenotype, and emerging biomarkers. Clinically, the available evidence supports a few practical points. MF is common rather than exceptional in advanced SI-NET, especially when imaging, surgical, and histologic data are combined. From a research perspective, MF can be treated as a stromal disease process that may be staged and monitored, although no antifibrotic treatment is currently proven. Over the next decade, multidimensional approaches that combine stromal biology, radiomics, and circulating markers may enable earlier diagnosis, risk stratification, and intervention to reduce the risk of MF progression and its downstream morbidity. The last five years have moved mesenteric fibrosis from a vague complication of SI-NETs toward a definable stromal disease with its own biology, imaging signatures, and candidate biomarkers. Yet almost all available data are retrospective, MF is rarely a primary endpoint, and no antifibrotic therapy is proven. The heterogeneity of MF definitions, endpoints, and analytical approaches across studies limits the quantitative pooling, so our conclusions are based on a qualitative synthesis rather than a meta-analysis. Most MF evidence derives from single-center retrospective cohorts, which carry a high risk of selection bias and incomplete confounder adjustment; therefore, effect estimates should be interpreted cautiously. Recent work on stromal proteomics, radiomics, and circulating transcripts sets the stage for a more mechanistic, fibrosis-focused research agenda. Deep phenotyping of the mesenteric tumor–stroma niche is a key priority. Future work should validate these pathology-led stromal and vascular markers in multicenter cohorts, link them to clinically meaningful MF endpoints (obstruction, ischemia, re-intervention, and bowel length preserved), and integrate pathology ground truth with

CT/MRI-derived radiomics and circulating transcript signatures to develop deployable risk models. Mechanistic studies and 3D co-culture systems that model the mesenteric niche could then be used to test candidate antifibrotic strategies targeting serotonin-linked pathways and core profibrotic signalling such as TGF-β and CTGF.

Conclusion

This study strengthened pathology-led risk profiling of mesenteric involvement in well-differentiated SI-NETs by integrating standardized histologic reassessment with whole-slide PSR collagen quantification and interface-focused vessel-wall modification scoring, applying these tools to compare primary-only vs mesenteric disease cases, characterize three phenotypes (primary-only, MTD, nodal), distinguish MTDs from nodes at the lesion level, and explore within-case primary–mesenteric collagen correlations. In a curated single-center resection cohort (2010–2024), a patient-level binary framework comparing patients with primary-only SI-NETs (no mesenteric metastasis) versus patients with SI-NETs showing any mesenteric metastasis (node or MTD) and a lesion-level framework (MTDs vs mesenteric nodal metastases) were applied to align practical diagnostic questions with measurable pathology outputs. At the patient level, the strongest and most pragmatic predictors of mesenteric involvement were conventional primary-tumor features. Compared with primary-only cases, patients with any mesenteric lesion had larger primary tumors (median 2.0 vs 1.5 cm; $p = 0.0378$; ROC AUC = 0.66) and markedly higher frequencies of primary vascular invasion (OR = 10.2; $p = 0.0014$) and perineural invasion (OR = 8.5; $p = 0.00042$). In contrast, compartment-specific primary-tumor collagen proportionate area (CPA) showed minimal discrimination for mesenteric involvement, supporting its interpretation as a descriptive stromal characteristic rather than a stand-alone classifier of mesenteric spread in this dataset. At the lesion level, two complementary pathology-based markers consistently supported discrimination of MTDs from nodal metastases. First, VWM at the lesion interface was strongly enriched in MTDs (17/19, 89.5%) compared with nodal metastases (12/29, 41.4%), corresponding to an OR of 12.04 ($p = 0.000828$) with sensitivity 0.895 and specificity 0.586. Second, mesenteric-lesion collagen burden was higher in MTDs than in nodes (median CPA 21.1% vs 15.7%; $p = 0.00158$; ROC AUC = 0.709), and an exploratory Youden-derived CPA threshold of at least 18% provided sensitivity 0.77 and specificity 0.61. Concordant positivity for CPA at least 18% together with VWM provided the strongest practical evidence favoring an MTD diagnosis, complementing (rather than replacing) the morphologic reference standard based on residual nodal architecture. Taken together, our data suggest two practical points. First, larger primary-tumor size and the presence of vascular and/or perineural invasion were associated with mesenteric involvement in this cohort. Second, among mesenteric lesions, vessel-wall modification and higher PSR-CPA tended to favour tumor deposits over nodal metastases, and using both features alongside morphology may help in difficult cases. Because this is a single-center retrospective series with

no formal inter-rater analysis, the operating characteristics and the 18% CPA threshold should be considered exploratory and need external validation. Future work should test these markers in multicentre cohorts, link them to clinically meaningful mesenteric endpoints (obstruction, ischemia, re-intervention, bowel length preserved), and integrate pathology ground truth with cross-sectional imaging, radiomics, and circulating biomarkers to support risk stratification of mesenteric disease in SI-NETs.

References

1. Mete O, Wenig BM. Update from the 5th edition of the world health organization classification of head and neck tumors: overview of the 2022 WHO classification of head and neck neuroendocrine neoplasms. Head and neck pathology. 2022 Mar;16(1):123-42.
2. Lamarca A, Bartsch DK, Caplin M, Kos-Kudla B, Kjaer A, Partelli S, Rinke A, Janson ET, Thirlwell C, van Velthuysen ML, Vullierme MP. European Neuroendocrine Tumor Society (ENETS) 2024 guidance paper for the management of well-differentiated small intestine neuroendocrine tumors. Journal of neuroendocrinology. 2024 Sep;36(9):e13423.
3. Pavel M, Öberg K, Falconi M, Krenning EP, Sundin A, Perren A, Berruti A, ESMO Guidelines Committee. Gastroenteropancreatic neuroendocrine neoplasms: ESMO Clinical Practice Guidelines for diagnosis, treatment and follow-up. Annals of Oncology. 2020 Jul 1;31(7):844-60.
4. Dasari A, Wallace K, Halperin DM, Maxwell J, Kunz P, Singh S, Chasen B, Yao JC. Epidemiology of Neuroendocrine Neoplasms in the US. JAMA Network Open. 2025 Jun 2;8(6):e2515798-.
5. White BE, Rous B, Chandrakumaran K, Wong K, Bouvier C, Van Hemelrijck M, George G, Russell B, Srirajaskanthan R, Ramage JK. Incidence and survival of neuroendocrine neoplasia in England 1995–2018: a retrospective, population-based study. The Lancet Regional Health–Europe. 2022 Dec 1;23.
6. Yang J, Kim MK. What every gastroenterologist should know about gastrointestinal NETs. Official journal of the American College of Gastroenterology| ACG. 2023 Apr 1;118(4):606-9.
7. Zhang XB, Fan YB, Jing R, Getu MA, Chen WY, Zhang W, Dong HX, Dakal TC, Hayat A, Cai HJ, Ashrafizadeh M. Gastroenteropancreatic neuroendocrine neoplasms: current development, challenges, and clinical perspectives. Military Medical Research. 2024 Jun 4;11(1):35.
8. Graf SD, Keber CU, Hattesohl A, Teply-Szymanski J, Hattesohl S, Guder M, Gercke N, Di Fazio P, Slater EP, Jesinghaus M, Denkert C. Mesenteric fibrosis in patients with small intestinal neuroendocrine tumors is associated with enrichment of alpha-smooth muscle actin-positive fibrosis and COMP-expressing stromal cells. Journal of Neuroendocrinology. 2024 Feb;36(2):e13364.

9. Spyroglou A, Violetis O, Iliakopoulos K, Vezakis A, Alexandraki K. Mesenteric Fibrosis in Neuroendocrine Neoplasms: A Systematic Review of New Thoughts on Causation and Potential Treatments. Current Oncology Reports. 2025 Apr 11:1-4.
10. L'huillier R, Poncet G, Pasquer A, Walter T, Lombard-Bohas C, Hervieu V, Cayot B, Valette PJ, Cheung H, Milot L. Surgical planning of small intestine neuroendocrine tumors: the concept of mesenteric tumor deposits. Endocrine Oncology. 2025 Jan 1;5(1).
11. Butz F, Supper L, Reinhard L, Dukaczewska A, Jann H, Fehrenbach U, Müller-Debus CF, Skachko T, Pratschke J, Goretzki PE, Mogl MT. Emergency surgery influences oncological outcome in small intestinal neuroendocrine tumors. Scandinavian Journal of Surgery. 2024 Dec;113(4):303-13.
12. Yogo A, Paciorek A, Kasai Y, Moon F, Hirose K, Corvera CU, Bergsland EK, Nakakura EK. Long-term survival outcomes after minimally invasive surgery for ileal neuroendocrine tumors. Annals of Surgical Oncology. 2024 Sep;31(9):5507-14.
13. Al Mansour L, De Mestier L, Haissaguerre M, Afchain P, Hadoux J, Lecomte T, Morland D, Cottereau AS, De Rycke O, Tlili G, Tordo J. Outcome on mesenteric mass response of small-intestinal neuroendocrine tumors treated by 177Lu-DOTATATE peptide receptor radionuclide therapy: the MesenLuth study, a national study from the French Group of Endocrine Tumors and Endocan-RENATEN Network. Journal of Nuclear Medicine. 2024 Feb 1;65(2):258-63.
14. Uhlig J, Nie J, Gibson J, Cecchini M, Stein S, Lacy J, Kunz P, Kim HS. Epidemiology, treatment and outcomes of gastroenteropancreatic neuroendocrine neoplasms. Scientific Reports. 2024 Dec 17;14(1):30536.
15. Blažević A, Iyer AM, Van Velthuysen ML, Hofland J, Franssen GJ, Feelders RA, Zajec M, Luider TM, de Herder WW, Hofland LJ. Proteomic analysis of small intestinal neuroendocrine tumors and mesenteric fibrosis. Endocrine-Related Cancer. 2023 Jun 1;30(6).
16. Sedlack AJ, Varghese DG, Naimian A, Yazdian Anari P, Bodei L, Hallet J, Riechelmann RP, Halfdanarson T, Capdevilla J, Del Rivero J. Update in the management of gastroenteropancreatic neuroendocrine tumors. Cancer. 2024 Sep 15;130(18):3090-105.
17. Huang J, Chan SC, Fung YC, Mak FY, Lok V, Zhang L, Lin X, Lucero-Prisno III DE, Xu W, Zheng ZJ, Elcarte E. Incidence, risk factors, and temporal trends of small

intestinal cancer: A global analysis of cancer registries. Gastroenterology. 2023 Sep 1;165(3):600-12.

18. Schafrat PJ, van Erning FN, Zwinderman K, Dekker E, Sarasqueta AF, de Vos-Geelen J, Bouwense SA, Goedegebuure RS, Vermeulen L, de Hingh IH, Sommeijer DW. Malignancies of the small intestine: incidence and trends in a nationwide registry. Cancer Epidemiology. 2025 Dec 1;99:102943.
19. Mousavi SE, Ilaghi M, Mahdavizadeh V, Ebrahimi R, Aslani A, Yekta Z, Nejadghaderi SA. A population-based study on incidence trends of small intestine cancer in the United States from 2000 to 2020. Plos one. 2024 Aug 19;19(8):e0307019.
20. Wu P, He D, Chang H, Zhang X. Epidemiologic trends of and factors associated with overall survival in patients with neuroendocrine tumors over the last two decades in the USA. Endocrine Connections. 2023 Dec 1;12(12).
21. Folkestad O, Hauso Ø, Mjønes P, Fougner R, Wasmuth HH, Fossmark R. Survival trends in patients with small intestinal neuroendocrine tumors—a cohort study in Central Norway. Cancers. 2023 Jun 21;15(13):3272.
22. Søreide K, Stättner S, Hallet J. Surgery as a principle and technical consideration for primary tumor resection of small bowel neuroendocrine tumors. Annals of Surgical Oncology. 2024 Feb;31(2):1125-37.
23. Mulders MC, Audhoe AS, Van Koetsveld PM, Feelders RA, Hofland LJ, De Herder WW, Kraaij R, Hofland J. Midgut neuroendocrine tumor patients have a depleted gut microbiome with a discriminative signature. European Journal of Cancer. 2024 Jan 1;197:113472.
24. Snorradottir S, Asgeirsdottir A, Rögnvaldsson S, Jonasson JG, Björnsson ES. Incidence and prognosis of patients with small intestinal neuroendocrine tumors in a population based nationwide study. Cancer Epidemiology. 2022 Aug 1;79:102197.
25. National Cancer Institute (2025). *Cancer Stat Facts: Small intestine cancer* (SEER Program). Available at: https://seer.cancer.gov/statfacts/html/smint.html (Accessed 23 October 2025).
26. Navin PJ, Ehman EC, Liu JB, Halfdanarson TR, Gupta A, Laghi A, Yoo DC, Carucci LR, Schima W, Sheedy SP. Imaging of small-bowel neuroendocrine neoplasms: AJR expert panel narrative review. American Journal of Roentgenology. 2023 Sep 7;221(3):289-301.
27. Kupietzky A, Dover R, Mazeh H. Surgical aspects of small intestinal neuroendocrine tumors. World Journal of Gastrointestinal Surgery. 2023 Apr 27;15(4):566.

28. Clift AK, Mahon H, Khan G, Boardman-Pretty F, Worker A, Marchini E, Buendia O, Fish P, Khan MS. Identifying patients with undiagnosed small intestinal neuroendocrine tumors in primary care using statistical and machine learning: model development and validation study. British Journal of Cancer. 2024 Jul 22;131(2):305-11.
29. Mulders MC, de Herder WW, Hofland J. What is carcinoid syndrome? A critical appraisal of its proposed mediators. Endocrine Reviews. 2024 May 7;45(3):351-60.
30. Mano Geran S, Krishnasamy Naido SN, Hline AT. Contemporary Management of Severe Carcinoid Heart Disease. Case Reports. 2025 Mar 19;30(6_Part_2):102989.
31. Algeri L, Falkman L, Spada F, Frassoni S, Bagnardi V, Boselli S, Cardinale D, Zanobini M, Crona J, Benini L, Tamayo D. Carcinoid heart disease in patients with advanced small-intestinal neuroendocrine tumors and carcinoid syndrome: a retrospective experience from two European referral centers. ESMO open. 2024 Nov 1;9(11):103959.
32. Baron T, Bergsten J, Albåge A, Lundin L, Sörensen J, Öberg K, Flachskampf FA. Cardiac imaging in carcinoid heart disease. Cardiovascular Imaging. 2021 Nov 1;14(11):2240-53.
33. Mattig I, Franke MR, Pschowski R, Brand A, Stangl K, Knebel F, Dreger H. Prevalence, one-year-incidence and predictors of carcinoid heart disease. Cardiovascular Ultrasound. 2023 Sep 26;21(1):18.
34. Grozinsky-Glasberg S, Davar J, Hofland J, Dobson R, Prasad V, Pascher A, Denecke T, Tesselaar ME, Panzuto F, Albåge A, Connolly HM. European Neuroendocrine Tumor Society (ENETS) 2022 guidance paper for carcinoid syndrome and carcinoid heart disease. Journal of Neuroendocrinology. 2022 May 25;34(7):e13146.
35. Cuthbertson DJ, Shankland R, Srirajaskanthan R. Diagnosis and management of neuroendocrine tumors. Clinical Medicine. 2023 Mar 1;23(2):119-24.
36. Gonzáles-Yovera JG, Roseboom PJ, Concepción-Zavaleta M, Gutiérrez-Córdova I, Plasencia-Dueñas E, Quispe-Flores M, Ramos-Yataco A, Alcalde-Loyola C, Massucco-Revoredo F, Paz-Ibarra J, Concepción-Urteaga L. Diagnosis and management of small bowel neuroendocrine tumors: A state-of-the-art. World Journal of Methodology. 2022 Sep 20;12(5):381.
37. Minordi LM, Larosa L, Barbaro B, Angelino A, Broglia D, Cipri C, Scaldaferri F, Manfredi R, Natale L. How the radiologist must reason for a correct diagnosis in patients with small bowel mural thickening studied by CT or MRI: a pictorial review. Current Problems in Diagnostic Radiology. 2023 Sep 1;52(5):393-411.

38. Pasieka JL. Multifocal small bowel neuroendocrine tumors. World Journal of Surgery. 2021 Jan;45(1):208-12.
39. Yoon JY, Kumta NA, Kim MK. The role of endoscopy in small bowel neuroendocrine tumors. Clinical Endoscopy. 2021 Apr 1;54(6):818-24.
40. Somech E, Halder D, Spitzer A, Barbolin C, Tyler M, Halperin R, Biton M, Tirosh A, Tirosh I. Subtypes and proliferation patterns of small intestine neuroendocrine tumors revealed by single-cell RNA sequencing. Elife. 2025 Jul 23;13:RP101153.
41. Elias E, Ardalan A, Lindberg M, Reinsbach SE, Muth A, Nilsson O, Arvidsson Y, Larsson E. Independent somatic evolution underlies clustered neuroendocrine tumors in the human small intestine. Nature Communications. 2021 Nov 4;12(1):6367.
42. Mäkinen N, Zhou M, Zhang Z, Kasai Y, Perez E, Kim GE, Thirlwell C, Nakakura E, Meyerson M. Whole genome sequencing reveals the independent clonal origin of multifocal ileal neuroendocrine tumors. Genome Medicine. 2022 Aug 3;14(1):82.
43. Daskalakis K, Tsoli M, Wallin G, Kogut A, Srirajaskanthan R, Harlow C, Giovos G, Weickert MO, Kos-Kudla B, Kaltsas G. Modified histopathological grading optimizes prediction of survival outcomes in small intestinal neuroendocrine tumors. The Journal of Clinical Endocrinology & Metabolism. 2024 Dec;109(12):e2222-30.
44. Van Den Heede K, Chidambaram S, Van Slycke S, Brusselaers N, Warfvinge CF, Ohlsson H, Gustafsson R, Nordenström E, Almquist M. Long-term survival of metastatic small intestine neuroendocrine tumors: a meta-analysis. Endocrine-Related Cancer. 2022 Mar 1;29(3):163-73.
45. Grillo F, Albertelli M, Brisigotti MP, Borra T, Boschetti M, Fiocca R, Ferone D, Mastracci L. Grade increases in gastroenteropancreatic neuroendocrine tumor metastases compared to the primary tumor. Neuroendocrinology. 2016 Aug 25;103(5):452-9.
46. Daskalakis K, Tsoli M, Wedin M, Kos-Kudla B, Kogut A, Srirajaskanthan R, Clement DS, Giovos G, Weickert MO, Kaltsas G. Longitudinal changes in ki-67 indices in small-intestinal neuroendocrine tumors and their impact on survival. Neuroendocrinology. 2025 Jun 16;115(5):402-10.
47. Landerholm K. Time trends in incidence and survival of small intestinal cancer in Sweden. BJS open. 2021 Jan;5(1):zraa044.
48. Slott C, Langer SW, Møller S, Krogh J, Klose M, Hansen CP, Kjaer A, Holmager P, Garbyal RS, Knigge U, Andreassen M. Outlook for 615 small intestinal neuroendocrine

tumor patients: Recurrence risk after surgery and disease-specific survival in advanced disease. Cancers. 2024 Jan 1;16(1):204.

49. Folkestad O, Wasmuth HH, Mjønes P, Fougner R, Hauso Ø, Fossmark R. Survival and disease recurrence in patients operated for small intestinal neuroendocrine tumors at a referral hospital. Surgical Oncology. 2020 Dec 1;35:336-43.
50. Sorbye H, Hjortland GO, Vestermark LW, Ladekarl M, Svensson J, Sundlöv A, Janson ET, Garresori H, Hofsli E, Kersten C, Elvebakken H. Characteristics and treatment outcome in a prospective cohort of 639 advanced high-grade digestive neuroendocrine neoplasms (NET G3 and NEC). The NORDIC NEC 2 study. British Journal of Cancer. 2025 May 17;133(3):316.
51. Sei Y, Feng J, Zhao X, Forbes J, Tang D, Nagashima K, Hanson J, Quezado MM, Hughes MS, Wank SA. Polyclonal crypt genesis and development of familial small intestinal neuroendocrine tumors. Gastroenterology. 2016 Jul 1;151(1):140-51.
52. Bolduan F, Müller-Bötticher N, Debnath O, Eichhorn I, Giesecke Y, Wetzel A, Sahay S, Zemojtel T, Jaeger M, Ungethuem U, Roderburg C. Small intestinal neuroendocrine tumors lack early genomic drivers, acquire DNA repair defects and harbor hallmarks of low REST expression. Scientific Reports. 2025 May 23;15(1):17969.
53. Singh PN, Gu W, Madha S, Lynch AW, Cejas P, He R, Bhattacharya S, Gomez MM, Oser MG, Brown M, Long HW. Transcription factor dynamics, oscillation, and functions in human enteroendocrine cell differentiation. Cell Stem Cell. 2024 Jul 5;31(7):1038-57.
54. Beumer J, Puschhof J, Bauzá-Martinez J, Martínez-Silgado A, Elmentaite R, James KR, Ross A, Hendriks D, Artegiani B, Busslinger GA, Ponsioen B. High-resolution mRNA and secretome atlas of human enteroendocrine cells. Cell. 2020 Jun 11;181(6):1291-306.
55. Smith CA, O'Flaherty EA, Guccio N, Punnoose A, Darwish T, Lewis JE, Foreman RE, Li J, Kay RG, Adriaenssens AE, Reimann F. Single-cell transcriptomic atlas of enteroendocrine cells along the murine gastrointestinal tract. PLoS One. 2024 Oct 8;19(10):e0308942.
56. Saint-Denis E, Frintu B, Goldsmith M, Ramos GP, Zeve D. Enteroendocrine cell differentiation: implications for human disease. Molecular and Cellular Endocrinology. 2025 Jun 26:112607.
57. McRae AN, Ticho AL, Liu Y, Ricardo-Silgado ML, Mangena NN, Jassir FF, Gonzalez-Izundegui D, Calderon G, Rohakhtar FR, Simon V, Li Y. Regulator of G-protein

signaling expression in human intestinal enteroendocrine cells and potential role in satiety hormone secretion in health and obesity. EBioMedicine. 2024 Sep 1;107.

58. Sanidad KZ, Rager SL, Carrow HC, Ananthanarayanan A, Callaghan R, Hart LR, Li T, Ravisankar P, Brown JA, Amir M, Jin JC. Gut bacteria–derived serotonin promotes immune tolerance in early life. Science immunology. 2024 Mar 15;9(93):eadj4775.
59. Nwako JG, Mccauley HA. Enteroendocrine cells regulate intestinal homeostasis and epithelial function. Molecular and cellular endocrinology. 2024 Nov 1;593:112339.
60. Rogoza O, Megnis K, Kudrjavceva M, Gerina-Berzina A, Rovite V. Role of somatostatin signalling in neuroendocrine tumors. International Journal of Molecular Sciences. 2022 Jan 27;23(3):1447.
61. Simbolo M, Vicentini C, Mafficini A, Fassan M, Pedron S, Corbo V, Mastracci L, Rusev B, Pedrazzani C, Landoni L, Grillo F. Mutational and copy number asset of primary sporadic neuroendocrine tumors of the small intestine. Virchows Archiv. 2018 Dec;473(6):709-17.
62. Fernandez-Cuesta L, Alcala N, Mathian E, Derks J, Thirlwell C, Dayton T, Marinoni I, Perren A, Walter T, Foll M. Basic science and translational implications of current knowledge on neuroendocrine tumors. The Journal of clinical investigation. 2025 Mar 3;135(5).
63. Zhang Z, Mäkinen N, Kasai Y, Kim GE, Diosdado B, Nakakura E, Meyerson M. Patterns of chromosome 18 loss of heterozygosity in multifocal ileal neuroendocrine tumors. Genes, Chromosomes and Cancer. 2020 Sep;59(9):535-9.
64. Schiller A, Hultmark A, Lindberg M, Socratous A, Luijts T, Van den Eynden J, Elf AK, Norrlund RR, Arvidsson Y, Elias E, Larsson E. Early initiation of small intestine neuroendocrine tumors. bioRxiv. 2025 May 20:2025-05.
65. Hofland J, de Herder WW. Gastrointestinal Neuroendocrine Tumors and the Carcinoid Syndrome. Endotext [Internet]. 2023 Aug 25.
66. van Riet J, van de Werken HJ, Cuppen E, Eskens FA, Tesselaar M, van Veenendaal LM, Klümpen HJ, Dercksen MW, Valk GD, Lolkema MP, Sleijfer S. The genomic landscape of 85 advanced neuroendocrine neoplasms reveals subtype-heterogeneity and potential therapeutic targets. Nature Communications. 2021 Jul 29;12(1):4612.
67. Tirosh A, Killian JK, Petersen D, Zhu YJ, Walker RL, Blau JE, Nilubol N, Patel D, Agarwal SK, Weinstein LS, Meltzer P. Distinct DNA methylation signatures in neuroendocrine tumors specific for primary site and inherited predisposition. The Journal of Clinical Endocrinology & Metabolism. 2020 Oct;105(10):3285-94.

68. Patte C, Pommier RM, Ferrari A, Fei-Lei Chung F, Ouzounova M, Moullé P, Richaud M, Khoueiry R, Hervieu M, Breusa S, Allio M. Comprehensive molecular portrait reveals genetic diversity and distinct molecular subtypes of small intestinal neuroendocrine tumors. Nature Communications. 2025 Mar 4;16(1):2197.
69. Klomp MJ, Refardt J, van Koetsveld PM, Campana C, Dalm SU, Dogan F, van Velthuysen ML, Feelders RA, de Herder WW, Hofland J, Hofland LJ. Epigenetic regulation of SST2 expression in small intestinal neuroendocrine tumors. Frontiers in Endocrinology. 2023 May 8;14:1184436.
70. Evans JS, Beaumont J, Braga M, Masrour N, Mauri F, Beckley A, Butt S, Karali CS, Cawthorne C, Archibald S, Aboagye EO. Epigenetic potentiation of somatostatin-2 by guadecitabine in neuroendocrine neoplasias as a novel method to allow delivery of peptide receptor radiotherapy. European Journal of Cancer. 2022 Nov 1;176:110-20.
71. Sharma R, Earla B, Baidoo KE, Zeiger MA, Madigan JP, Escorcia FE, Sadowski SM. Upregulation of somatostatin receptor type 2 improves 177Lu-DOTATATE therapy in receptor-deficient pancreatic neuroendocrine tumor model. Molecular cancer therapeutics. 2023 Sep 5;22(9):1052-62.
72. Papantoniou D, Grönberg M, Thiis-Evensen E, Sorbye H, Landerholm K, Welin S, Janson ET. Treatment efficacy in a metastatic small intestinal neuroendocrine tumor grade 2 cohort. Endocrine-Related Cancer. 2023 Mar 1;30(3).
73. Prakash J, Shaked Y. The interplay between extracellular matrix remodeling and cancer therapeutics. Cancer discovery. 2024 Aug 2;14(8):1375-88.
74. Hung LY, Alves ND, Del Colle A, Talati A, Najjar SA, Bouchard V, Gillet V, Tong Y, Huang Z, Browning KN, Hua J. Intestinal epithelial serotonin as a novel target for treating disorders of gut-brain interaction and mood. Gastroenterology. 2025 Apr 1;168(4):754-68.
75. Grundeken E, El Aidy S. Enteroendocrine cells: the gatekeepers of microbiome-gut-brain communication. npj Biofilms and Microbiomes. 2025 Sep 1;11(1):179.
76. McIntyre RS. Serotonin 5-HT2B receptor agonism and valvular heart disease: implications for the development of psilocybin and related agents. Expert Opinion on Drug Safety. 2023 Oct 3;22(10):881-3.
77. Hörsch D, Anthony L, Gross DJ, Valle JW, Welin S, Benavent M, Caplin M, Pavel M, Bergsland E, Öberg K, Kassler-Taub KB. Long-term treatment with telotristat ethyl in patients with carcinoid syndrome symptoms: results from the TELEPATH study. Neuroendocrinology. 2022 May 3;112(3):298-310.

78. Hodgetts H, Martins MC, Chen L, Hall AR, Luong TV, Mandair D, Caplin M, Rombouts K. Telotristat ethyl affects tumor-fibroblast crosstalk in small intestinal neuroendocrine tumors. Journal of Neuroendocrinology. 2025 Nov;37(11):e70094.
79. Lauricella E, Mandriani B, Cavallo F, Pezzicoli G, Chaoul N, Porta C, Cives M. Angiogenesis in NENs, with a focus on gastroenteropancreatic NENs: from biology to current and future therapeutic implications. Frontiers in Oncology. 2022 Aug 17;12:957068.
80. Vesely C, Wong YN, Childs A, Akarca AU, Dhami P, Vaikkinen H, Conde L, Herrero J, Ogunbiyi O, Gander A, Luong TV. Systematic evaluation of the immune environment of small intestinal neuroendocrine tumors. Clinical Cancer Research. 2022 Jun 13;28(12):2657-68.
81. Strosberg J, Mizuno N, Doi T, Grande E, Delord JP, Shapira-Frommer R, Bergsland E, Shah M, Fakih M, Takahashi S, Piha-Paul SA. Efficacy and safety of pembrolizumab in previously treated advanced neuroendocrine tumors: results from the phase II KEYNOTE-158 study. Clinical cancer research. 2020 May 1;26(9):2124-30.
82. Zhang M, Zhang B. Extracellular matrix stiffness: mechanisms in tumor progression and therapeutic potential in cancer. Experimental Hematology & Oncology. 2025 Apr 10;14(1):54.
83. Liu ZL, Chen HH, Zheng LL, Sun LP, Shi L. Angiogenic signaling pathways and anti-angiogenic therapy for cancer. Signal transduction and targeted therapy. 2023 May 11;8(1):198.
84. Chan JA, Geyer S, Zemla T, Knopp MV, Behr S, Pulsipher S, Ou FS, Dueck AC, Acoba J, Shergill A, Wolin EM. Phase 3 trial of cabozantinib to treat advanced neuroendocrine tumors. New England Journal of Medicine. 2025 Feb 13;392(7):653-65.
85. Bergsland EK, Geyer S, Asmis TR, Behr SC, Kuebler JP, Kumthekar P, Mazza G, Maitland ML, Niedzwiecki D, Nixon AB, Schwartz LH. Randomized Phase II Trial of Pazopanib Versus Placebo in Patients With Advanced Extrapancreatic Neuroendocrine Tumors (Alliance A021202). Journal of Clinical Oncology. 2025 Oct 10;43(29):3170-83.
86. Huang J, Zhang L, Wan D, Zhou L, Zheng S, Lin S, Qiao Y. Extracellular matrix and its therapeutic potential for cancer treatment. Signal transduction and targeted therapy. 2021 Apr 23;6(1):153.
87. Collins JT, Nguyen A, Omole AE, Badireddy M. Anatomy, abdomen and pelvis, small intestine. InStatPearls [Internet] 2025 Feb 18. StatPearls Publishing.

88. Medscape. (2025, March 19). *Small Intestine Anatomy: Overview, gross anatomy, vascular supply*. Retrieved October 26, 2025.
89. Vasic T, Stimec M, Stimec BV, Ignjatovic D. Lymphatic and vascular anatomy define surgical principles for bowel-sparing radical treatment of ileal tumors. Surgical Endoscopy. 2025 Apr;39(4):2711-20.
90. Radiopaedia.org. (2024, December 19). *Superior mesenteric artery*. https://doi.org/10.53347/rID-1701 (Accessed October 26, 2025).
91. Reinehr MD, Vuille-dit-Bille RN, Soll C, Mittal A, Samra JS, Staerkle RF. Anatomy of the neural fibers at the superior mesenteric artery—a cadaver study. Langenbeck's Archives of Surgery. 2022 Sep;407(6):2347-54.
92. Groh AM, Lamont J, de Oliveira C, Fanous J, Rajakumar N, Power NE, Beveridge TS. Characterizing the autonomic neural connections between the abdominal aortic and superior hypogastric plexuses: A multimodal neuroanatomical study. Autonomic Neuroscience. 2021 May 1;232:102785.
93. Reintam Blaser A, Koitmäe M, Laisaar KT, Forbes A, Kase K, Kiisk E, Murruste M, Reim M, Starkopf J, Tamme K. Radiological diagnosis of acute mesenteric ischemia in adult patients: a systematic review and meta-analysis. Scientific Reports. 2025 Mar 22;15(1):9875.
94. Swafford EP, Magge DR. Acute mesenteric ischemia secondary to metastatic neuroendocrine tumor: a case analysis and review of the literature. Journal of Surgical Case Reports. 2024 Nov 1;2024(11).
95. Daskalakis K, Wedin M, Tsoli M, Kogut A, Srirajaskanthan R, Sarras K, Kattiparambil S, Giovos G, Weickert MO, Kos-Kudla B, Kaltsas G. Association of lymph node metastases, grade and extent of mesenteric lymph node dissection in locoregional small intestinal neuroendocrine tumors with recurrence-free survival. Journal of neuroendocrinology. 2022 Nov;34(11):e13205.
96. Fata CR, Gonzalez RS, Liu E, Cates JM, Shi C. Mesenteric tumor deposits in midgut small intestinal neuroendocrine tumors are a stronger indicator than lymph node metastasis for liver metastasis and poor prognosis. The American journal of surgical pathology. 2017 Jan 1;41(1):128-33.
97. Hua J, Xu J, Liang C, Meng Q, Zhang B, Yu X, Wang W, Shi S. Reappraisal of tumor deposit as a prognostic factor in pancreatic cancer. Annals of Surgical Oncology. 2023 May 1;30(5):3038-44.

98. Chan K, Chauhan A, Shi C. AJCC Cancer Staging System Version 9: practice-informing updates for gastroenteropancreatic neuroendocrine tumors. Annals of Surgical Oncology. 2024 Aug;31(8):4834-6.
99. Liu Q, Polydorides AD. Diagnosis and prognostic significance of extramural venous invasion in neuroendocrine tumors of the small intestine. Modern Pathology. 2020 Nov 1;33(11):2318-29.
100. Kmiotek E, Lakda S, Borakati A, Ogunbiyi O, Mandair D, Caplin M, Toumpanakis C, Mirnezami R. Management strategies and outcomes for small intestinal neuroendocrine tumors with involvement of the superior mesenteric vessels: a systematic review. Current Oncology. 2023 Oct 18;30(10):9192-204.
101. Bartsch DK, Krasser-Gercke N, Rinke A, Mahnken A, Jesinghaus M, Eilsberger F, Maurer E. Outcome of Debulking the Mesenteric Mass in Symptomatic Patients with Locally Advanced Small Intestine Neuroendocrine Tumors. Cancers. 2025 Apr 14;17(8):1318.
102. Bala M, Catena F, Kashuk J, De Simone B, Gomes CA, Weber D, Sartelli M, Coccolini F, Kluger Y, Abu-Zidan FM, Picetti E. Acute mesenteric ischemia: updated guidelines of the World Society of Emergency Surgery. World journal of emergency surgery. 2022 Oct 19;17(1):54.
103. Asmundo L, Rizzetto F, Blake M, Anderson M, Mojtahed A, Bradley W, Shenoy-Bhangle A, Fernandez-del Castillo C, Qadan M, Ferrone C, Clark J. Advancements in neuroendocrine neoplasms: imaging and future frontiers. Journal of Clinical Medicine. 2024 Jun 2;13(11):3281.
104. Dromain C, Vullierme MP, Hicks RJ, Prasad V, O'Toole D, de Herder WW, Pavel M, Faggiano A, Kos-Kudla B, Oberg K, Krejs GJ. ENETS consensus guidelines for synoptic reporting of radiology studies. JOURNAL OF NEUROENDOCRINOLOGY. 2022 Mar 1;34(3).
105. Gonzalez RS, La Rosa S, Ma C, Polydorides AD, Shi C, Yang Z, Cox B, Karamchandani DM. Substantial Interobserver Agreement Exists in Distinguishing Tumor Deposits From Nodal Metastases in Small Bowel Neuroendocrine Tumors. ARCHIVES OF PATHOLOGY & LABORATORY MEDICINE. 2024 May 1;148(5):581-7.
106. Gonzalez RS, Cates JM, Shi C. Number, not size, of mesenteric tumor deposits affects prognosis of small intestinal well-differentiated neuroendocrine tumors. Modern Pathology. 2018 Jan 1;31(10):1560-6.

107. Lardière-Deguelte S, de Mestier L, Appéré F, Vullierme MP, Zappa M, Hoeffel C, Noaves M, Brixi H, Hentic O, Ruszniewski P, Cadiot G. Toward a preoperative classification of lymph node metastases in patients with small intestinal neuroendocrine tumors in the era of intestinal-sparing surgery. Neuroendocrinology. 2016 Oct 8;103(5):552-9.

108. Blažević A, Brabander T, Zandee WT, Hofland J, Franssen GJ, van Velthuysen ML, Feelders RA, De Herder WW. Evolution of the mesenteric mass in small intestinal neuroendocrine tumors. Cancers. 2021 Jan 25;13(3):443.

109. Pennazio M, Rondonotti E, Despott EJ, Dray X, Keuchel M, Moreels T, Sanders DS, Spada C, Carretero C, Valdivia PC, Elli L. Small-bowel capsule endoscopy and device-assisted enteroscopy for diagnosis and treatment of small-bowel disorders: European Society of Gastrointestinal Endoscopy (ESGE) Guideline–Update 2022. Endoscopy. 2023 Jan;55(01):58-95.

110. Lee HH, Kim JS, Goong HJ, Lee SH, Oh EH, Park J, Kim MC, Nam K, Yang YJ, Kim TJ, Nam SJ. Use of device-assisted enteroscopy in small bowel disease: an expert consensus statement by the Korean Association for the Study of Intestinal Diseases. Intestinal research. 2023 Jan 31;21(1):3-19.

111. Kim SE, Kim HJ, Koh M, Kim MC, Kim JS, Nam JH, Cho YK, Choe AR. A practical approach for small bowel bleeding. Clinical endoscopy. 2023 May 11;56(3):283-9.

112. Gangi A, Siegel E, Barmparas G, Lo S, Jamil LH, Hendifar A, Nissen NN, Wolin EM, Amersi F. Multifocality in small bowel neuroendocrine tumors. Journal of Gastrointestinal Surgery. 2018 Feb 1;22(2):303-9.

113. Bosch EM, Laskaratos FM, Sodergren M, Faiz O, Humphries A. The Role of Small-Bowel Endoscopy in the Diagnosis and Management of Small-Bowel Neuroendocrine Tumours. Journal of Clinical Medicine. 2024 Nov 15;13(22):6877.

114. Yano T, Yamamoto H. Endoscopic Diagnosis of Small Bowel Tumor. Cancers. 2024 Apr 27;16(9):1704.

115. Li R, Ye S, Zhou C, Liu F, Li X. A systematic review and meta-analysis of magnetic resonance and computed tomography enterography in the diagnosis of small intestinal tumors. PeerJ. 2023 Dec 21;11:e16687.

116. Gupta P, Lamichane S, Bhatia H, Singhal M, Sharma V, Singh H, Kumar R, Sandhu MS. Imaging of small bowel tumors and mimics. Journal of Gastrointestinal and Abdominal Radiology. 2024 Jan;7(01):055-64.

117. Ramachandran A, Madhusudhan KS. Advances in the imaging of gastroenteropancreatic neuroendocrine neoplasms. World Journal of Gastroenterology. 2022 Jul 14;28(26):3008.

118. Fehrenbach U, Xin S, Hartenstein A, Auer TA, Dräger F, Froböse K, Jann H, Mogl M, Amthauer H, Geisel D, Denecke T. Automatized hepatic tumor volume analysis of neuroendocrine liver metastases by gd-eob mri—A deep-learning model to support multidisciplinary cancer conference decision-making. Cancers. 2021 May 31;13(11):2726.

119. Maino C, Vernuccio F, Cannella R, Cortese F, Franco PN, Gaetani C, Giannini V, Inchingolo R, Ippolito D, Defeudis A, Pilato G. Liver metastases: The role of magnetic resonance imaging. World Journal of Gastroenterology. 2023 Sep 28;29(36):5180.

120. Jasti R, Carucci LR. Small bowel neoplasms: a pictorial review. Radiographics. 2020 Jul;40(4):1020-38.

121. Alija L, De Backer A. Neuroendocrine Small Bowel Tumor. Journal of the Belgian Society of Radiology. 2025 Sep 17;109(1).

122. Danti G, Flammia F, Matteuzzi B, Cozzi D, Berti V, Grazzini G, Pradella S, Recchia L, Brunese L, Miele V. Gastrointestinal neuroendocrine neoplasms (GI-NENs): Hot topics in morphological, functional, and prognostic imaging. La radiologia medica. 2021 Dec;126(12):1497-507.

123. Merola E, Fanciulli G, Pes GM, Dore MP. Artificial intelligence in the diagnosis of gastro-entero-pancreatic neuroendocrine neoplasms: Potential benefits and current limitations. Journal of Neuroendocrinology. 2025 Nov;37(11):e70087.

124. Galgano SJ, Iravani A, Bodei L, El-Haddad G, Hofman MS, Kong G. Imaging of neuroendocrine neoplasms: monitoring treatment response—AJR Expert Panel Narrative Review. American Journal of Roentgenology. 2022 May 5;218(5):767-80.

125. Flicek KT, Nehra AK, Fidler JL, Sheedy SP. Imaging of the Small Bowel Tumors. Radiologic Clinics. 2025 May 1;63(3):345-59.

126. Hope TA, Allen-Auerbach M, Bodei L, Calais J, Dahlbom M, Dunnwald LK, Graham MM, Jacene HA, Heath CL, Mittra ES, Wright CL. SNMMI procedure standard/EANM practice guideline for SSTR PET: imaging neuroendocrine tumors. Journal of Nuclear Medicine. 2023 Feb 1;64(2):204-10.

127. Hope TA, Bergsland EK, Bozkurt MF, Graham M, Heaney AP, Herrmann K, Howe JR, Kulke MH, Kunz PL, Mailman J, May L. Appropriate use criteria for

somatostatin receptor PET imaging in neuroendocrine tumors. Journal of Nuclear Medicine. 2018 Jan 1;59(1):66-74.

128. Poletto G, Cecchin D, Sperti S, Filippi L, Realdon N, Evangelista L. Head-to-head comparison between peptide-based radiopharmaceutical for PET and SPECT in the evaluation of neuroendocrine tumors: a systematic review. Current issues in molecular biology. 2022 Nov 7;44(11):5516-30.

129. Becx MN, Minczeles NS, Brabander T, de Herder WW, Nonnekens J, Hofland J. A clinical guide to peptide receptor radionuclide therapy with 177Lu-DOTATATE in neuroendocrine tumor patients. Cancers. 2022 Nov 24;14(23):5792.

130. Prela O, Caveney B, Strawderman M, Linehan D, Galka E, Schoeniger L, Hezel A, Badri N, Carpizo DR. A Reassessment of the Clinical Utility of 68Ga-DOTATATE PET/CT in Patients With Gastroenteropancreatic Neuroendocrine Tumors. Journal of Surgical Oncology. 2025 Jan 5.

131. Al-Adhami D, Abdlkadir AS, Lee ST, Sharma P, Obeidat N, Al-Alawi H, Son MH, Khalaf A, Al-Ibraheem AN. False Positive Findings of 68Ga-DOTATOC PET/CT: A Systematic Review. Molecular Imaging and Radionuclide Therapy. 2025 Oct 8;34(3):256.

132. Capdevila Castillon J. Consensus on molecular imaging and theranostics in neuroendocrine neoplasms. EUROPEAN JOURNAL OF CANCER, 2021, vol. 146, p. 56-73. 2021 Mar 1.

133. Franchina M, Cavalcoli F, Falco O, La Milia M, Elvevi A, Massironi S. Biochemical markers for neuroendocrine tumors: traditional circulating markers and recent development—a comprehensive review. Diagnostics. 2024 Jun 18;14(12):1289.

134. Marotta V, Zatelli MC, Sciammarella C, Ambrosio MR, Bondanelli M, Colao A, Faggiano A. Chromogranin A as circulating marker for diagnosis and management of neuroendocrine neoplasms: more flaws than fame. Endocrine-related cancer. 2018 Jan 1;25(1):R11-29.

135. Rossi RE, Lavezzi E, Jaafar S, Cristofolini G, Laffi A, Nappo G, Carrara S, Bertuzzi AF, Uccella S, Repici A, Zerbi A. Urinary 5-hydroxyindolacetic acid measurements in patients with neuroendocrine tumor-related carcinoid syndrome: state of the art. Cancers. 2023 Aug 11;15(16):4065.

136. Das S, Stockton SS, Hassan SA. Carcinoid heart disease management: a multi-disciplinary collaboration. The Oncologist. 2023 Jul 1;28(7):575-83.

137. Kerolles M, Mulders MC, Mirzaian M, van den Berg SA, Feelders RA, de Herder WW, Hofland J. Serum 5-hydroxyindoleacetic acid measurements for the diagnosis and follow-up of carcinoid syndrome. The Journal of Clinical Endocrinology & Metabolism. 2025 May 2:dgaf263.

138. Bevere M, Masetto F, Carazzolo ME, Bettega A, Gkountakos A, Scarpa A, Simbolo M. An overview of circulating biomarkers in neuroendocrine neoplasms: a clinical guide. Diagnostics. 2023 Aug 31;13(17):2820.

139. Öberg K, Califano A, Strosberg JR, Ma S, Pape U, Bodei L, Kaltsas G, Toumpanakis C, Goldenring JR, Frilling A, Paulson S. A meta-analysis of the accuracy of a neuroendocrine tumor mRNA genomic biomarker (NETest) in blood. Annals of Oncology. 2020 Feb 1;31(2):202-12.

140. Gertner J, Tsoli M, Hayes AR, O'Mahony LF, Laskaratos FM, Glover T, Karia P, Butt MF, Eastwood O, Mandair D, Caplin M. The clinical utility of the NETest in patients with small intestinal neuroendocrine neoplasms (Si-NENs): a "real-life" study. Cancers. 2024 Jul 10;16(14):2506.

141. Gagliardi I, Campolo F, Borges de Souza P, Rossi L, Albertelli M, Grillo F, Caputi L, Mazza M, Faggiano A, Zatelli MC. Comparative targeted genome profiling between solid and liquid biopsies in gastroenteropancreatic neuroendocrine neoplasms: a proof-of-concept pilot study. Neuroendocrinology. 2025 Jun 24;115(5):422-33.

142. Sorbye H, Hjortland GO, Vestermark LW, Sundlov A, Assmus J, Couvelard A, Perren A, Langer SW. NETest in advanced high-grade gastroenteropancreatic neuroendocrine neoplasms. Journal of Neuroendocrinology. 2024 Nov;36(11):e13428.

143. Rindi G, Mete O, Uccella S, Basturk O, La Rosa S, Brosens LA, Ezzat S, De Herder WW, Klimstra DS, Papotti M, Asa SL. Overview of the 2022 WHO classification of neuroendocrine neoplasms. Endocrine pathology. 2022 Mar;33(1):115-54.

144. Milione M, Parente P, Grillo F, Zamboni G, Mastracci L, Capella C, Fassan M, Vanoli A. Neuroendocrine neoplasms of the duodenum, ampullary region, jejunum and ileum. Pathologica. 2021 Feb 1;113(1):12.

145. Gao R, Zhang X, Chen X, Lin Y, Jin L, Zheng H, Yu X. Comparison of insulinoma-associated protein 1 (INSM1) with traditional neuroendocrine markers in gastrointestinal and pancreatic mixed neuroendocrine-non-neuroendocrine neoplasms (MiNENs). Diagnostic Pathology. 2024 Oct 29;19(1):144.

146. Juhlin CC, Zedenius J, Höög A. Metastatic neuroendocrine neoplasms of unknown primary: clues from pathology workup. Cancers. 2022 Apr 28;14(9):2210.

147. Sultana Q, Kar J, Verma A, Sanghvi S, Kaka N, Patel N, Sethi Y, Chopra H, Kamal MA, Greig NH. A comprehensive review on neuroendocrine neoplasms: presentation, pathophysiology and management. Journal of Clinical Medicine. 2023 Aug 5;12(15):5138.

148. Volante M, Brizzi MP, Faggiano A, Rosa SL, Rapa I, Ferrero A, Mansueto G, Righi L, Garancini S, Capella C, De Rosa G. Somatostatin receptor type 2A immunohistochemistry in neuroendocrine tumors: a proposal of scoring system correlated with somatostatin receptor scintigraphy. Modern Pathology. 2007 Nov;20(11):1172-82.

149. Yu J, Cao F, Zhao X, Xie Q, Lu M, Li J, Yang Z, Sun Y. Correlation and comparison of somatostatin receptor type 2 immunohistochemical scoring systems with 68Ga-DOTATATE positron emission tomography/computed tomography imaging in gastroenteropancreatic neuroendocrine neoplasms. Neuroendocrinology. 2022 Mar 22;112(4):358-69.

150. Luchini C, Pantanowitz L, Adsay V, Asa SL, Antonini P, Girolami I, Veronese N, Nottegar A, Cingarlini S, Landoni L, Brosens LA. Ki-67 assessment of pancreatic neuroendocrine neoplasms: systematic review and meta-analysis of manual vs. digital pathology scoring. Modern Pathology. 2022 Jun 1;35(6):712-20.

151. Grillo F, Valle L, Ferone D, Albertelli M, Brisigotti MP, Cittadini G, Vanoli A, Fiocca R, Mastracci L. KI-67 heterogeneity in well differentiated gastro-entero-pancreatic neuroendocrine tumors: when is biopsy reliable for grade assessment?. Endocrine. 2017 Sep;57(3):494-502.

152. Bourdeleau P, Couvelard A, Ronot M, Lebtahi R, Hentic O, Ruszniewski P, Cros J, de Mestier L. Spatial and temporal heterogeneity of digestive neuroendocrine neoplasms. Therapeutic advances in medical oncology. 2023 Jun;15:17588359231179310.

153. Wang SJ, Whitman J, Paciorek A, Le BK, Nakakura EK, Behr SC, Joseph N, Zhang L, Hope TA, Bergsland EK. Baseline tumor growth rate highlights the heterogeneity of well differentiated gastroenteropancreatic neuroendocrine tumors and predicts for increases in Ki67 index over time. Journal of Neuroendocrinology. 2023 Apr;35(4):e13260.

154. Couvelard A, Cazes A, Cros J. Updates in histopathological classification and tissue biomarkers of digestive neuroendocrine neoplasms: What the clinician should know. Best Practice & Research Clinical Endocrinology & Metabolism. 2023 Sep 1;37(5):101795.

155. Vesterinen T, Säilä J, Blom S, Pennanen M, Leijon H, Arola J. Automated assessment of Ki-67 proliferation index in neuroendocrine tumors by deep learning. Apmis. 2022 Jan;130(1):11-20.

156. Saetiew K, Angkathunyakul N, Hunnangkul S, Pongpaibul A. Digital image analysis of Ki67 hotspot detection and index counting in gastroenteropancreatic neuroendocrine neoplasms. Annals of Diagnostic Pathology. 2024 Aug 1;71:152295.

157. Das S, Shi C, Koyama T, Huang Y, Gonzalez R, Idrees K, Bailey CE, Berlin J. Peritoneal carcinomatosis in well-differentiated small-intestinal neuroendocrine tumors with mesenteric tumor deposits. Journal of medical & surgical pathology. 2019 Jul 5;4(1):1.

158. Chauhan A, Chan K, Halfdanarson TR, Bellizzi AM, Rindi G, O'Toole D, Ge PS, Jain D, Dasari A, Anaya DA, Bergsland E. Critical updates in neuroendocrine tumors: Version 9 American Joint Committee on Cancer staging system for gastroenteropancreatic neuroendocrine tumors. CA: a cancer journal for clinicians. 2024 Jul;74(4):359-67.

159. Resch A, Langner C. Lymph node staging in colorectal cancer: old controversies and recent advances. World journal of gastroenterology: WJG. 2013 Dec 14;19(46):8515.

160. Kankava K, Maisonneuve P, Mangogna A, Centonze G, Cattaneo L, Prinzi N, Pusceddu S, Fazio N, Pisa E, Di Domenico S, Bertani E. Prognostic features of gastro-entero-pancreatic neuroendocrine neoplasms in primary and metastatic sites: Grade, mesenteric tumor deposits and emerging novelties. Journal of Neuroendocrinology. 2021 Aug;33(8):e13000.

161. Clift AK, Drymousis P, von Roon A, Humphries A, Goldin R, Bomanji J, Leaman S, Wasan H, Habib N, Frilling A. Management of Small Bowel Neuroendocrine Tumours: 10 Years' Experience at a Tertiary Referral Centre. Cancers. 2023 Sep 6;15(18):4438.

162. Polydorides AD, Liu Q. Evaluation of pathologic prognostic factors in neuroendocrine tumors of the small intestine. The American Journal of Surgical Pathology. 2022 Apr 1;46(4):547-56.

163. Grillo F, Albertelli M, Malandrino P, Dotto A, Pizza G, Cittadini G, Colao A, Faggiano A. Prognostic effect of lymph node metastases and mesenteric deposits in neuroendocrine tumors of the small bowel. The Journal of Clinical Endocrinology & Metabolism. 2022 Dec 1;107(12):3209-21.

164. National Cancer Institute, Surveillance, Epidemiology, and End Results (SEER) Program. (2023). SEER Inquiry System: Question 20230074—Extent of Disease/EOD Regional Nodes—Small intestine. https://seer.cancer.gov/seer-inquiry/inquiry-detail/20230074/

165. Burgart LJ, Chopp WV, Jain D. Protocol for the Examination of Specimens From Patients with Well-Differentiated Neuroendocrine Tumors (Carcinoid Tumors) of the Duodenum and Ampulla of Vater.

166. van Velthuysen ML, Couvelard A, Rindi G, Fazio N, Hörsch D, Nieveen van Dijkum EJ, Klöppel G, Perren A. ENETS standardized (synoptic) reporting for neuroendocrine tumor pathology. Journal of Neuroendocrinology. 2022 Mar;34(3):e13100.

167. Bonomi A, Fumagalli Romario U, Funicelli L, Conti G, Realis Luc M, Ceci F, Pozzi S, Radice D, Fazio N, Bertani E. Diagnosis and staging of small intestinal neuroendocrine tumors with CT enterography and PET with Gallium-68: preoperative risk stratification protocol. Langenbeck's Archives of Surgery. 2024 Feb 16;409(1):63.

168. College of American Pathologists. *Cancer protocol templates*. Retrieved November 4, 2025, from https://www.cap.org/protocols-and-guidelines/cancer-reporting-tools/cancer-protocol-templates

169. Reinhard L, Mogl MT, Benz F, Dukaczewska A, Butz F, Dobrindt EM, Tacke F, Pratschke J, Goretzki PE, Jann H. Prognostic differences in grading and metastatic lymph node pattern in patients with small bowel neuroendocrine tumors. Langenbeck's Archives of Surgery. 2023 Jun 19;408(1):237.

170. Lavie D, Ben-Shmuel A, Erez N, Scherz-Shouval R. Cancer-associated fibroblasts in the single-cell era. Nature cancer. 2022 Jul;3(7):793-807.

171. Mai Z, Lin Y, Lin P, Zhao X, Cui L. Modulating extracellular matrix stiffness: a strategic approach to boost cancer immunotherapy. Cell death & disease. 2024 May 1;15(5):307.

172. Hernández Fernaud JR, Kay EJ, Paterson K, Riera-Domingo C, Sumpton D, Däbritz JH, Tardito S, Boldrini C, Athineos D, Dhayade S, Stepanova E. Cancer-

associated fibroblasts require proline synthesis by PYCR1 for the deposition of pro-tumorigenic extracellular matrix.

173. Ratnayake GM, Laskaratos FM, Mandair D, Caplin ME, Rombouts K, Toumpanakis C. What causes desmoplastic reaction in small intestinal neuroendocrine neoplasms?. Current Oncology Reports. 2022 Oct;24(10):1281-6.

174. Blažević A, Iyer AM, van Velthuysen ML, Hofland J, van Koestveld PM, Franssen GJ, Feelders RA, Zajec M, Luider TM, de Herder WW, Hofland LJ. Aberrant tryptophan metabolism in stromal cells is associated with mesenteric fibrosis in small intestinal neuroendocrine tumors. Endocrine Connections. 2022 Apr 1;11(4).

175. Andrews SG, Forsythe SD, Madigan JP, Sadowski SM. Multifaceted modeling of small intestinal neuroendocrine tumors. Endocrine Oncology. 2024 Jan 1;4(1).

176. Snider JC, Riley LA, Mallory NT, Bersi MR, Umbarkar P, Gautam R, Zhang Q, Mahadevan-Jansen A, Hatzopoulos AK, Maroteaux L, Lal H. Targeting 5-HT2B receptor signaling prevents border zone expansion and improves microstructural remodeling after myocardial infarction. Circulation. 2021 Mar 30;143(13):1317-30.

177. Löfdahl A, Tornling G, Wigén J, Larsson-Callerfelt AK, Wenglén C, Westergren-Thorsson G. Pathological insight into 5-HT2B receptor activation in fibrosing interstitial lung diseases. International Journal of Molecular Sciences. 2020 Dec 28;22(1):225.

178. Pagire HS, Pagire SH, Jeong BK, Choi WI, Oh CJ, Lim CW, Kim M, Yoon J, Kim SS, Bae MA, Jeon JH. Discovery of a peripheral 5HT2A antagonist as a clinical candidate for metabolic dysfunction-associated steatohepatitis. Nature communications. 2024 Jan 20;15(1):645.

179. Herrera-Martínez AD, Fuentes-Fayos AC, Sanchez-Sanchez R, Montero AJ, Sarmento-Cabral A, Gálvez-Moreno MA, Gahete MD, Luque RM. Does telotristat have a role in preventing carcinoid heart disease?. International Journal of Molecular Sciences. 2024 Feb 7;25(4):2036.

180. Blažević A, Iyer AM, Van Velthuysen ML, Hofland J, Oudijk L, De Herder WW, Hofland LJ, Feelders RA. Sexual dimorphism in small-intestinal neuroendocrine tumors: lower prevalence of mesenteric disease in premenopausal women. The Journal of Clinical Endocrinology & Metabolism. 2022 May 1;107(5):e1969-75.

181. Vitale G, Carra S, Alessi Y, Campolo F, Pandozzi C, Zanata I, Colao A, Faggiano A, NIKE Group. Carcinoid syndrome: preclinical models and future therapeutic strategies. International Journal of Molecular Sciences. 2023 Feb 10;24(4):3610.

182. Koumarianou A, Alexandraki KI, Wallin G, Kaltsas G, Daskalakis K. Pathogenesis and clinical management of mesenteric fibrosis in small intestinal neuroendocine neoplasms: a systematic review. Journal of Clinical Medicine. 2020 Jun 8;9(6):1777.

183. Giambelluca D, Cannella R, Midiri M, Salvaggio G. The “spoke wheel” sign in mesenteric carcinoid. Abdominal Radiology. 2019 May 15;44(5):1949-50.

184. Hospices Civils de Lyon. (2019). *Assessment of an optimized and standardized computerized tomography (CT) reading grid for preoperative planning improvement of small bowel neuroendocrine tumors (NET) (POPINET) (NCT03958188)* [Clinical trial registration]. ClinicalTrials.gov. https://clinicaltrials.gov/study/NCT03958188

185. Marasco M, Romano E, Arrivi G, Prosperi D, Rinzivillo M, Caruso D, Mercantini P, Rossi M, Faggiano A, Panzuto F. Exploring carcinoid syndrome in neuroendocrine tumors: insights from a multidisciplinary narrative review. Cancers. 2024 Nov 14;16(22):3831.

186. Nadim B, Boyko A, Kavanaugh M, Prabhu R, Auer B, Shah H. Neuroendocrine Neoplasms: A Primer on Imaging and Nonsurgical Therapies. Roentgen Ray Review. 2025 Mar 6.

187. Speca S, Giusti I, Rieder F, Latella G. Cellular and molecular mechanisms of intestinal fibrosis. World journal of gastroenterology: WJG. 2012 Jul 28;18(28):3635.

188. Shah MH, Goldner WS, Benson AB, Bergsland E, Blaszkowsky LS, Brock P, Chan J, Das S, Dickson PV, Fanta P, Giordano T. Neuroendocrine and adrenal tumors, version 2.2021, NCCN clinical practice guidelines in oncology. Journal of the National Comprehensive Cancer Network. 2021 Jul 28;19(7):839-68.

189. Hanna MG, Ardon O. Digital pathology systems enabling quality patient care. Genes, Chromosomes and Cancer. 2023 Nov;62(11):685-97.

190. Laskaratos FM, Mandair D, Hall A, Alexander S, von Stempel C, Bretherton J, Luong T, Watkins J, Ogunbiyi O, Rombouts K, Caplin M. Clinicopathological correlations of mesenteric fibrosis and evaluation of a novel biomarker for fibrosis detection in small bowel neuroendocrine neoplasms. Endocrine. 2020 Mar;67(3):718-26.

191. Calvaruso V, Burroughs AK, Standish R, Manousou P, Grillo F, Leandro G, Maimone S, Pleguezuelo M, Xirouchakis I, Piero Guerrini G, Patch D. Computer-assisted image analysis of liver collagen: relationship to Ishak scoring and hepatic venous pressure gradient. Hepatology. 2009 Apr;49(4):1236-44.

192. Calvaruso V, Dhillon AP, Tsochatzis E, Manousou P, Grillo F, Germani G, Patch D, O'Beirne J, Burroughs AK. Liver collagen proportionate area predicts decompensation in patients with recurrent hepatitis C virus cirrhosis after liver transplantation. Journal of gastroenterology and hepatology. 2012 Jul;27(7):1227-32.

193. Soon G, Wee A. Updates in the quantitative assessment of liver fibrosis for nonalcoholic fatty liver disease: histological perspective. Clinical and molecular hepatology. 2020 Nov 19;27(1):44.

194. Ball L, Barisione E, Mastracci L, Campora M, Costa D, Robba C, Battaglini D, Micali M, Costantino F, Cittadini G, Patroniti N. Extension of collagen deposition in COVID-19 post mortem lung samples and computed tomography analysis findings. International Journal of Molecular Sciences. 2021 Jul 13;22(14):7498.

195. Serdjebi C, Bertotti K, Huang P, Wei G, Skelton-Badlani D, Leclercq IA, Barbes D, Lepoivre B, Popov YV, Julé Y. Automated whole slide image analysis for a translational quantification of liver fibrosis. Scientific reports. 2022 Nov 4;12(1):17935.

196. Courtoy GE, Leclercq I, Froidure A, Schiano G, Morelle J, Devuyst O, Huaux F, Bouzin C. Digital image analysis of picrosirius red staining: a robust method for multi-organ fibrosis quantification and characterization. Biomolecules. 2020 Nov 22;10(11):1585.

197. Almici E, Arshakyan M, Carrasco JL, Martínez A, Ramírez J, Enguita AB, Monsó E, Montero J, Samitier J, Alcaraz J. Quantitative image analysis of fibrillar collagens reveals novel diagnostic and prognostic biomarkers and histotype-dependent aberrant mechanobiology in lung cancer. Modern Pathology. 2023 Jul 1;36(7):100155.

198. Hashemi Z, Hui T, Wu A, Matouba D, Zukowski S, Nejati S, Lim C, Bruzzese J, Lin C, Seabold K, Mills C. Epithelial-specific loss of Smad4 alleviates the fibrotic response in an acute colitis mouse model. Life Science Alliance. 2024 Dec 1;7(12).

199. Naoumov NV, Brees D, Loeffler J, Chng E, Ren Y, Lopez P, Tai D, Lamle S, Sanyal AJ. Digital pathology with artificial intelligence analyses provides greater insights into treatment-induced fibrosis regression in NASH. Journal of Hepatology. 2022 Nov 1;77(5):1399-409.

200. Voon W, Hum YC, Tee YK, Yap WS, Nisar H, Mokayed H, Gupta N, Lai KW. Evaluating the effectiveness of stain normalization techniques in automated grading of invasive ductal carcinoma histopathological images. Scientific Reports. 2023 Nov 22;13(1):20518.

201. Hoque MZ, Keskinarkaus A, Nyberg P, Seppänen T. Stain normalization methods for histopathology image analysis: A comprehensive review and experimental comparison. Information Fusion. 2024 Feb 1;102:101997.

202. Rivenson Y, Wang H, Wei Z, de Haan K, Zhang Y, Wu Y, Günaydın H, Zuckerman JE, Chong T, Sisk AE, Westbrook LM. Virtual histological staining of unlabelled tissue-autofluorescence images via deep learning. Nature biomedical engineering. 2019 Jun;3(6):466-77.

203. Cristoforetti A, Masè M, Ravelli F. Model-Based Approach for the Semi-Automatic Analysis of Collagen Birefringence in Polarized Light Microscopy. Applied Sciences. 2023 Feb 24;13(5):2916.

204. Evans AJ, Brown RW, Bui MM, Chlipala EA, Lacchetti C, Milner Jr DA, Pantanowitz L, Parwani AV, Reid K, Riben MW, Reuter VE. Validating whole slide imaging systems for diagnostic purposes in pathology. Archives of pathology & laboratory medicine. 2022 Apr 1;146(4):440-50.

205. Pillar N, Li Y, Zhang Y, Ozcan A. Virtual staining of nonfixed tissue histology. Modern Pathology. 2024 May 1;37(5):100444.

206. den Braber-Ymker M, Vonk MC, Grünberg K, Lammens M, Nagtegaal ID. Intestinal hypomotility in systemic sclerosis: a histological study into the sequence of events. Clinical Rheumatology. 2021 Mar;40(3):981-90.

207. Biel C, Kastermans A, Heidema J, Pehrsson M, Henstra C, Mortensen J, Faber KN, Olinga P. Fibrogenesis in Human Mucosa and Muscularis Precision-Cut Intestinal Slices. Cells. 2024 Jun 22;13(13):1084.

208. Baidoo N, Crawley E, Knowles CH, Sanger GJ, Belai A. Total collagen content and distribution is increased in human colon during advancing age. PloS one. 2022 Jun 17;17(6):e0269689.

209. Gordon IO, Bettenworth D, Bokemeyer A, Srivastava A, Rosty C, De Hertogh G, Robert ME, Valasek MA, Mao R, Li J, Harpaz N. International consensus to standardise histopathological scoring for small bowel strictures in Crohn's disease. Gut. 2022 Mar 1;71(3):479-86.

210. Bettenworth D, Baker ME, Fletcher JG, Jairath V, Lu C, Bemelman W, d'Haens G, d'Hoore A, Dignass A, Dotan I, Feakins R. A global consensus on the definitions, diagnosis and management of fibrostenosing small bowel Crohn's disease in clinical practice. Nature Reviews Gastroenterology & Hepatology. 2024 Aug;21(8):572-84.

211. Albertelli M, Grillo F, Lo Calzo F, Puliani G, Rainone C, Colao AA, Faggiano A, NIKE group. Pathology reporting in neuroendocrine neoplasms of the digestive system: everything you always wanted to know but were too afraid to ask. Frontiers in endocrinology. 2021 Apr 23;12:680305.

212. Grillo F, Pigozzi S, Ceriolo P, Calamaro P, Fiocca R, Mastracci L. Factors affecting immunoreactivity in long-term storage of formalin-fixed paraffin-embedded tissue sections. Histochemistry and cell biology. 2015 Jul;144(1):93-9.

213. Grillo F, Campora M, Pigozzi S, Bonadio S, Valle L, Ferro J, Paudice M, Dose B, Mastracci L. Methods for restoration of ki67 antigenicity in aged paraffin tissue blocks. Histochemistry and Cell Biology. 2021 Aug;156(2):183-90.

214. Gonzalez J, Bahmad HF, Ocejo S, Abreu A, Popp M, Gogola S, Fernandez V, Recine M, Poppiti R. The usefulness of elastin staining to detect vascular invasion in cancer. International Journal of Molecular Sciences. 2023 Oct 17;24(20):15264.

215. Liebig C, Ayala G, Wilks JA, Berger DH, Albo D. Perineural invasion in cancer: a review of the literature. Cancer: Interdisciplinary International Journal of the American Cancer Society. 2009 Aug 1;115(15):3379-91.

216. Warner TF, O'Reilly G, Angus McL. Lee G. Mesenteric occlusive lesion and ileal carcinoids. Cancer. 1979 Aug;44(2):758-62.

217. Daskalakis K, Karakatsanis A, Stålberg P, Norlén O, Hellman P. Clinical signs of fibrosis in small intestinal neuroendocrine tumors. Journal of British Surgery. 2017 Jan;104(1):69-75.

218. Rodríguez Laval V, Pavel M, Steffen IG, Baur AD, Dilz LM, Fischer C, Detjen K, Prasad V, Pascher A, Geisel D, Denecke T. Mesenteric fibrosis in midgut neuroendocrine tumors: functionality and radiological features. Neuroendocrinology. 2018 Feb 22;106(2):139-47.

219. Landau M, Wisniewski S, Davison J. Jejunoileal Neuroendocrine Tumors Complicated by Intestinal Ischemic Necrosis Are Associated With Worse Overall Survival. Archives of Pathology & Laboratory Medicine. 2016 May 1;140(5).

220. Laskaratos FM, Hall A, Alexander S, von Stempel C, Bretherton J, Luong TV, Watkins J, Ogunbiyi O, Toumpanakis C, Mandair D, Caplin M. Sa1697–Is Computed Tomography an Accurate Diagnostic Modality for the Detection of Mesenteric Fibrosis in Midgut Neuroendocrine Tumours?. Gastroenterology. 2019 May 1;156(6):S-369.

221. Druce MR, Bharwani N, Akker SA, Drake WM, Rockall A, Grossman AB. Intra-abdominal fibrosis in a recent cohort of patients with neuroendocrine (‘carcinoid’)

tumors of the small bowel. QJM: An International Journal of Medicine. 2010 Mar 1;103(3):177-85.

222. Laskaratos FM, Walker M, Wilkins D, Tuck A, Ramakrishnan S, Phillips E, Gertner J, Megapanou M, Papantoniou D, Shah R, Banks J. Evaluation of clinical prognostic factors and further delineation of the effect of mesenteric fibrosis on survival in advanced midgut neuroendocrine tumors. Neuroendocrinology. 2018 Aug 28;107(3):292-304.

223. Walsh JC, Schaeffer DF, Kirsch R, Pollett A, Manzoni M, Riddell RH, Albarello L. Ileal "carcinoid" tumors—small size belies deadly intent: high rate of nodal metastasis in tumors≤ 1 cm in size. Human pathology. 2016 Oct 1;56:123-7.

224. Pasquer A, Walter T, Hervieu V, Forestier J, Scoazec JY, Lombard-Bohas C, Poncet G. Surgical management of small bowel neuroendocrine tumors: specific requirements and their impact on staging and prognosis. Annals of surgical oncology. 2015 Dec;22(Suppl 3):742-9.

225. Ranot JM, Hamid JS, Montazeri A, Harper K, McCudden C, Moyana TN. Well-Differentiated Jejunoileal Neuroendocrine Tumors and Corresponding Liver Metastases: Mesenteric Fibrogenesis and Extramural Vascular Invasion in Tumor Progression. Cancers. 2025 Apr 28;17(9):1486.

226. Anthony PP, Drury RA. Elastic vascular sclerosis of mesenteric blood vessels in argentaffin carcinoma. Journal of Clinical Pathology. 1970 Mar 1;23(2):110-8.

227. Qizilbash AH. Carcinoid tumors, vascular elastosis, and ischemic disease of the small intestine. Diseases of the Colon & Rectum. 1977 Oct;20(7):554-60.

228. Harvey JN, Denyer ME, DaCosta P. Intestinal infarction caused by carcinoid associated elastic vascular sclerosis: early presentation of a small ileal carcinoid tumor. Gut. 1989 May 1;30(5):691-4.

229. Ronot M, Vullierme MP. Morphological imaging of gastrointestinal and lung neuroendocrine neoplasms. Current Opinion in Endocrine and Metabolic Research. 2021 Aug 1;19:1-7.